การปลูกและการกำหนดลักษณะเฉพาะผลึกเดี่ยวของโพแทสเซียมไดไฮโดรเจน
ฟอสเฟตบริสุทธิ์และถูกเจือด้วยไทโอยูเรีย

นายยุทธพงษ์ อินทร์กง

วิทยานิพนธ์นี้เป็นส่วนหนึ่งของการศึกษาตามหลักสูตรปริญญาวิทยาศาสตรดุษฎีบัณฑิต
สาขาวิชาฟิสิกส์
มหาวิทยาลัยเทคโนโลยีสุรนารี
ปีการศึกษา 2555

# GROWTH AND CHARACTERIZATION OF PURE AND

# THIOUREA DOPED POTASSIUM DIHYDROGEN

# PHOSPHATE SINGLE CRYSTALS

**Yutthapong  Inkong**

**A Thesis Submitted in Partial Fulfillment of the Requirements for the**

**Degree of Doctor of Philosophy in Physics**

**Suranaree University of Technology**

**Academic Year 2012**

# GROWTH AND CHARACTERIZATION OF PURE AND

# THIOUREA DOPED POTASSIUM DIHYDROGEN

# PHOSPHATE SINGLE CRYSTALS

Suranaree University of Technology has approved this thesis submitted in
partial fulfillment of the requirements for the Degree of Doctor of Philosophy.

Thesis Examining Committee

_____

(Assoc. Prof. Dr. Santi Maensiri)

Chairperson

_____

(Assoc. Prof. Dr. Prapun Manyum)

Member (Thesis Advisor)

_____
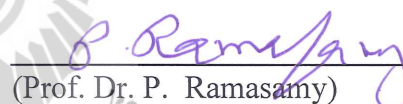
(Prof. Dr. P. Ramasamy)

Member

_____

(Asst. Prof. Dr. Rattikorn Yimnirun)

Member

_____

(Dr. Worawat Meevasana)

Member

_____                    _____
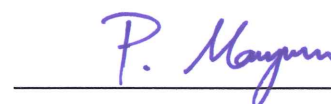
(Prof. Dr. Sukit Limpijumnong)            (Assoc. Prof. Dr. Prapun Manyum)

Vice Rector for Academic Affairs          Dean of Institute of Science

ยุทธพงษ์ อินทร์กง : การปลูกและการกำหนดลักษณะเฉพาะผลึกเดี่ยวของโพแทสเซียม
ไดไฮโดรเจนฟอสเฟตบริสุทธิ์และถูกเจือด้วยไทโอยูเรีย (GROWTH AND
CHARACTERIZATION OF PURE AND THIOUREA DOPED POTASSIUM
DIHYDROGEN PHOSPHATE SINGLE CRYSTALS) อาจารย์ที่ปรึกษา :
รองศาสตราจารย์ ดร.ประพันธ์ แม่นยำ, 150 หน้า.

ผลึกเดี่ยวของสารโพแทสเซียมไดไฮโดรเจนฟอสเฟตบริสุทธิ์และที่ถูกเจือด้วยไทโอยูเรีย
ถูกปลูกขึ้นด้วยวิธีการปลูกผลึกแบบดั้งเดิมและวิธีการปลูกผลึกแบบเอสอาร์ ผลึกที่ปลูกได้ถูกนำมา
กำหนดลักษณะเฉพาะ โดยโครงสร้างของผลึก, พารามิเตอร์ของแลตทิสและหมู่ฟังก์ชันของผลึก
ได้รับการยืนยันจากการศึกษาการเลี้ยวเบนของรังสีเอกซ์และการศึกษาฟูเรียร์ทรานสฟอร์ม
อินฟราเรด ค่าพารามิเตอร์ของแลตทิสของผลึกที่ปลูกได้สอดคล้องกับค่ามาตรฐานไอซีเอสดี ไม่
สังเกตุพบรูปแบบของสารไทโอยูเรียในรูปแบบการเลี้ยวเบนของรังสีเอกซ์ ความสมบูรณ์ของผลึก
ถูกตรวจสอบโดยการศึกษาการเลี้ยวเบนของรังสีเอกซ์ที่มีความละเอียดสูง พบว่าผลึกโพแทสเซียม
ไดไฮโดรเจนฟอสเฟตบริสุทธิ์ปราศจากโครงสร้างของขอบเกรนและปรากฏความพร่องแบบ
อินเตอร์สติเชียลในผลึกที่ถูกเจือด้วยไทโอยูเรีย อัตตราการเกิด ผลึกที่ปลูกโดยวิธีเอสอาร์ในทิศ
$\langle 001 \rangle$ สูงกว่าในทิศอื่น ค่าพารามิเตอร์ทางแสงคำนวณได้จากค่าการส่องผ่าน จากการวิเคราะห์การ
ส่องผ่านพบว่า ผลึกที่ปลูกโดยวิธีเอสอาร์ มีค่าการส่องผ่าน ที่ดีในช่วงความยาวคลื่นแสงที่ตา
มองเห็น และช่วงอินฟราเรด ในทิศ $\langle 001 \rangle$ และ $\langle 011 \rangle$ แต่มีค่าการส่องผ่าน ต่ำในทิศ $\langle 010 \rangle$ ซึ่ง
เป็นสมบัติที่จำเป็นต่อการนำไปประยุกต์ใช้ทางด้านทัศนศาสตร์ไม่เชิงเส้น พลังงานแถบห้าม
ทางด้านทัศนศาสตร์ของผลึกเดี่ยวที่ปลูกได้มีค่ามากกว่าพลังงานดูดกลืนช่วงแสงมองเห็นได้ ผล
จากการวัดความแข็งระดับจุลภาคแสดงให้เห็นว่าผลึกที่ปลูกได้มีแลตทิสที่แข็งแรง และความแข็ง
ของผลึกที่ปลูกโดยวิธีเอสอาร์ในทิศ $\langle 001 \rangle$ ทั้งผลึกบริสุทธิ์และผลึกที่ถูกเจือสูงกว่าในทิศอื่น
นอกจากนี้ยังได้ศึกษา ค่าคงตัวไดอิเล็กตริกและ การสูญเสียทาง ไดอิเล็กตริก ในรูป ของฟังก์ชันของ
ความถี่ ซึ่งพบว่าค่าคงตัวไดอิเล็กตริกของผลึกมีค่าลดลงเล็กน้อยเมื่อความถี่เพิ่มขึ้น ส่วนค่าการ
สูญเสียทาง ไดอิเล็กตริก มีการ ลดลงแบบฟังก์ชันเอกซ์โปแนนเชียลเมื่อความถี่เพิ่มขึ้น ซึ่งค่าการ
สูญเสียทางไดอิเล็กตริกมีค่าต่ำนั้นเป็นตัวบ่งบอกว่าผลึกมีความพร่องต่ำด้วย

สาขาวิชาฟิสิกส์        ลายมือชื่อนักศึกษา _____
ปีการศึกษา 2555        ลายมือชื่ออาจารย์ที่ปรึกษา_____
                ลายมือชื่ออาจารย์ที่ปรึกษาร่วม_____

YUTTHAPONG INKONG : GROWTH AND CHARACTERIZATION OF

PURE AND THIOUREA DOPED POTASSIUM DIHYDROGEN

PHOSPHATE SINGLE CRYSTALS. THESIS ADVISOR : ASSOC. PROF.

PRAPUN MANYUM, D.Phil. 150 PP.

SINGLE CRYSTAL GROWTH/KDP/SR TECHNIQUE

Single crystals of pure and thiourea doped Potassium dihydrogen phosphate

(KDP) were grown by conventional slow evaporation and Sankaranarayanan–

Ramasamy (SR) techniques. The grown crystals were characterized. Structure, lattice

parameters and functional groups in the crystals were confirmed by powder X–ray

diffraction and FTIR studies. The lattice parameters of the grown crystals were

corresponded with the standard ICSD. No peaks of thiourea were observed in XRD

patterns. The perfection of the grown crystals was investigated by high–resolution X–

ray diffraction (HRXRD). It was found that the pure KDP crystal is free from

structural grain boundaries and the interstitial defect presented in thiourea doped

crystal. The growth rate of SR technique in $\langle 001 \rangle$–direction is higher than another

direction. The optical parameters of the grown crystals were calculated from the

transmittance. The optical transmission spectrum reveals that the crystals grown by

SR technique in $\langle 001 \rangle$ and $\langle 011 \rangle$–directions have good optical transmittance in the

visible and IR regions but low transmittance in $\langle 010 \rangle$–direction. The transmittance is

a crucial condition which makes them promising materials for NLO applications. The

optical band gap energy of grown single crystals is greater than the absorption energy

of visible light. Microhardness measurement reveals that the crystals have a hard

lattice and the crystals grown by SR technique in $\langle 001 \rangle$–direction is higher in hardness than another direction both of pure and doped crystals. The dielectric constant and dielectric loss were studied as a function of frequency. It was found that the dielectric constant slightly decreases with increasing frequency. The values of dielectric loss generally decrease exponentially with frequency. Low values of dielectric loss indicate that the crystals have very low defects.

School of Physics        Student's  Signature_____

Academic Year 2012      Advisor's  Signature_____

                        Co-advisor's  Signature_____

# ACKNOWLEDGEMENT

# CONTENTS

# CONTENTS (Continued)

# CONTENTS (Continued)

# CONTENTS (Continued)

# CONTENTS (Continued)

# LIST OF TABLES

# LIST OF FIGURES

# LIST OF FIGURES (Continued)

# LIST OF FIGURES (Continued)

# LIST OF FIGURES (Continued)

# LIST OF FIGURES (Continued)

# LIST OF FIGURES (Continued)

# LIST OF ABBEVIATIONS

| | |
|---|---|
| $A$ | Surface area |
| ADP | Ammonium dihydrogen phosphate |
| ATR | Attenuated total reflection |
| $C$ | Capacitance |
| C | Actual concentration |
| $C_0$ | Equilibrium concentration |
| $\Delta C$ | Concentration driving force |
| $c.c.$ | Complex conjugate |
| DC | Direct current |
| DFG | Difference-frequency generation |
| DKDP | Potassium deuterium phosphate |
| $d$ | Diagonal length |
| $d_{hkl}$ | Inter–planar spacing |
| $E$ | Energy |
| $E_g$ | Energy band gap |
| $\vec{E}$ | Electric field |
| EDTA | Ethylene diamine tetra acetic acid |
| FWHM | Full width at half maximum |
| FTIR | Fourier transforms infrared |
| $H_v$ | Vickers hardness number |

# LIST OF ABBEVIATIONS (Continued)

| | |
|---|---|
| HRXRD | High–resolution X–ray diffraction |
| $h$ | Planck's constant |
| $I_0$ | Incident beam |
| $I_A$ | Absorbed beams |
| $I_R$ | Reflected beams |
| $I_T$ | Transmitted beams |
| KBr | Potassium bromide |
| KDP | Potassium dihydrogen phosphate |
| $k$ | Extinction coefficient |
| $\ell$ | Length |
| $N$ | Complex refractive index |
| NLO | Nonlinear optics |
| $n$ | Meyer's index |
| $n$ | Refractive index |
| $P$ | Load |
| $\vec{P}(t)$ | Polarization |
| $R$ | Reflectance |
| S | Supersaturation ratio |
| SFG | Sum frequency generation |
| SHG | Second harmonic generation |
| SR | Sankaranarayanan – Ramasamy |

# LIST OF ABBEVIATIONS (Continued)

| | |
|---|---|
| SSA | Sulfosalicylic acid |
| $T$ | Transmittance |
| TGS | Triglycine sulphate |
| t | Time |
| UV-Vis | Ultra violet-visible spectrophotometer |
| XRD | X-ray diffractometer |
| $\alpha$ | Absorption coefficient |
| $\varepsilon_0$ | Permittivity of free space |
| $\varepsilon_r$ | Relative permittivity |
| $\varepsilon_r'$ | Real part of dielectric constant |
| $\varepsilon_r''$ | Dielectric loss |
| $\theta$ | Angle |
| $\kappa$ | Dielectric constant or relative permittivity |
| $\lambda$ | Wavelength |
| $\sigma$ | Supersaturation |
| $\sigma_v$ | Yield strength |
| $\chi^{(n)}$ | n–th order susceptibility |
| $\omega$ | Angular frequency |

# CHAPTER I

# INTRODUCTION

## 1.1 Rationale of the Study

One can say that nowadays technologies have come from the studies and developments of single crystals growth. A single crystal is a solid material which has the same arrangement of atoms, molecules, or ions (called "crystal lattice") in an orderly and repeating pattern extending in all three spatial dimensions of the whole specimen. Single crystals have been employed in electronic industry, photonic industry, fiber optic communications, semiconductors, non-linear optics, computer industries, etc. The process of crystal formation via mechanisms of crystal growth is called "crystallization". Crystal growth is related to various fields covering solid state physics, theoretical physics, chemistry, materials science, chemical engineering, metallurgy, crystallography, mineralogy, etc. Clearly, it is more difficult to prepare single crystals than polycrystalline materials, however, there are two important reasons for growing single crystals,

1. Many physical properties of solids are obscured or complicated by the effect of grain boundaries.

2. The full range of tensor relationships between applied physical cause and observed effect can be obtained only if the full internal symmetry of the crystal structure is maintained throughout the specimen (Santhanaraghavan and Ramasamy, 2000).

The single crystals growth studies in the present days are mainly focused on investigating new materials and applications of crystals for the above mentioned fields. Hence, in order to achieve high performance from the device, good quality single crystals are needed. Growth of single crystals has become inevitable for any further developments in materials research. Large size single crystals are essential for device fabrication (Pritula, Kolybayeva, Salo and Puzikov, 2007; Maunier *et al.*, 2007; Arivanandhan, Sankaranarayanan and Ramasamy, 2005) and efforts are taken to grow large crystals in short durations by fast growth techniques (Zaitseva *et al.*, 1999; Zhuang *et al.*, 2011; Nakatsuka, Fujioka, Kanabe and Fujita, 1997).

In the past few decades, there has been a growing interest in crystal growth process, particularly in view of the increasing demand of nonlinear optical (NLO) materials. The wide range of applicability of NLO single crystal is evident in the fields of semiconductors, polarizers, infrared detectors, solid state lasers, piezoelectric, acousto-optic, optical modulation, optical switching, frequency shifting, telecommunications and signal processing, and optical data storage. The growth of single crystals and their characterization towards device fabrication has assumed great motivation due to their significance in both academic research and applied research (Varjula, Ramanand and Das, 2008; Raj and Das, 2007; Anandha Babu and Ramasamy, 2009).

Investigations were initially focused on purely inorganic materials, which were the first to demonstrate second-order nonlinear optical properties. Attention was later directed towards organic materials. (Anandha babu and Ramasamy, 2010). The organic materials are being widely used for the development of optical devices, because they posses fast and large nonlinear response, low cost, over a broad

frequency range, inherent synthetic flexibility and high optical damage threshold (Hussaini, Dhumane, Rabbani, Karmuse, Dongre and Shirsat, 2007). However, organic materials are poor in thermal and chemical stability and mechanical hardness. It is difficult to grow large size, high quality single crystals Anandha babu, Perumal Ramasamy and Ramasamy, 2009). The organic additive such as thiourea has emerged a new class of promising nonlinear materials because of its superior qualities over inorganic materials, called semi–organic materials (Vijayan, Ramesh Babu, Gunasekaran, Gopalakrishana and Ramasamy, 2003).

Currently, Potassium dihydrogen phosphate (KDP) and potassium deuterium phosphate (DKDP) are widely used in nonlinear optical materials, electro–optic modulators, Q–switches, second and third harmonic generation, and high–power laser frequency conversion devices because of their good nonlinear properties, clear optical transparency, larger sizes crystal grown, high laser damage threshold and easy growth by low temperature solution growth method (Rashkovich, 1991; Javidi, Faripour, Esmaeil Nia, Sepehri and Akbari, 2008; Dhanaraj *et al.*, 2008; Balamurugan, Ramasamya, Sharmab, Inkong and Manyum, 2009).

The National Ignition Facility (NIF) at Lawrence Livermore National Laboratory (LLNL, USA) has used KDP single crystal in large–aperture laser systems (about $40 \times 40 \ \text{cm}^2$) for nuclear fusion experiments. KDP crystals were used for two functions: frequency conversion and optical switches (Goldhar and Henesian, 1986).

KDP crystal is easily grown by solution method because of its wide metastable zone and non toxic vapor. The aims of this thesis are to study growth of pure KDP single crystals and thiourea added KDP single crystals by both conventional slow evaporation and Sankaranarayanan – Ramamsamy methods. The reason for choosing

thiourea as a dopant is due to its well known optical nonlinearity (Crasta, Ravindrachary, Bhajantri and Gonsalves, 2004). The study also includes the characterization of the grown single crystals with various instruments to compare the properties both of pure and thiourea–dopped crystal and the crystals grown by both techniques.

## 1.2 Research Objectives

1.2.1 To grow pure and thiourea–doped KDP single crystals by slow evaporation method and by SR method,

1.2.2 To characterize the grown crystals with various techniques,

1.2.3 To optimize the growth conditions for thiourea doped KDP crystals with improved quality.

## 1.3 Scope and Limitations of the Study

1.3.1 Growth of pure and thiourea doped KDP single crystals by conventional and SR methods.

1.3.2 Characterization of the grown crystals by micro hardness, XRD, FTIR, UV–Vis and dielectric properties measurement.

## 1.4 Research Procedure

### 1.4.1 Growth of Single Crystals

1.4.1.1 The seed crystals of pure KDP and thiourea doped KDP are prepared by solution method.

1.4.1.2 The single crystals are grown from seed crystal by both slow evaporation and SR methods.

**1.4.2 Characterizations**

1.4.2.1 The powder XRD of pure and doped sample is used for lattice parameter evaluation.

1.4.2.2 FTIR spectrum provides the functional groups of thiourea doped KDP.

1.4.2.3 UV-Vis spectrum investigates the optical properties of the grown crystals.

1.4.2.4 Micro hardness test is used for testing the hardness of the crystal.

1.4.2.5 Dielectric constant and dielectric loss are evaluated.

## 1.5 Expected Results

1.5.1 The skill and expertise for solution growth.

1.5.2 The skill and expertise for crystal characterization.

1.5.3 The crystals with good qualities for applications.

## 1.6 References

Anandha Babu, G. and Ramasamy, P. (2009). Synthesis, crystal growth and characterization of novel semiorganic nonlinear optical crystal: dichlorobis(l–proline)zinc(II). **Materials Chemistry and Physics**. 113: 727–733.

Anandha Babu, G. and Ramasamy, P. (2010). Growth and characterization of an organic NLO material ammonium malate. **Current Applied Physics**. 10: 214–220.

Anandha babu, G., Perumal Ramasamy, R. and Ramasamy, P. (2009). Synthesis, crystal growth and characterization of an efficient nonlinear optical D–$\pi$–A type single crystal: 2–Aminopyridinium 4–nitrophenolate 4–nitrophenol. **Materials Chemistry and Physics**. 117: 326–330.

Arivanandhan, M., Sankaranarayanan, K. and Ramasamy, P. (2008). Growth of longest <1 0 0> oriented benzophenone single crystal from solution at ambient temperature. **Journal of Crystal Growth**. 310: 1493–1496.

Balamurugan, S., Bhagavannarayana, G. and Ramasamy, P. (2008). Growth of unidirectional potassium dihydrogen orthophosphate single crystal by SR method and its characterization. **Materials Letters**. 62(24): 3963–3965.

Balamurugan, S., Ramasamya, P., Sharmab, S. K., Inkong, Y. and Manyum, P. (2009). Investigation of SR method grown <001> directed KDP single crystal and its characterization by high–resolution X–ray diffractometry (HRXRD), laser damage threshold, dielectric, thermal analysis, optical and hardness studies. **Materials Chemistry and Physics**. 117: 465–470.

Crasta, V., Ravindrachary, V., Bhajantri, R. F. and Gonsalves, R. (2004). Growth and characterization of an organic NLO crystal: 1–(4–methylphenyl)–3–(4–methoxyphenyl) –2–propen–1–one. **Journal of Crystal Growth**. 267, 129–133.

Dhanaraj, P. V., Mahadevan, C. K., Bhagavannarayana. G., Ramasamy, P. and Rajesh, N. P. (2008). Growth and characterization of KDP crystals with potassium carbonate as additive. **Journal of Crystal Growth**. 310: 5341–5346.

Goldhar, J. and Henesian, M. A. (1986). Large-Aperture Electrooptical Switches with Plasma Electrodes. **IEEE Journal of Quantum Electronics**. QE–22 (7): 1137–1147.

Hussaini, S. S., Dhumane, N. R., Rabbani, G., Karmuse, P., Dongre, V. G. and Shirsat, M. D. (2007). Growth and high frequency dielectric study of pure and thiourea doped KDP crystals. **Crystal Research and Technology**. 42(11): 1110–1116.

Javidi, S., Faripour, H., Esmaeil Nia, M., Sepehri, K. F. and Ali Akbari, N. (2008). Development of a KDP crystal growth system based on TRM and characterization of the grown crystals. **Semiconductor Physics, Quantum Electronics & Optoelectronics**. 11(3): 248–251.

Jonie Varjula, A., Ramanand, A. and Jerome Das, S. (2008). Growth, thermal and mechanical properties of new nonlinear optical barium bis–paranitrophenolate paranitrophenol tetrahydrate single crystal**. Materials Research Bulletin**. 43: 431–436.

Justin Raj, C. and Jerome Das, S. (2007). Growth and characterization of nonlinear optical active L–alanine formate crystal by modified Sankaranarayanan–Ramasamy (SR) method. **Journal of Crystal Growth**. 304: 191–195.

Maunier, C., Bouchut, P., Bouillet, S., Cabane, H., Courchinoux, R., Defossez, P., Poncetta, J. C. and Ferriou-Daurios, N. (2007). Growth and characterization of large KDP crystals for high power lasers. **Optical Materials**. 30: 88–90.

Nakatsuka, M., Fujioka, K., Kanabe, T. and Fujita, H. (1997). Rapid growth over 50 mm/day of water-soluble KDP crystal. **Journal of Crystal Growth**. 171: 531–537.

Pritula, I. M., Kolybayeva, M. I., Salo, V. I. and V. M. Puzikov. (2007). Defects of large–size KDP single crystals and their influence on degradation of the optical properties. **Optical Materials**. 30: 98–100.

Rashkovich, L. N. (1991). **KDP – Family Single Crystals**. New York: Adam Hilger.

Santhanaraghavan, P. and Ramasamy, P. (2000). **Crystal Growth Processes and Methods**. Kumbakonam, India: KRU publications.

Vijayan, N., Ramesh Babu, R., Gunasekaran, M., Gopalakrishana, R. and Ramasamy, P. (2003). Growth, optical, thermal and mechanical studies of methyl 4 – hydroxybenzoate single crystals. **Journal of Crystal Growth**. 256: 174–182.

Zaitseva, N., Atherton, J., Rozsa, R., Carman, L., Smolsky, I., Runkel, M., Ryon, R. and James, L. (1999). Design and benefits of continuous filtration in rapid growth of large KDP and DKDP crystals. **Journal of Crystal Growth**. 197: 911–920.

Zaitseva, N., Carmana, L. and Smolskyb, I. (2002). Habit control during rapid growth of KDP and DKDP crystals. **Journal of Crystal Growth**. 241: 363–373.

Zhuang, X., Ye, L., Zheng, G., Su, G., He, Y., Lin, X. and Xu, Z. (2011). The rapid growth of large–scale KDP single crystal in brief procedure. **Journal of Crystal Growth**. 318(1): 700–702.

# CHAPTER II

# REVIEW OF THE LITERATURE

## 2.1 Review of the Literature

Nonlinear optical materials (NLO) have a nonlinear response to the electric field associated with the light of a laser beam, leading to a variety of optical phenomena such as the generation of new light frequencies or the alteration of the material's optical properties. This nonlinearity is typically only observed at very high electric field strength (about $10^8$ V/m) such as those provided by pulsed lasers. This is the reason why the first nonlinear phenomena (Second harmonic generation, SHG) was discovered by P. A. Franken and co-workers at the University of Michigan, Ann Arbor, in 1961, shortly after the demonstration of the first working laser by Maimann in 1960 (Boyd, 2003; He and Liu, 1999).

Potassium dihydrogen phosphate (KDP) is currently used widely in nonlinear optical materials. Many research groups are making effort to improve KDP single crystal, either properties or crystal growth processes. Impurity ions of bivalent metal ($Ni^{2+}$, $Co^{2+}$, $Fe^{2+}$, $Mn^{2+}$, $Ba^{2+}$, $Ca^{2+}$, $Sr^{2+}$) and trivalent metal ($Fe^{3+}$, $Mn^{3+}$, $Y^{3+}$, $La^{3+}$) doped KDP crystal, have resulted in an increase in the crystal growth rate and optical transparency of doped crystals have increased as compared to that of pure KDP crystals (Miroslawa Raka $et\ al.$, 2005; Eremina $et\ al.$, 2005; Rashkovich and Kronsky, 1997). The hardness of KDP is increased with $Mn^{2+}$ doping (Riscob, Shakir, Vijayan, Ganesh and Bhagavannarayana, 2012) but the hardness value of

$La^{3+}$ added KDP is lower than the pure KDP (Kannan, Bairava Ganesh, Sathyalakshmi, Rajesh and Ramasamy 2006; Javidi, Esmaeil Nia, Aliakbari and Taheri, 2008).

Optical transmission of pyramidal and prismatic faces of KDP crystal grown by conventional method was studied by Fujioka, Matsuo, Kanabe, Fujita and Nakatsuka (1997). The absorption coefficient of pyramidal face was 0.02 cm$^{-1}$ at wavelength of 285 nm. For the rapidly grown crystal, the absorption coefficient of pyramidal sector at 285 nm was 0.05 cm$^{-1}$ and that of prismatic sector was 0.94 cm$^{-1}$. After thermal conditioning the laser damage threshold was 15.6 J/cm$^2$ in the pyramidal face and 19.6 J/cm$^2$ in the prismatic face. Optical transmission of KDP doped with 1 wt% of organic reagent sulfosalicylic acid (SSA) (Li, Su, Zhuang, Li, and He, 2004), in the ultraviolet (UV) region, is higher than the KDP crystal grown from pure solution by conventional method. The damage threshold of KDP crystal from SSA-added solution was 9.45 J/cm$^2$ and reached to 14.9 J/cm$^2$ (1.06 μm, 1 ns). They concluded that the laser damage thresholds are nearly the same for pure and SSA–doped samples, and the addition of small quantity of SSA in their experiment does not affect crystal quality in any way.

The hardness value of pure KDP crystal and organic additives (urea, thiourea and ethylene diamine tetra acetic acid, EDTA) added KDP have been studied by Rajesh *et al*. (2002). They added 2 mol% of the additives and growth run was carried out between the temperature of 45 and 35°C with the cooling rates of 0.1 to 0.8 °C/day. The results of microhardness test of the crystals are shown in Figure 2.1. The hardness value of KDP crystal is found to increase with organic additives of urea, thiourea and EDTA, respectively.
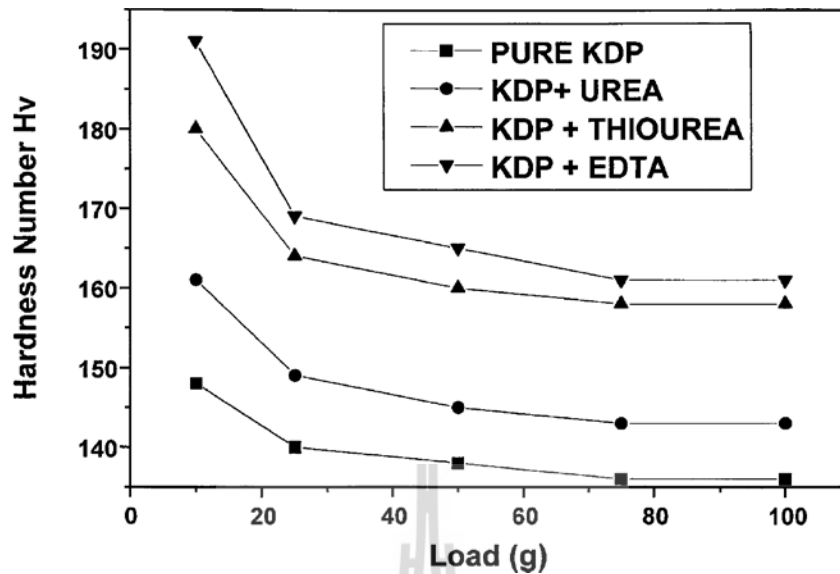
**Figure 2.1** Variation of microhardness with indenter load for Pure KDP, KDP with

urea, KDP with thiourea, and KDP with EDTA (Rajesh *et al.*, 2002).

The SHG efficiency of pure and L–arginine doped KDP were studied by using a Q–switched, mode-locked Nd : YAG laser which generated about 2.7 mJ/pulse at 1064 nm (Parikh, Dave, Parekh and Joshi, 2007). The intensity of the second harmonic output pulses with 532 nm from different samples were measured. They found that the second harmonic signal strength and the second harmonic generation efficiency increases as the doping concentration of L–arginine was increase. Second harmonic signal output of Pure KDP, KDP + 0.3% L–arginine and KDP + 0.4% L–arginine are 405, 540 and 705 mV, respectively.

Hussani *et al.* (2007), studied pure and 2 mol% thiourea doped KDP crystal. They used laser with wavelength of 1064 nm from Q switched Nd: YAG laser to studied nonlinear optical property. The output power of 2 mol% thiourea doped KDP crystal was found as 553 mV, which is 1.99 times higher than pure KDP, while for higher concentration of thiourea doping in KDP, there was found an enhancement in

SHG property. This indicates that the SHG efficiency of thiourea doped KDP crystal is higher than that of pure KDP. This is due to the fact that the sulfur present in thiourea, which is more electro negative. This causes more delocalization of electrons in the case of thiourea doped KDP crystals.  For high frequency dielectric study using transmission line wave–guide method in X–band and at microwave frequencies of 8 and 12 GHz at room temperature, the dielectric constant decrease as frequency increase.

## 2.2 Methods of Crystal Growth

A single crystal is defined by long-range atomic order extending over many atomic diameters, and having a repetitive structure. As a result, crystals have rigidity, fixed shape, and mechanical strength (Encyclopedia of Materials: Science and Technology, 2001). Growth of crystal process and crystallization time ranges from minutes, hours, days and to months. Single crystals should be produced by the transport of crystal constituents in the solid, liquid or vapor phase. Then crystal growth could be classified into three methods as follows,

1. Growth from solid or solid growth.

2. Growth from solution or solution growth or melt growth.

3. Growth from vapor or vapor growth.

This thesis deals with the growth of crystals from aqueous solution. Hence, in the following sections, the solution growth technique has been discussed in detail.

## 2.3 Solution Growth

A solution is a homogeneous mixture of two or more substances. Homogeneous means that the components of the mixture form a single phase. A solute is a substance dissolved in another substance, known as a solvent. The concentration of a solute in a solution is a measure of how much of that solute is dissolved in the solvent. A saturated solution is in thermodynamic equilibrium with the solid phase at a specified temperature. The solutions containing more dissolved solid than that represented by equilibrium saturation are called supersaturated. This state is an essential requirement for all crystallization conditions.

Growth of crystals from aqueous solutions is the crystallization of substances from supersaturated solutions in suitable condition. The used solvents are water, organic liquids and their mixtures, and melts of some chemical compounds. Based on the growth temperature, solution growth can be divided in to two techniques :

1. Low temperature solution growth.
2. High temperature solution growth.

In crystallization from low temperature solutions, the growth temperatures usually do not exceed 70 - 80°C and in growth from high temperature solutions, the growth temperatures generally do not exceed 1200 - 1300°C. However, in both low and high temperature growths, the highest possible growth temperature is the boiling point of the solvent used (Encyclopedia of Materials: Science and Technology, 2001). In this thesis, only low temperature solution growth is presented.

## 2.4 Low Temperature Solution Growth

The mechanism of crystallization from solutions is governed by the interaction of ions or molecules of the solute and the solvent which is based on the solubility of substance on the thermodynamical parameters process; temperature, pressure and solvent concentration (Chernov, 1989). The advantage of low temperature solution is that the growth apparatus is relatively simple and cheap which gives a good degree of control of accuracy of $\pm 0.01^{\circ}\text{C}$. Due to the precise temperature control, supersaturation can be very accurately controlled and low growth temperature introduces small thermal stresses and reduces the possibility of major thermal shock to the crystal both during growth and removal from the apparatus. Water is the solvent in about 90% of the crystals produced by low temperature solution method. Rates of growth from solution are in the range of 0.1 to 1 mm/day. The disadvantages are the slow growth rate and the solvent inclusion into the growing crystal. After many studies of several research groups about the processes of solution growth, now give good quality crystals for applications (Zaitseva and Carman, 2001; Ramesh Babu *et al.*, 2006).

The method of crystal growth from low temperature solutions is widely used for the growth of many important crystals, when the materials are unstable at high temperatures and also when there is phase transformation below melting point. The growth duration time involves weeks, months and sometimes years. Though the grown crystal has been well perfected, it involves meticulous work, much patience and even a little amount of luck. A failure or a contaminated raw material can destroy months of work (Santhanaraghavan and Ramasamy, 2000).

## 2.5 Nucleation

Nucleation is an important phenomenon in crystal growth and is the precursor of the overall crystallization process. Nucleation is the process of formation of very small particles, or nuclei, of the substance in solutions, which are capable of continuously growing into crystals. Nucleation may occur spontaneously or it may be induced by other particles (dust, impurity, etc.) and they are usually referred to as homogeneous and heterogeneous nucleation respectively. These are called primary nucleation. If nucleation was induced by the presence of a crystal, it's referred to as secondary nucleation. Hence, the nucleation process can be expressed by the following:

Nucleation

 — Primary nucleation
   — Homogeneous : spontaneously
   — Heterogeneous : induced by other particles
 — Secondary nucleation : induced by seed crystal
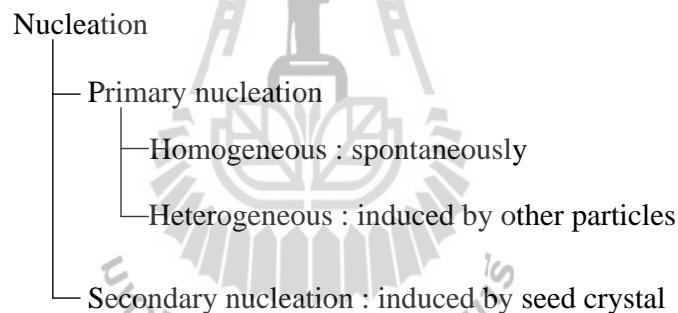
Growth of crystals from solutions can occur if some degree of supersaturation or supercooling has been achieved first in the system. There are three steps involved in the crystallization process (Santhanaraghavan and Ramasamy, 2000).

  1. achievement of supersaturation or supercooling.

  2. formation of crystal nuclei.

  3. successive growth of crystals to get distinct faces.

.

## 2.6 Expression of Supersaturation

Crystal growth from low temperature solutions must occur only in the metastable zone with a desired supersaturation ($\sigma$). The growth rate increases with the maximum value of supersaturation. Supersaturation is determined by the width of the metastable zone. The relations of concentration driving force ($\Delta C$), the supersaturation ratio (S) and relative supersaturation ($\sigma$) are as follows:

The concentration driving force 
$$\Delta C = C - C_0 \tag{2.1}$$

where $C$ is the actual concentration of the solution at a given temperature, $T$ and $C_0$ is the equilibrium concentration at a given temperature, $T$.

Supersaturation ratio 
$$S = \frac{C}{C_0} \tag{2.2}$$

Relative supersaturation 
$$\sigma = \frac{C - C_0}{C_0} \tag{2.3}$$

$$\sigma = S - 1 \tag{2.4}$$

If the concentration of a solution can be measured at a given temperature and the corresponding equilibrium saturation concentration is known, then it is easier to calculate the relative supersaturation. The solubility diagram is given in Figure 2.2.
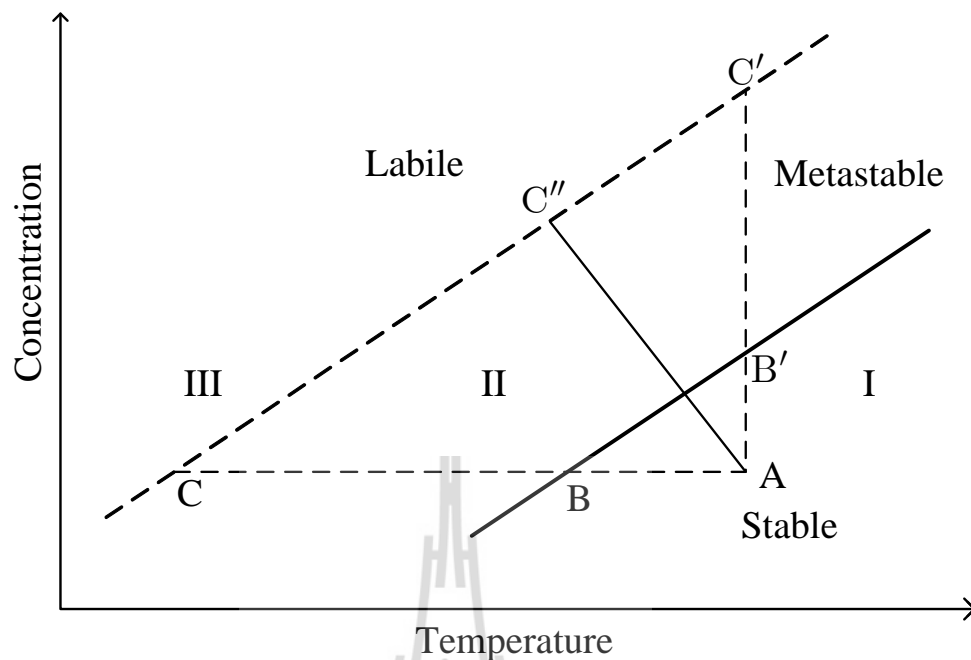
**Figure 2.2** Solubility Diagram (Santhanaraghavan and Ramasamy, 2000).

The solid line is the normal solubility curve of solution. It is separated into two regions, unsaturated (below solid line, region I, called stable zone) and supersaturated solutions (above solid line, region II called metastable zone and III, called labile zone). Crystals can be grown only from supersaturated solutions. Numerous nucleations can occur spontaneously in the labile zone. Metastable zone refers to the level of supersaturation where spontaneous nucleation cannot occur and a seed crystal is essential to facilitate growth. Normally, the word "crystal growth" means a crystallization process by the seed crystal.

1. The stable (undersaturated) zone, where crystallization is not possible.

2. The metastable zone, between the solubility and supersolubility curves, where spontaneous crystallization is impossible. Only if a seed crystal is placed in such a region, growth process would occur.

3. The unstable or labile (supersaturation) zone, where spontaneous crystallization is uncontrolled.

## 2.7 Supersaturation Achievement Technique

In low temperature solution growth, crystals can be grown if the solution is maintained in supersaturated condition. Three principal methods are used to achieve the required supersaturation:

1. Slow cooling method.

2. Slow evaporation method.

3. The temperature gradient method.

### 2.7.1 Slow Cooling Method

Crystal growth by slow cooling method is commonly used for producing small specimens for research purposes and this method gives good quality crystals. The apparatus for this method is simple (a water bath, a solution container and a temperature controller), only temperature was controlled to control the solution supersaturation. In the beginning, (see solubility diagram in Figure 2.2), if a seed crystal is at point A, at this point crystallization process is not achieved. when temperature decreases from point A to B, the crystallization process is initiated when the solution temperature reaches to point B and concentration in supersaturated. The growing seed always remains in the metastable zone, between point B and C. Since the volume of the crystal is finite and the amount of the substance placed in it is limited, the supersaturation requires systematic cooling. The temperature range at which such crystallization usually occurs is within 45 to 75 °C and the lower limit of cooling is the room temperature.

### 2.7.2 Slow Evaporation Method

This method is similar to the slow cooling method in view of the apparatus requirements. The temperature is fixed constant and provision is made for the evaporation of the solvent. Then, the growth rate is controlled by controlling the evaporation rate. In almost all cases, the vapor pressure of the solvent above the solution is higher than the vapor pressure of the solute. Therefore the solvent evaporates more rapidly and the solution becomes supersaturated (Petrov, 1969). In the solubility diagram (Figure 2.2), supersaturation is along the part $A \rightarrow B' \rightarrow C'$. With non-toxic solvents like water, it is permissible to allow evaporation into the atmosphere. Typical growth conditions involve temperature stabilization to about $\pm 0.01^{\circ}C$ and rates of evaporation of a few $mm^3 / hr$. This method can be used with materials, which have very small temperature coefficient of stability.

### 2.7.3 Temperature Gradient Method

This method involves the transport of the materials from a hot region to a cooler region where the solution is supersaturated and the crystal grows. The material transport is ensured by gravitational, thermal, or forced convection. The main advantages of this method are:

1. Crystal grows at a fixed temperature.

2. This method is insensitive to changes in temperature provided both the source and the growing crystal undergo the same change.

3. Economy of solvent and solute.

On the other hand, changes in the small temperature differences between the source and the crystal zones have a large effect on the growth rate (Santhanaraghavan and Ramasamy, 2000).

Excellent quality crystals of nonlinear optic materials such as Ammonium dihydrogen phosphate (ADP), Potassium dihydrogen phosphate (KDP) and Triglycine sulphate (TGS) are commercially grown for use in devices by the low temperature solution growth method.

## 2.8 Solution Growth by Sankaranarayanan – Ramasamy  Method

In the year 2005, the novel method of solution growth called Sankaranarayanan – Ramasamy (SR) method was reported (Sankaranarayanan and Ramasamy, 2005). The schematic diagram of the experimental set up is shown in Figure 2.3. The equipment consists of a growth ampoule made out of glass with seed mounting pad at the bottom. An outer glass shield tube protects and holds the inner growth ampoule. A ring heater positioned at the top of the growth ampoule is connected to the temperature controller and it provides the necessary temperature for solvent evaporation. The temperature around the growth ampoule is selected based on the solvent used and is controlled with the aid of the temperature controller. The rate of growth of crystal depends on the rate of solvent evaporation (Sankaranarayanan and Ramasamy, 2005). The advantages of SR method are the growth of single crystals with specific orientation (or unidirectional) and i) the achievement of solute-crystal conversion efficiency of 100%, and ii) reduction of the preparation and maintenance of growth solution. In conventional solution growth method, to grow a large size crystal, a large amount of solution in a large container is necessarily used and only a small fraction of the solute is converted to a bulk crystal. For the SR method, the size of the ampoule is the size of grown crystal (Balamurugan, Lenin, Bhagavannarayana and Ramasamy, 2007).
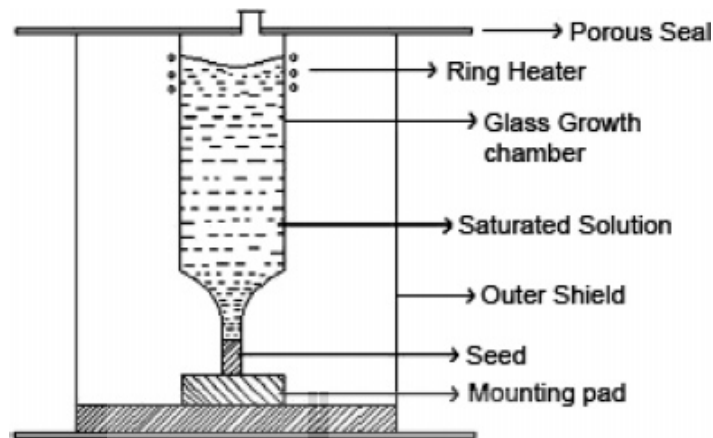
**Figure 2.3** Schematic diagram of the SR method experimental setup

(Sankaranarayanan and Ramasamy, 2005).

## 2.9 Nonlinear Optics

Nonlinear optics (NLO) describes the behavior of light in nonlinear media, in which the dielectric polarization (the dipole moment per unit volume) $\vec{P}(t)$ at time t responds nonlinearly to the electric field $\vec{E}$ of the light. NLO is a very useful technology in the area of laser technology, optical communication and data storage technology. NLO is a completely new effect in which light of one wavelength is transformed to light of another wavelength.

In order to describe nonlinear effects by considering the relationship between polarization $\vec{P}(t)$ with electric field $\vec{E}$ , in the case of conventional linear optics,

$$\vec{P}(t) = \varepsilon_0 \chi^{(1)} \vec{E} \qquad (2.5)$$

where $\chi^{(1)}$ is the linear susceptibility and $\varepsilon_0$ is the permittivity of free space $(\varepsilon_0 = 8.8542 \times 10^{-12}$ F / m$)$. In nonlinear response, with very high electric field, the polarization can be expressed as a power series:

$$\vec{P}(t) = \varepsilon_0 \left[ \chi^{(1)}\vec{E}(t) + \chi^{(2)}\vec{E}^2(t) + \chi^{(3)}\vec{E}^3(t) + ..... \right]$$

$$= \varepsilon_0\chi^{(1)}\vec{E}(t) + \varepsilon_0\chi^{(2)}\vec{E}^2(t) + \varepsilon_0\chi^{(3)}\vec{E}^3(t) + .....$$

$$= \vec{P}^{(1)}(t) + \vec{P}^{(2)}(t) + \vec{P}^{(3)}(t) + ..... \tag{2.6}$$

where $\chi^{(2)}$ and $\chi^{(3)}$ are the second and third order nonlinear susceptibilities, respectively. The terms $\vec{P}^{(1)}(t)$, $\vec{P}^{(2)}(t)$ and $\vec{P}^{(3)}(t)$ are the first, second and third order nonlinear polarizations, respectively.

For example, in condensed matter, the calculation for $\chi^{(1)}$ is of the order of unity, and $\chi^{(2)} \simeq 1.94 \times 10^{-12}$ m / V and $\chi^{(3)} \simeq 3.78 \times 10^{-24}$ m$^2$ / V$^2$. By comparing these values with actual measured values $\chi^{(2)}$ and $\chi^{(3)}$ are very small, hence, high electric fields like laser can reveal nonlinear properties.

$\chi^{(1)}$ is the linear term responsible for material's linear optical properties like, refractive index, dispersion, birefringence and absorption.

$\chi^{(2)}$ is the quadratic term which describes second harmonic generation in noncentro-symmetric materials.

$\chi^{(3)}$ is the cubic term responsible for third harmonic generation, stimulated Raman scattering, phase conjugation and optical bi-stability. (Boyd, 2003)

## 2.10 Second Harmonic Generation

Second harmonic generation is the first nonlinear optical phenomenon after the discovery of the laser. P. A. Franken and coworkers focused a pulsed ruby laser with a wavelength of 694 nm into a quartz crystal and found that light at twice of the laser frequency (at 347 nm) was generated. Figure 2.4 shows the experiment of Franken (Franken *et al.*, 1961).
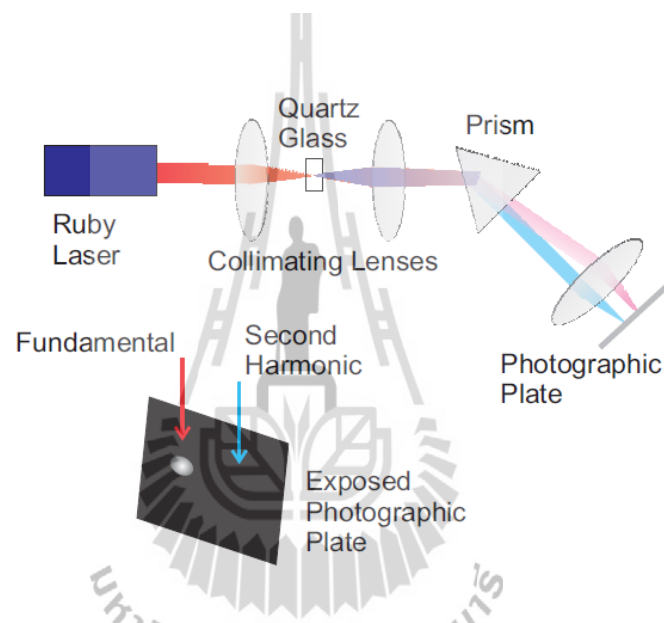


**Figure 2.4** The experiment used by Franken and coworkers to demonstrate second harmonic generation (Kuzyk, 2010).

A prism was used to separate the fundamental from the second harmonic, and the two beams were recorded on photographic film. The film's appearance is shown in the inset of Figure 1.4. Since the second harmonic signal is weak, the spot on the film appeared as a tiny spec. So, in the original paper, an arrow points to the location of the second harmonic spot, but the tiny spot is not visible. (Kuzyk, 2010).

In most crystalline materials, the nonlinear susceptibility $\chi^{(2)}$ depends on the direction of propagation, polarization of the electric field and the orientation of the

optic axis of the crystal. From equation (2.6), the second order nonlinear polarizations term is $\vec{P}^{(2)}(t) = \varepsilon_0 \chi^{(2)} \vec{E}^2$. Here a laser beam is incident toward a crystal for which the second-order susceptibility $\chi^{(2)}$ is nonzero. The electric field of laser light is represented as

$$\vec{E}(t) = E e^{-i\omega t} + c.c. \tag{2.7}$$

(*c.c.* stands for complex conjugate.)

Then, the second order nonlinear polarization $\vec{P}^{(2)}(t)$ becomes

$$\vec{P}^{(2)}(t) = 2\varepsilon_0 \chi^{(2)} E E^* + \varepsilon_0 \chi^{(2)} E e^{-i(2\omega)t} + c.c. \tag{2.8}$$

In equation (2.8) the second order polarization $\vec{P}^{(2)}(t)$ consists of a zero frequency (the first term) and a contribution at frequency $2\omega$ (the second term). This means that the contribution can lead to the generation of radiation at the double frequency (second harmonic frequency).

Under proper experimental conditions, the process of second harmonic generation can be so efficient that nearly all of the power in the incident beam at frequency $\omega$ is converted to the second harmonic frequency $2\omega$. For example, the Nd:YAG laser operates in the near infrared at a wavelength of 1,060 nm. Second harmonic generation media is routinely used to convert to the wavelength of 530 nm, in the middle of the visible spectrum (Boyd, 2003). Figure 2.5 illustrates configurations for optical second harmonic generation in materials.
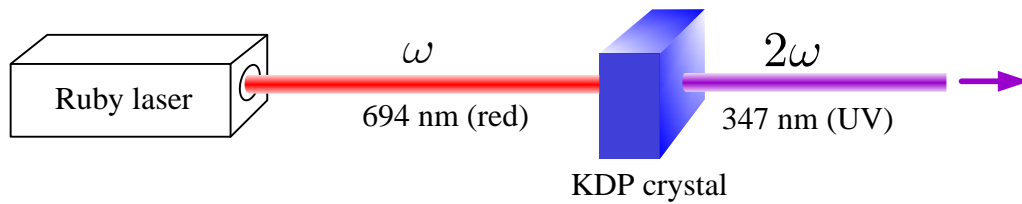
**Figure 2.5** Optical second-harmonic generation in nonlinear medium (Adopted

from: Bloembergen : http://www.coqus.at/fileadmin/quantum/coqus/

documents/Bahaa_Saleh/CH21–Nonlinear–Optics.pdf).

Second harmonic generation can consider the interaction in terms of the

exchange of photons between the various frequency components of the field.

According to the picture illustrated in part (b) of Figure 2.6, two photons of frequency

$\omega$ are destroyed, and a photon of frequency $2\omega$ is simultaneously created. The solid

line in the figure represents the atomic ground state, and the dashed lines represent the

virtual levels. These levels are not energy of the free atom but rather represent the

combined energy of one of the energy of the atom and of one or more photons of the

radiation field.
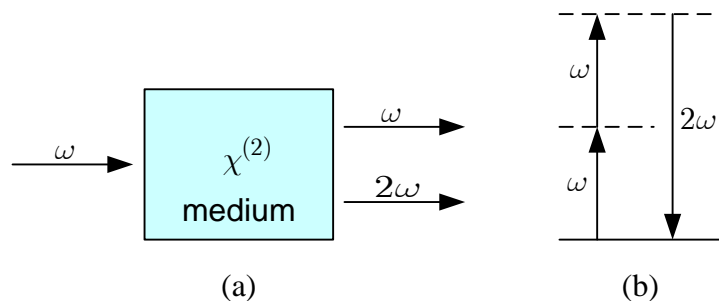


**Figure 2.6** (a) Geometry of second–harmonic generation. (b) Energy–level diagram

describing second–harmonic generation (Adopted from : Boyd, 2003).

The electric field made up of two frequencies $\omega_1$ and $\omega_2$ which propagates through a nonlinear medium is represented as

$$\vec{E}(t) = E_1 e^{-i\omega_1 t} + E_2 e^{-i\omega_2 t} + c.c. \tag{2.9}$$

The expression of $\vec{P}^{(2)}(t)$ is given by

$$\vec{P}^{(2)}(t) = \varepsilon_0 \chi^{(2)} \Big[ E_1^2 e^{-i(2\omega_1)t} + E_2^2 e^{-i(2\omega_2)t}$$
$$+ 2E_1 E_2 e^{-i(\omega_1 + \omega_2)t}$$
$$+ 2E_1 E_2^* e^{-i(\omega_1 - \omega_2)t}$$
$$+ 2(E_1^2 + E_2^2)e^0 + c.c. \Big] \tag{2.10}$$

Thus the medium exhibits second order linearity. The second-order susceptibility gives rise to several different nonlinear optical phenomenas. The complex amplitudes of the various frequency components of the nonlinear polarization are labeled each expressed by the name of the physical process that $2\omega_1$ and $2\omega_2$ as second harmonic generation (SHG), $\omega_3 = \omega_1 + \omega_2$ as sum frequency generation (SFG) see Figure 2.7, $\omega_3 = \omega_1 - \omega_2$ as difference – frequency generation (DFG) see Figure 2.8, and $\omega = 0$ as optical rectification (OR).

Optical rectification is a steady (non–time–varying) polarization density that creates a DC potential difference across the plates of a capacitor within which the nonlinear material is placed (Figure 2.9). The generation of a DC voltage as a result of an intense optical field represents optical rectification.
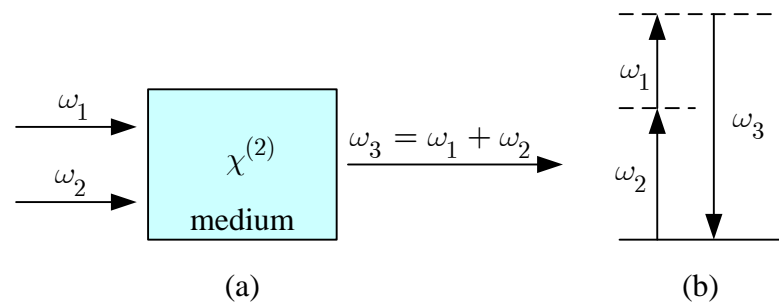
**Figure 2.7** Sum-frequency generation. (a) Geometry of second-harmonic generation.

(b) Energy-level diagram (Adopted from : Boyd, 2003).
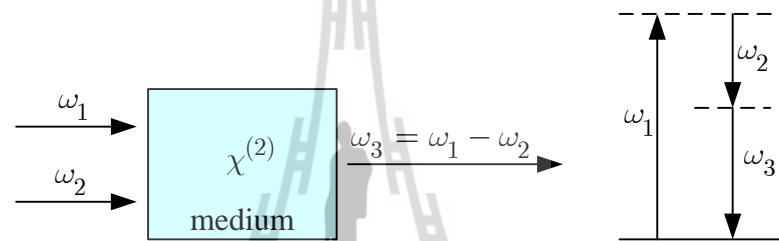


**Figure 2.8** Difference-frequency generation. (a) Geometry of second-harmonic

generation. (b) Energy-level diagram (adopted from : Boyd, 2003).
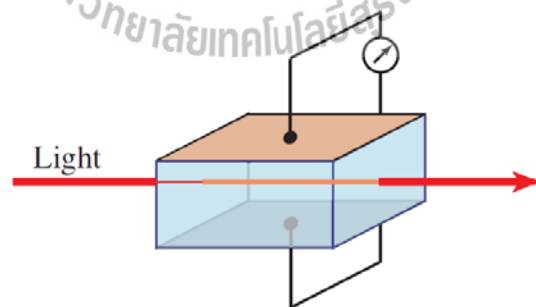


**Figure 2.9** Optical rectification the transmission of an intense beam of light through a

nonlinear crystal generates a DC voltage across it. (Bloembergen :

http://www.coqus.at/fileadmin/quantum/coqus/documents/Bahaa_Saleh/

CH21–Nonlinear–Optics.pdf).

## 2.11 Potassium Dihydrogen Phosphate Crystal

Potassium dihydrogen phosphate (KDP, $KH_2PO_4$) or monopotassium phosphate or monobasic potassium phosphate and its isomorphs are representative of hydrogen bonded (Figure 2.10) systems which have extremely interesting properties like piezoelectric, ferroelectric, electro-optic and nonlinear optical properties (Santhanaraghavan and Ramasamy, 2000; Xu, Xue and Henryk Ratajczak, 2005; Hussaini, Dhumanel, Rabbani, Karmuse, Dongre and Shirsat, 2007). They have attracted the interests of many theoretical and experimental researches, probably because of their comparatively simple structure and very fascinating properties associated with hydrogen bond system involving large isotope effect and easily grown by solution as good quality crystals.

A crystallochemical analogue of KDP, ammonium dihydrogen phosphate (ADP, $NH_4H_2PO_4$) has also found fairly wide practical applications and is used as a piezoelectric transducer in microphones, gramophones and other sound reproduction devices. They were very first materials to be used and exploited for their nonlinear optical and electro-optical properties, are still used widely in nonlinear optical devices and continue to be popular as electro-optic materials.

$$K^+O^- - P - OH$$
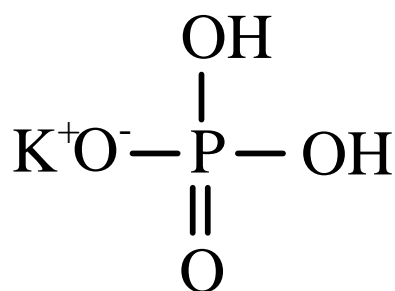
**Figure 2.10** Structure formula of KDP crystal.
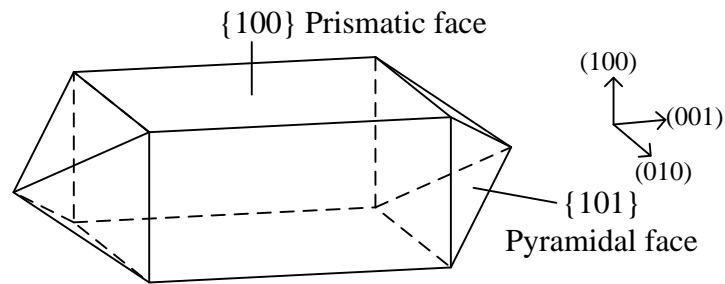
**Figure 2.11** Prismatic face and pyramidal face of KDP crystal.

The morphology of KDP crystal has prismatic faces with pyramidal ends as shown in Figure 2.11. Usually, KDP crystal grows faster along the "c" direction (pyramidal) compared to "a" and "b" (prismatic) directions at normal pH (Santhanaraghavan and Ramasamy, 2000). The structure of KDP belongs to tetragonal system with the class $\overline{4}2m$. It has molecular mass of 136.086 g and specific gravity: 2.3325 $g/cm^3$. The unit cell dimensions are $a = b = 7.448$ $\overset{\circ}{A}$ and $c = 6.977$ $\overset{\circ}{A}$. Vickers hardness is $122 \pm 17$ along a–direction and $183 \pm 12$ along c–direction (Nikogosyan, 2005). There are four formula units per cell. The structure is most easily pictured as built up from potassium atoms and phosphate groups as shown in Figure 2.12.

The structure of KDP consists of two interpenetrating body–centered lattices of $PO_4$ tetrahedra and two interpenetrating body–centered K lattices, the phosphate and potassium lattices being separated along the c–axis. Every $PO_4$ is linked to four other $PO_4$ groups by hydrogen bonds, which lie very nearly perpendicular to the

ferroelectric c-axis. The linkage is such that there is a hydrogen bond between the upper oxygen of one $PO_4$ groups and lower oxygen of a neighboring group. As revealed by the neutron studies, only two hydrogen atoms are normally located nearest in any $PO_4$ group, giving rise to a formal ionic configuration $K^+$ $(H_2PO_4^-)$. KDP has a phase transition to ferroelectric from its paraelectric state at 123 K.
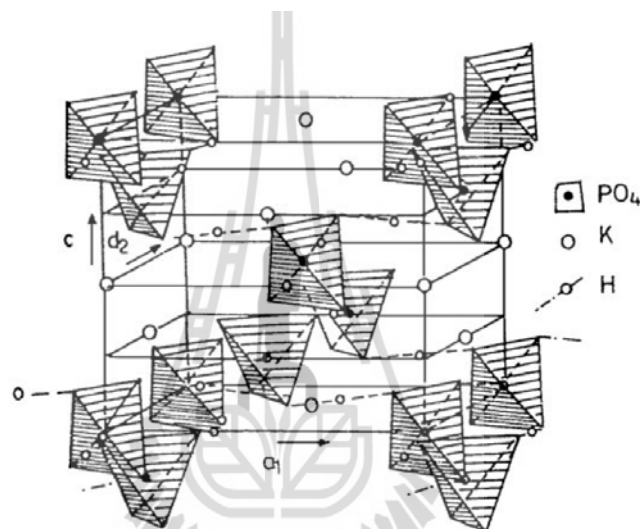


**Figure 2.12** The structure of KDP (Encyclopedia of Materials, 2001).

## 2.12 References

Boyd, R. W. (2003). **Nonlinear Optics**. 2$^{nd}$ Ed.  San diago: Acadamic press.

Chernov, A. A. (1989). Formation of crystals in solutions. **Contemporary Physics**. 30 : 251.

Eremina, T. A., Kuznetsov, V. A., Eremin, N. N., Okhrimenko, T. M., Furmanova, N. G., Efremova, E.P.and Mirosława Rak. (2005). On the mechanism of impurity influence on growth kinetics and surface morphology of KDP crystals–II : experimental study of influence of bivalent and trivalent impurity ions on

growth kinetics and surface morphology of KDP crystals. **Journal of Crystal Growth**. 273: 586–593.

Franken, P. A., Hill, A. E., Peters, C. W., and Weinreich, G. (1961). Generation of Optical Harmonics. **Physical Review Letters**. 7: 118–119.

Fujioka, K., Matsuo, S., Kanabe, T., Fujita, H. and Nakatsuka, H. (1997). Optical properties of rapidly grown KDP crystal improved by thermal conditioning. **Journal of Crystal Growth**. 181: 265–271.

HE, G. S. and Liu, S. H. (1999). **Physics of Nonlinear Optics**. Singapore: World Scientific.

Hussaini, S. S., Dhumane1, N. R., Rabbani, G., Karmuse, P., Dongre, V. G. and Shirsat, M. D. (2007). Growth and high frequency dielectric study of pure and thiourea doped KDP crystals. **Crystal Research and Technology**. 42(11): 1110–1116.

Javidi, S., Esmaeil Nia, M., Aliakbari, N. and Taheri, F. (2008). Effect of La3+ ions on the habit of KDP crystals Semiconductor Physics. **Quantum Electronics & Optoelectronics**. 11(4): 342–344.

Kannan1, V., Bairava Ganesh1, R., Sathyalakshmi1, R., Rajesh N. P. and Ramasamy, P. (2006). Influence of $La^{3+}$ ions on growth and NLO properties of KDP single crystals. **Crystal Research and Technology**. 41(7): 678–682.

Kuzyk, M. G. (2010). **Nonlinear Optics**. [On-line] (Available: http://www. NLOsource.com.)

Li, G., Su, G., Zhuang, X., Li, Z., and He, Y. (2004). Rapid growth of KDP crystal with new additive. **Journal of Crystal Growth.** 269: 443–447

Nikogosyan, D. N. (2005) **Nonlinear Optical Crystals: A Complete Survey**. New York: Springer.

Parikh, K. D., Dave, D. J., Parekh, B. B., and Joshi, M. J. (2007). Thermal, FT–IR and SHG efficiency studies of L–arginine doped KDP crystals. **Bulletin of Materials Science**. 30 (2):105–112.

Patel, A. R. and Arora, S. K. (1976).  Growth of strontium tartrate tetrahydrate single crystals in silica gels.  **Journal of Materials Science**. 11(5): 843.

Rajesh, N. P., Kannan, V., Santhana Raghavan, P., Ramasamy, P. and  Lan, C. W. (2002). Optical and microhardness studies of KDP crystals grown from aqueous solutions with organic additives. **Materials Letters**. 52: 326–328.

Ramesh Babu, R., Sethuramana, K., Gopalakrishnan, R. and Ramasamy, P. (2006) Growth of L–lysine monohydrochloride dihydrate bulk single crystal by Sankaranarayanan – Ramasamy (SR) method.  **Journal of Crystal Growth**. 297: 356–360.

Rashkovich,  L. N. and  Kronsky, N. V. (1997). Influence of $Fe^{3+}$ and $Al^{3+}$ ions on the kinetics of steps on the $\{1\ 0\ 0\}$ faces of KDP. **Journal of Crystal Growth**. 182: 434–441.

Riscob, B., Shakir, M., Vijayan, N., Ganesh, V. and Bhagavannarayana, G. (2012). Effect of Mn(II) doping on crystalline perfection, nonlinear, optical and mechanical properties of KDP single crystals. **Applied Physics A**. 107: 477–484**.**

Sankaranarayanan, K. and Ramasamy, P. (2005). Unidirectional seeded single crystal growth from solution of benzophenone. **Journal of Crystal Growth**. 280: 467–473.

Santhanaraghavan, P. and Ramasamy, P. (2000). **Crystal Growth Processes and Methods.** Kumbakonam, India: KRU publications.

Verbiest, T., Clays, K. and Rodriguez, V. (2009). **Second–Order Nonlinear Optical Characterization Techniques : An Introduction.** New York: CRC Press**.**

Xu, D., Xue, D. and Henryk Ratajczak, H. (2005). Morphology and structure studies of KDP and ADP crystallites in the water and ethanol solutions. **Journal of Molecular Structure**. 740: 37–45.

Zaitseva, N. and Carman, L. (2001). Rapid Growth of KDP–type Crystals. **Crystals Progress in Crystal Growth and Characterization Materials**. 1–118.

Zheltikov, A., L'Huillier, A. and Ferenc Krausz, F. (2007). **Springer Handbook of Lasers and Optics**. Springer.

# CHAPTER III

# EXPERIMENTAL TECHNIQUES

# FOR CHARACTERIZATIONS

## 3.1 Introduction

An introduction of the various characterization techniques used in this present work has been discussed in this chapter. Powder X–ray diffractometer has been used to study the structure of the grown crystals. The infrared (IR) spectroscopy is a widely used technique for investigating chemical compounds of the interested material. The UV–Vis spectrum gives the optical transmittance and absorption of the grown crystals. The Vicker's hardness measurement is used for investigating the mechanical behaviors of the grown crystals. The dielectric study which is measurement of dielectric properties of the crystals is also discussed.

## 3.2 X–Ray Powder Diffractometer

X–ray powder diffraction is a powerful analytical tool that is widely used in material science, chemistry, mineral science and also in many industries. The molecular structures, lattice parameters, size and shape of the unit cell of the grown single crystals in this work were investigated by X–ray powder diffractometer.

### 3.2.1. X–Ray Source

X–rays are generated when electrons with high kinetic energies collided with a metal plate target anode such as Copper, Molybdenum, Tungsten or Iron, inside the evacuated X–ray tube as shown in Figure 3.1. The voltage and current depend on the target metal, for example, for copper 25 – 40 kV and 40 mA are used. The incident electron from the cathode filament has sufficient energy to hit the anode plate. The electron of anode atom goes to an exited state. When an atom returns to the ground state the X–rays are emitted. This process is called Bremsstrahlung. The emitted radiation in this case is of continuous wavelength known as white radiation. The X–rays emitted out from X–ray tube pass through thin beryllium windows. However, most of energy (about 98 percent) is converted into heat, then the target metal must be cooled by water.
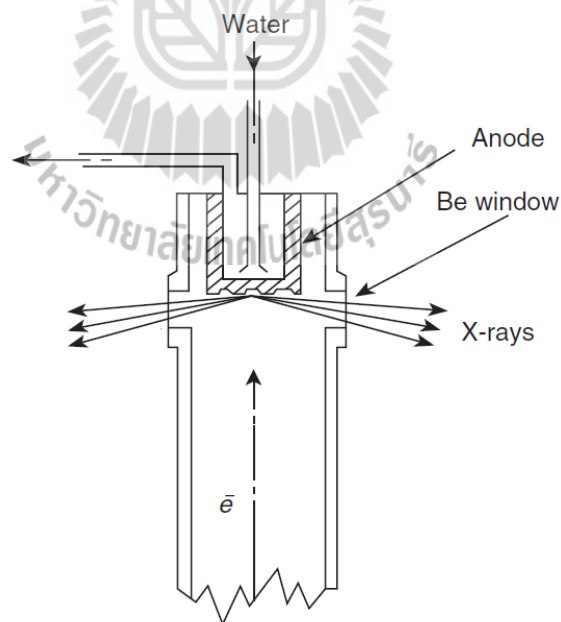
**Figure 3.1** Schematic drawing of an X–ray tube. (Shmueli, 2007).
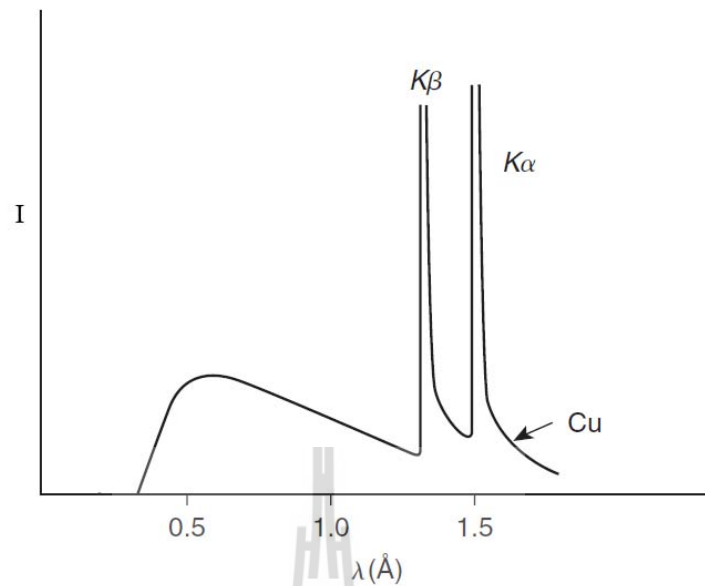
**Figure 3.2** The X–ray spectrum of copper target. (Shmueli, 2007).

The X–ray spectrum using a copper target is shown in Figure 3.2. The spectrum shows continuous and two peaks of characteristic radiation that are designated the $K_\alpha$ and $K_\beta$ lines. The wavelengths of the $K_\alpha$ and $K_\beta$ lines are unique characteristic for a metal. For copper, the $K_\alpha$ and $K_\beta$ lines occur at a wavelength of 1.5406 and 1.3922 Å, respectively. The characteristic radiation is explained as follows. The electrons in K shell (n = 1) of anode are knocked out by high energy electrons from cathode, leaving excited atoms. Then, electrons in higher energy (L, M, ...shell; n = 2, 3,…) undergoes transition to lower energy levels emitting energy of a characteristic wavelength. The electrons from L shell to K shell create the $K_\alpha$ line, and from M shell to K shell is $K_\beta$ line, indicated in Figure 3.3.
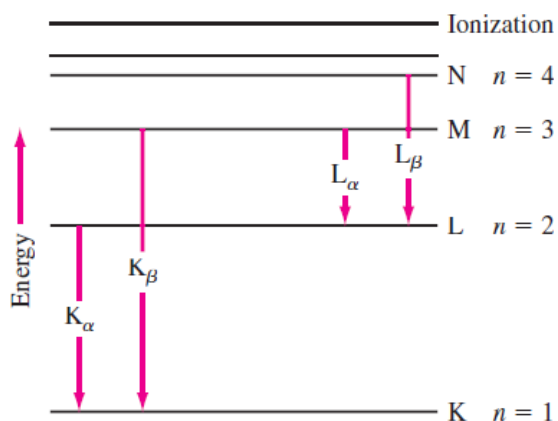
**Figure 3.3** Electron transitions of $K_\alpha$ and $K_\beta$ radiation. (Avarible : highered.

mcgraw – hill.com/sites/dl/.../sample_ch03.pdf).

In general, the commercial diffractometer uses the single-wavelength of X-rays by $Cu\,K_\alpha$ radiation with a wavelength of 1.5406 Å because of its high intensity. To select suitable wavelength, the absorption edge technique is used.

### 3.2.2 A Typical X-Ray Powder Diffraction System

The basic components of an X–ray diffractometer are X–ray source, X–ray detector and goniometer. Goniometer is an instrument that measures at a given angle. The distance from the X–ray source to the sample is the same as from the sample to the detector and this is called focusing circle. This method is called Bragg–Brentano parafocusing. Figure 3.4 shows the X–ray diffractometer used in this work. There are 2 types of goniometer, the $\theta : \theta$ and the $2\theta : \theta$. In the $\theta : \theta$ goniometer, the sample is stationary, the X–ray tube and the detector both simultaneously rotate over the angular range $\theta$. In the $2\theta : \theta$ goniometer, the X–ray tube is stationary, the sample holder rotates by the angle theta and the detector simultaneously rotates by the angle $2\theta$ (Scintag Inc; 1999), as shown in Figure 3.5.

**Figure 3.4** The components of an X–ray diffractometer model BRUKER AXS D500. (The Center for Scientific and Technological Equipment, Suranaree University of Technology).
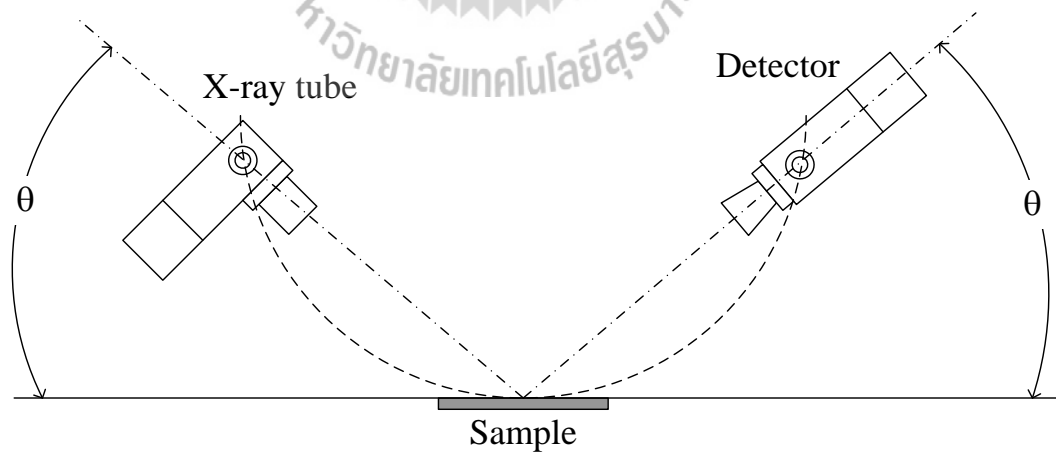


(a)

**Figure 3.5** The schematic of Bragg-Brentano setup (a) $\theta : \theta$ goniometer and (b) $2\theta : \theta$ goniometer. (adopted from : Scintag Inc, 1999).

(b)
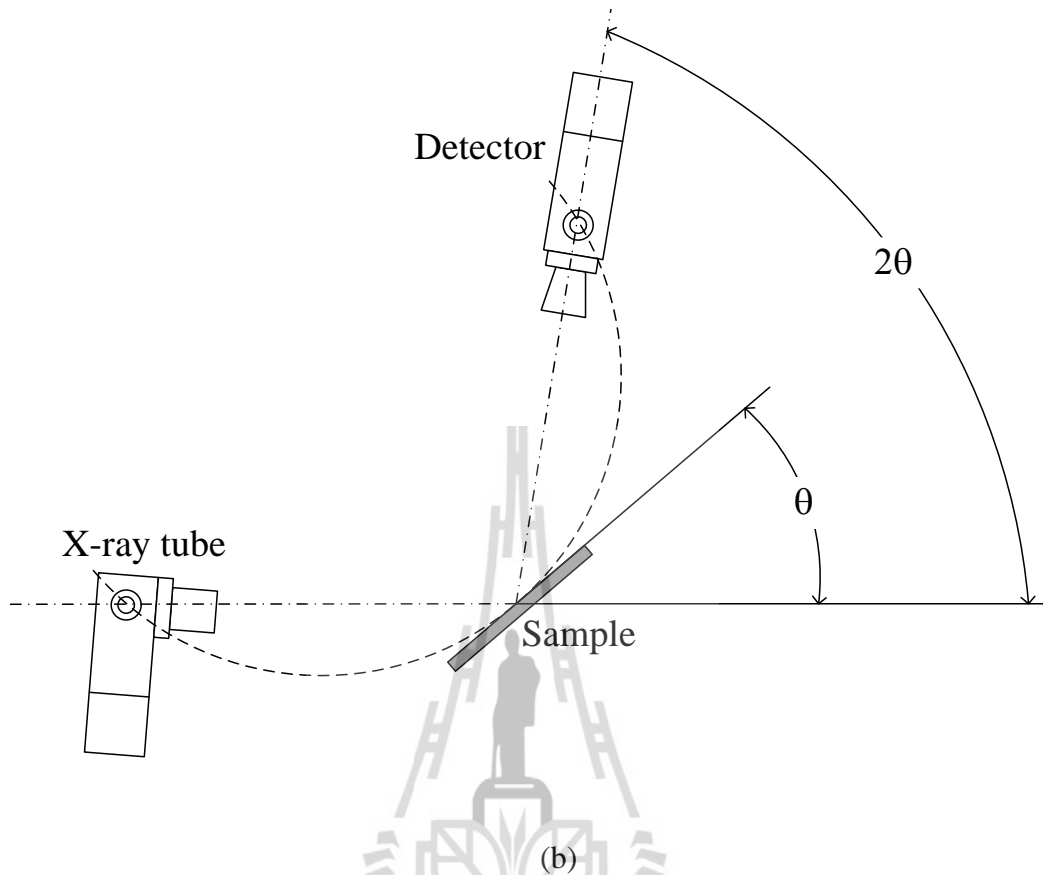
**Figure 3.5** (continued) The schematic of Bragg-Brentano setup (a) $\theta : \theta$ goniometer
and (b) $2\theta : \theta$ goniometer. (adopted from : Scintag Inc, 1999).

### 3.2.3 X–Ray Powder Diffraction Pattern

The condition of X–ray diffracted by the specimen where the combination of
the wavelength $(\lambda)$ of the X–ray, the angle $(\theta)$ between the incident beam and the
diffracting plane, and the inter-planar spacing $(d_{hkl})$ must be corresponded with the
Bragg's law as

$$2d_{hkl}\sin\theta = n\lambda \tag{3.1}$$

where $n$ is integer, normally $n = 1$.
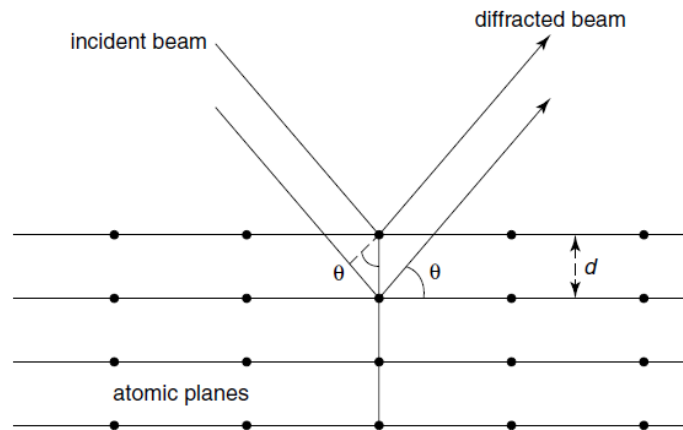
**Figure 3.6** The schematic of incident beam diffracted by a crystal lattice.

(Shmueli, 2007).

A typical result from an X–ray powder diffraction pattern consists of a plot of diffracted intensities versus the detector angle $2\theta$ as shown in Figure 3.7.
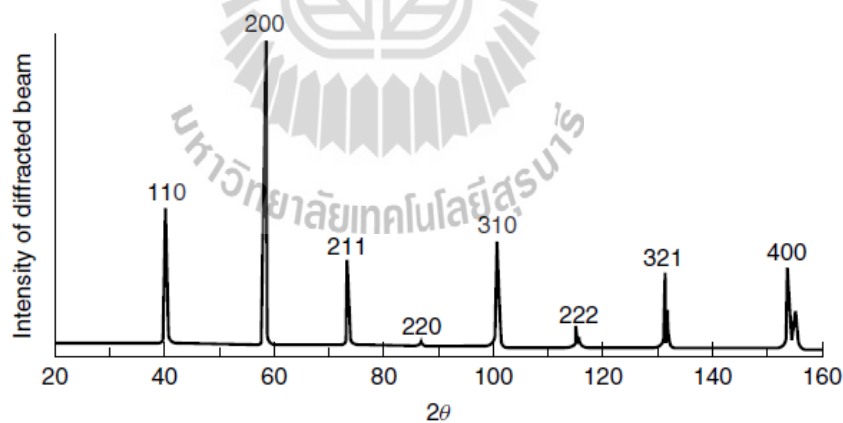


**Figure 3.7** X–Ray diffraction pattern of tungsten. (Guy and Hren; 1974 ).

The peaks indicate angles at which all of the conditions for X–ray diffraction have corresponded. Inter-planar spacing or d–spacing $(d_{hkl})$ for different crystal systems and their Miller indices $hkl$ and parameters $a$, $b$ and $c$ which give the lengths of the unit cell are shown in Table 3.1.

**Table 3.1** Crystal parameters of different crystal systems.

| Crystal system | d-spacing |
|---|---|
| Cubic | $\dfrac{1}{d_{hkl}^2} = \dfrac{h^2 + k^2 + l^2}{a^2}$ |
| Tetragonal | $\dfrac{1}{d_{hkl}^2} = \dfrac{h^2 + k^2}{a^2} + \dfrac{l^2}{c^2}$ |
| Orthorhombic | $\dfrac{1}{d_{hkl}^2} = \dfrac{h^2}{a^2} + \dfrac{k^2}{b^2} + \dfrac{l^2}{c^2}$ |
| Hexagonal | $\dfrac{1}{d_{hkl}^2} = \dfrac{4}{3}\left(\dfrac{h^2 + hk + k^2}{a^2}\right) + \dfrac{l^2}{c^2}$ |
| Trigonal/ Rhombohedral | $\dfrac{1}{d_{hkl}^2} = \dfrac{(h^2 + k^2 + l^2)\sin^2\alpha + 2(hk + kl + hl)(\cos^2\alpha - \cos\alpha)}{a^2(1 - 3\cos^2\alpha + 2\cos^3\alpha)}$ |
| Monoclinic | $\dfrac{1}{d_{hkl}^2} = \dfrac{h^2}{a^2\sin^2\beta} + \dfrac{k^2}{b^2} + \dfrac{l^2}{c^2\sin^2\beta} - \dfrac{2hl\cos\beta}{ac\sin^2\beta}$ |
| Triclinic | $\dfrac{1}{d_{hkl}^2} = \dfrac{1}{V^2}\left\{ \begin{array}{l} h^2b^2c^2\sin^2\alpha + k^2a^2c^2\sin^2\beta + l^2a^2b^2\sin^2\gamma \\ +2kla^2bc(\cos\beta\cos\gamma - \cos\alpha) \\ +2hlab^2c(\cos\alpha\cos\gamma - \cos\beta) \\ +2hkabc^2(\cos\alpha\cos\beta - \cos\gamma) \end{array} \right\}$ <br> $V = abc(1 - \cos^2\alpha - \cos^2\beta - \cos^2\gamma + 2\cos\alpha\cos\beta\cos\gamma)^{1/2}$ |

## 3.3 High Resolution X–Ray Powder Diffractometer

To evaluate the crystalline perfection of the specimen crystals, high–resolution X–ray diffraction (HRXRD) analysis was carried out. A multicrystal X–ray diffractometer developed at National Physical Laboratory (NPL), New Delhi (Lal and Bhagavannarayana, 1989) was used to record high-resolution rocking or diffraction curves (DCs). In this system, a fine focus ($0.4 \times 8$ mm$^2$ ; 2 kW Mo) X–ray source energized by a well–stabilized Philips X–ray generator (PW 1743) was employed.

The well–collimated and monochromated $MoK_{\alpha1}$ beam obtained from the three monochromator Si crystals set in dispersive $(+,-,-)$ configuration has been used as the exploring X–ray beam. This arrangement improves the spectral purity ($\Delta\lambda/\lambda << 10^{-5}$) of the $MoK_{\alpha1}$ beam. The divergence of the exploring beam in the horizontal plane (plane of diffraction) was estimated to be $\ll 3$ arc sec. The specimen crystal is aligned in the $(+,-,-,+)$ configuration. Schematic of configuration of monochromator is shown in Figure 3.8. Due to dispersive configuration of the third monochromator crystal with respect to the $2^{nd}$ monochromator, the spectral quality of the diffracted beam emerged from the $3^{rd}$ monochromator is highly perfect ($\Delta\lambda / \lambda \ll 10^{-5}$; horizontal divergence $\ll 3$ arc seconds) and hence though the lattice constant of the monochromator crystal and the specimen are different, the unwanted experimental dispersion broadening in the diffraction curve of the specimen crystal ($\Delta FWHM = \Delta\lambda / \lambda (\tan\theta_M - \tan\theta_S)$; $\theta_M$ and $\theta_S$ being the Bragg diffraction angles of monochromator and the specimen crystals) is insignificant. The advantage of dispersion configuration $(+,-,-)$ over the non–dispersive configuration $(+,-,+)$ of monochromators is well described in the recent article (Bhagavannarayana and Kushwaha, 2010). The specimen can be rotated about a vertical axis, which is perpendicular to the plane of diffraction, with minimum angular interval of 0.4 arc sec. The diffracted intensity is measured by using a scintillation counter. The DCs were recorded by changing the glancing angle (angle between the incident X–ray beam and the surface of the specimen) around the Bragg diffraction peak position $\theta_B$ (taken zero as reference point) starting from a suitable arbitrary glancing angle ($\theta$). The detector was kept at the same angular position $2\theta_B$ with wide opening for its slit,

the so–called ω scan (Bhagavannarayana and Kushwaha, 2010). The omega scan is very appropriate to record the short range order scattering caused by the defects or by the scattering from local Bragg diffractions from agglomerated point defects or due to low angle and very low angle structural grain boundaries (Senthilkumar, MoorthyBabu and Bhagavannarayana, 2011). Before recording the diffraction curve, to remove the non–crystallized solute atoms which remained on the surface of the crystal and also to ensure the surface planarity, the specimens were first lapped and chemically etched in a non–preferential etchant of water and acetone mixture in 1:2 volume ratio.
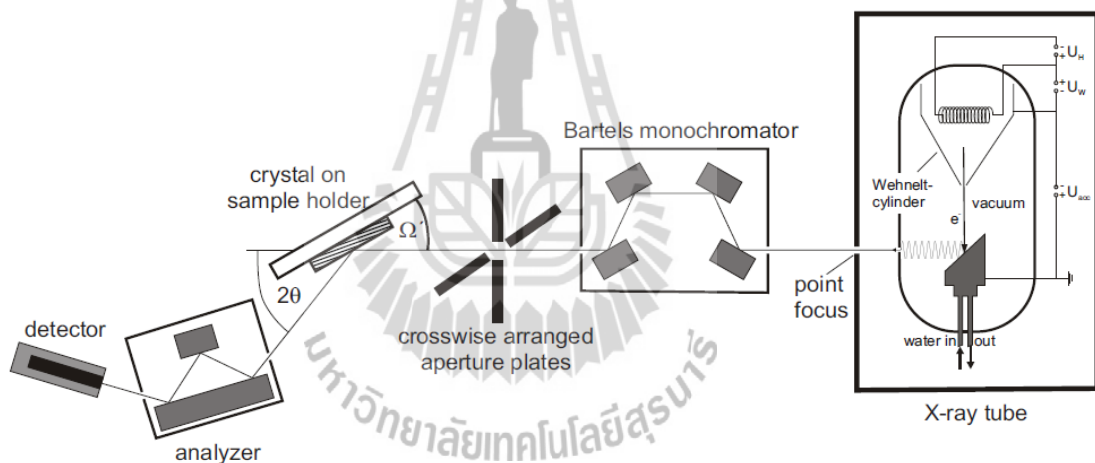


**Figure 3.8** Optical path of the X–ray beam for the used goniometer.

(Walter Schottky Institute, 2009).

## 3.4 Fourier Transforms Infrared Spectroscopy

The infrared (IR) spectroscopy is a widely used technique for investigating chemical structure of the interested unknown material. It is concerned with the absorption of IR region energy of the electromagnetic spectrum by a molecule, ion or functional group of the sample. When the sample absorbs IR spectrum, it causes

vibration of the molecules. The absorption frequency is dependent on the vibrational frequency of the molecules (Åmand and Tullin, n.d.). There are two types of molecular vibrations, stretching and bending. For example, the vibrations of water ($H_2O$) are shown in Figure 3.9. Because water is non–linear molecule, hence it has three fundamental vibrations (Barton (II), 2002).



symmetrical stretching      asymmetrical stretching      scissoring (bending)
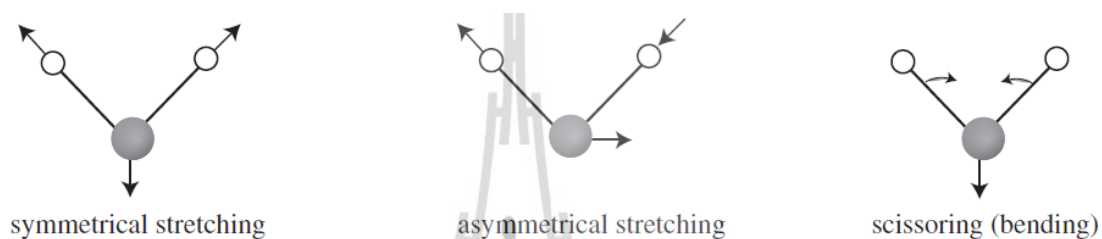
**Figure 3.9** Fundamental vibrational modes of water. (Available: orgchem.colorado. edu/Spectroscopy/.../IRtheory.pdf Ref.).

The IR spectrum is covering the range from 14,000 to 10 $cm^{-1}$ approximately. It is generally divided into three regions. The near IR approximately from 14,000 – 4,000 $cm^{-1}$ (0.8 – 2.5 μm in wavelength), the middle IR approximately from 4,000 – 400 $cm^{-1}$ (2.5 – 25 μm) and the far IR approximately from 400 – 10 $cm^{-1}$ (25 – 1000 μm). The middle IR is commonly used in laboratory.

Fourier transforms infrared (FT–IR) spectroscopy is a mathematical technique to use Fourier transforms convert the complex raw data into the actual spectrum. There are many techniques which are used to obtain an infrared spectrum. The technique called attenuated total reflection (ATR) with middle IR is today the most widely used FT–IR tool (PIKE Technologies [On–line] and PerkinElmer, Inc. [On–line], n.d.). The ATR technique uses a small amount of sample and no Potassium

bromide (KBr) is used for matrix. The schematic diagram of ATR technique is given in Figure 3.10.
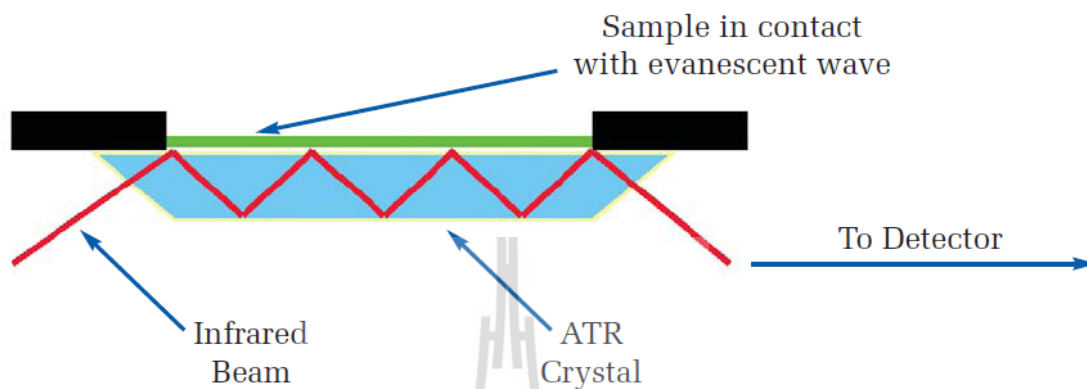


**Figure 3.10** A multiple reflection ATR system. (PerkinElmer, Inc. [On-line], n.d.).

The ATR transmission spectra of a pure KDP Sample is shown in Figure 3.11 and some absorption frequencies of IR region are given in Table 3.2
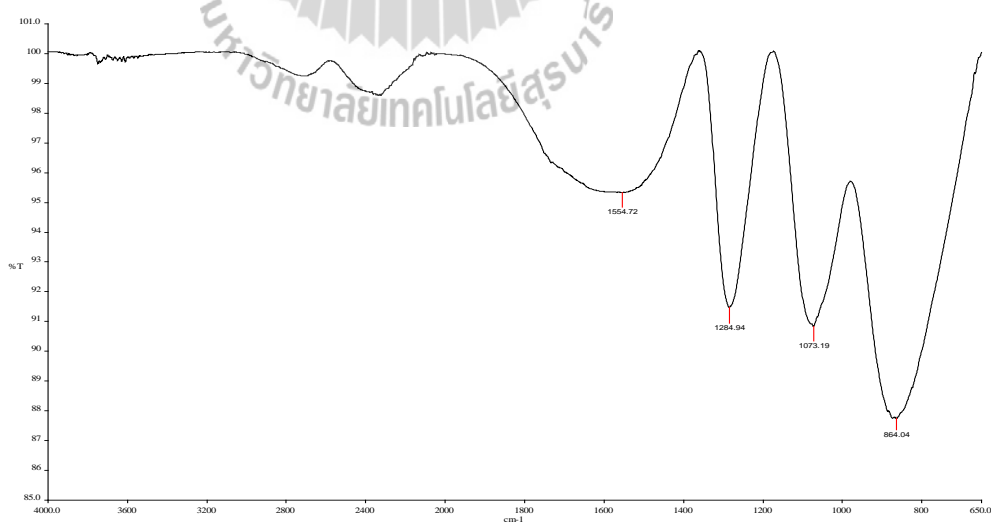


**Figure 3.11** Transmission spectra of pure KDP.

**Table 3.2** IR frequencies of Functional Group [On–line].

| Functional Group | Wave no. (cm$^{-1}$) | Description |
|---|---|---|
| C–O | 1000 – 1200 | |
| C=C | 1575 – 1650 | Short (sharp, short) |
| C=O | 1600 – 1800 | Huge band |
| C≡C | 2100 – 2200 | Short, narrow |
| C≡N (nitrile) | 2240 – 2260 | Sharp, narrow |
| N–H (amine) | 3300 – 3500 | Like alcohol, 1°–amines have 2 peaks |
| sp$^3$ C–H | 2850 – 3000 | Tallest C–H Band |
| sp$^2$ C–H | 3000 – 3100 | |
| sp C–H | ~3300 | Narrow, short |
| O–H (alcohol) | 3300 – 3600 | Strong and broad |
| O–H(acids) | 2500 – 3000 | Very broad (over ~ 500 cm$^{-1}$) |

## 3.5 UV-Vis Spectrophotometer

The optical properties of grown crystal were investigated by the ultra violet–visible (UV–Vis) spectrophotometer. The transmission, absorption and refraction in the regions ultraviolet to visible spectrum with wavelength of 200 – 1,100 nm were studied. The energy ($E$) of light or photon is defined by the relationship

$$E = h\nu = \frac{hc}{\lambda} \tag{3.2}$$

where $h$ is a Planck's constant, which has a value of $6.63 \times 10^{-34}$ J·s and $c$ is velocity of light in vacuum.

Figure 3.12 shows the schematic representation of double beam UV–Vis spectrophotometer. It consists of light sources, monochromator (grating), beam splitter system (mirrors), standard sample cuvette, focusing lens and detector system.

A spectrophotometer detects the transmittance intensity of spectrum with certain frequency which is passed through the sample. The instrument compares the intensity of the transmitted beam with the reference beam.
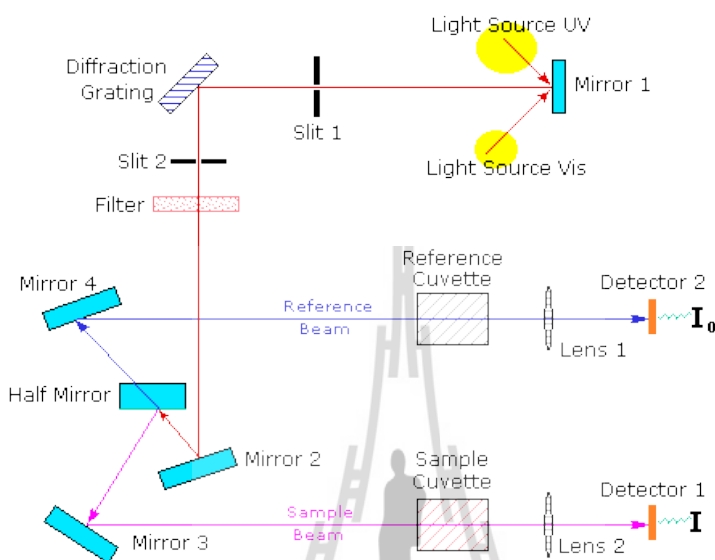


**Figure 3.12** The schematic of double beam UV–Vis spectrophotometer. (available:
http://www2.chemistry.msu.edu/faculty/reusch/virttxtjml/spectrpy/uv–
vis/uvspec.htmRef.).

When light is directed to the sample, transmission, absorption and reflection occur. The intensity of the incident beam ($I_0$) to the sample must equal the sum of the intensities of the transmitted ($I_T$), absorbed ($I_A$), and reflected ($I_R$) beams, Hence

$$I_T + I_A + I_R = I_0 \tag{3.3}$$

or
$$T + A + R = 1 \tag{3.4}$$

where the transmittance,
$$T = \frac{I_T}{I_0} \tag{3.5}$$

the absorbance, $$A = \frac{I_A}{I_0} \qquad (3.6)$$

the reflectance, $$R = \frac{I_R}{I_0} \qquad (3.7)$$

In general, a spectrophotometer detects the transmittance intensity of spectrum with certain frequency which is passed through the sample. The instrument compares the intensity of the transmitted beam with the reference beam. The percentage of transmittance ($\%T$) is given by:

$$\%T = \frac{I_T}{I_0} \times 100\% \qquad (3.8)$$

The relationship between absorbance and transmittance is

$$A = \log \frac{I_0}{I_T} = \log \frac{1}{T} \qquad (3.9)$$

then $$A = -\log T = \alpha \ell \qquad (3.10)$$

where $\alpha$ is the absorption coefficient, $\ell$ is the length of given sample. Equation (3.10) is known as the Beer–Lambert law (Callister and Rethwisch, 2010; Tilley, 2004; Miller, 1995).

Absorption of a photon occurs by the excitation of an electron of a sample from the valence band across the energy band gap ($E_g$) to the conduction band and emitting photon when it comes down to valence band, as demonstrated in Figure 3.13.
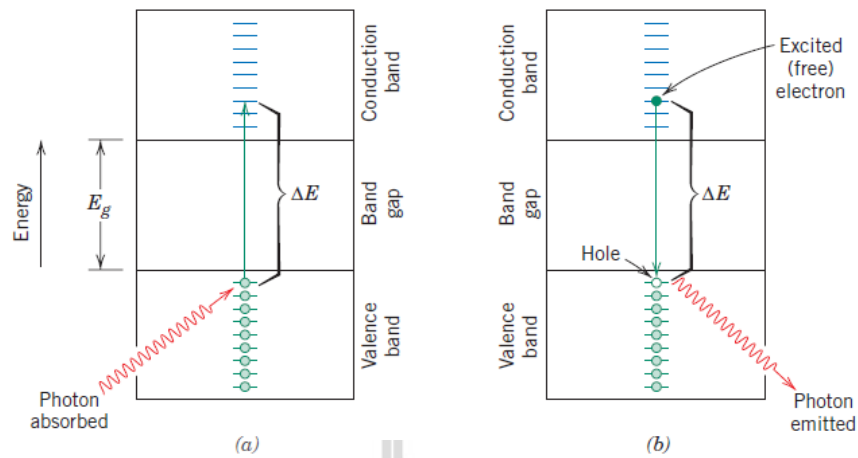
**Figure 3.13** The photon absorption and emitting of electron in solid. (Callister, Jr. and

Rethwisch, 2010).

The energy band gap and the absorption coefficient has relation as follows

(Bassani and Pastori Parravicini, 1975 ; Dresselhaus, on–line; Robert, Justin Raj,

Krishnan and Jerome Das, 2010),

$$\alpha = \frac{C(h\nu - E_g)^{\frac{1}{2}}}{h\nu}$$
(3.11)

where $C$ is constant.

The relationship between reflectance and transmittance is

$$T = (1 - R)^2 e^{-\alpha \ell}$$
(3.12)

When light travels into the transparent materials, the velocity decreases and

there is bending of a ray of light, this phenomenon is called refraction. The index of

refraction, or refractive index ( $n$ ) is defined as

$$n = \frac{c}{v}$$
(3.13)

where $v$ is the velocity of light in the medium.

In general case, the refractive index is a complex quantity, called complex refractive index ( $N$ ) which is defined by

$$N = n + ik \tag{3.14}$$

Where $n$ is normal refractive index and $k$ is extinction coefficient (Tilley, 2004; Miller, 1995; Fox, 2007).

The reflectance and the absorption coefficient are related to $n$ and $k$ by the expressions, (the refractive index of air is equal to 1)

$$R = \left| \frac{N-1}{N+1} \right|^2 = \frac{(n-1)^2 + k^2}{(n+1)^2 + k^2} \tag{3.15}$$

And

$$\alpha = \frac{4\pi k}{\lambda} \tag{3.16}$$

In the case of good transparent material $k$ is neglected, then equation (3.15) becomes,

$$R = \frac{(n-1)^2}{(n+1)^2} \tag{3.17}$$

## 3.6 Microhardness Studies

Hardness of a material is a measure of its resistance to deformation when a force is applied. Hardness studies are carried to understand the mechanical properties of material such as the plasticity of the crystal, elastic constants or yield stress etc (Lal, Bamzai and Kotru ; 2002). The hardness property is basically related to the crystal structure of the material (Karan, Sen Gupta and Sen Gupta, 2001).

There are many methods for measuring hardness of materials depending on indentation type. Microhardness commonly refers to static indentations with loads not

exceeding 1 kg. The Vicker's hardness test method is used in this work. The Vickers diamond pyramid indenter where opposite faces contains an angle $\theta = 136^\circ$ is presented in Figure 3.14.
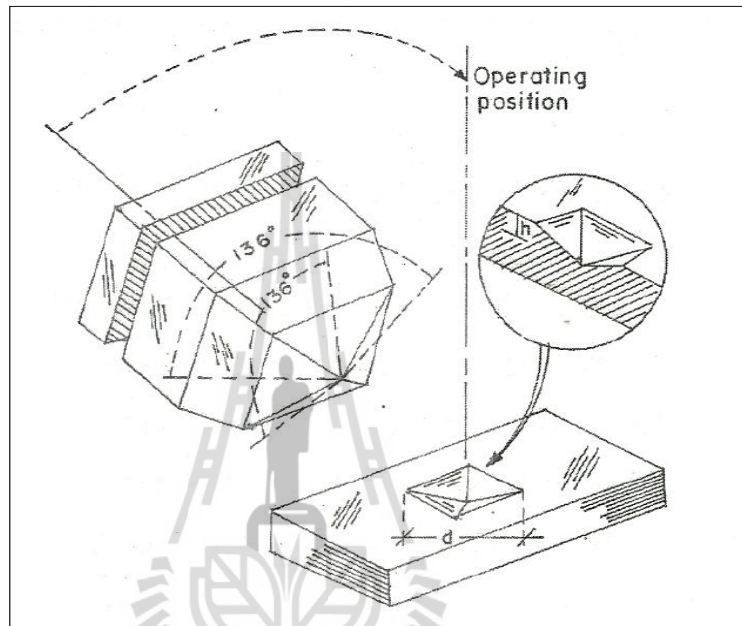


**Figure 3.14** The schematic of Vickers indenter. (Available:http://www.metallography .com/amp/micro.htm).

The base of the Vickers pyramid is square. The unit of hardness is known as the Vickers hardness number ($H_v$). The $H_v$ number is defined as the ratio of the load ($P$) applied to the surface area ($A$) of the indentation.

$$A = \frac{d^2}{2\sin(\theta/2)} \tag{3.18}$$

$$H_v = \frac{P}{A} = \frac{2\sin(\theta/2)P}{d^2} \tag{3.19}$$

Because $\theta = 136^\circ$ then equation (3.19) becomes,

$$H_v = \frac{1.8544P}{d^2} \tag{3.20}$$

where $d$ is the diagonal length of the indentation mark.

The relation between load and the size of indentation is given by Meyer's law as

$$P = k_1 d^n \tag{3.21}$$

where $k_1$ is a constant, $n$ the Meyer's index (or work-hardening coefficient).

Hardness values are measured from the observed size of the impression remaining after a loaded indenter. Since the material takes sometime to revert to the elastic mode after every indentation, a correction $x$, known as the measure of dislocation density of the material is applied to the d value and the Kick's law is related as (Justin Raj, Dinakaran, Krishnan, Milton Boaz, Robert and Jerome Das, 2008)

$$P = k_2(d + x)^2 \tag{3.22}$$

Form equations (3.21) and (3.22) is got,

$$k_1 d^n = k_2(d + x)^2$$

$$d^{n/2} = \left(\frac{k_2}{k_1}\right)^{1/2} d + \left(\frac{k_2}{k_1}\right)^{1/2} x \tag{3.23}$$

The yield strength ($\sigma_v$) of the material can be found out using the relation (Justin Raj *et al.*, 2008)

$$\sigma_v = \frac{H_v}{2.9}\left\{[1 - (2 - n)] \times \left[\frac{12.5(2 - n)}{1 - (2 - n)}\right]^{2-n}\right\} \tag{3.24}$$

## 3.7 Dielectric Properties Studies

A dielectric is a nonconducting material or insulator which has the unique characteristic of being able to store energy when an external electric field is applied (Agilent Technologies, 2006). When a dielectric is placed in an electric field, it can be polarized which is called dielectric polarization as shown in Figure 3.15. The charged particles of dielectric are rearranged toward the field. This creates an internal electric field which reduces the overall field within the dielectric itself (on-line: http://en.wikipedia.org). When a dielectric is inserted between the plates of a capacitor, the capacitance increases with factor $\kappa$, known as dielectric constant or relative permittivity (Serway and Jewett, 2004).
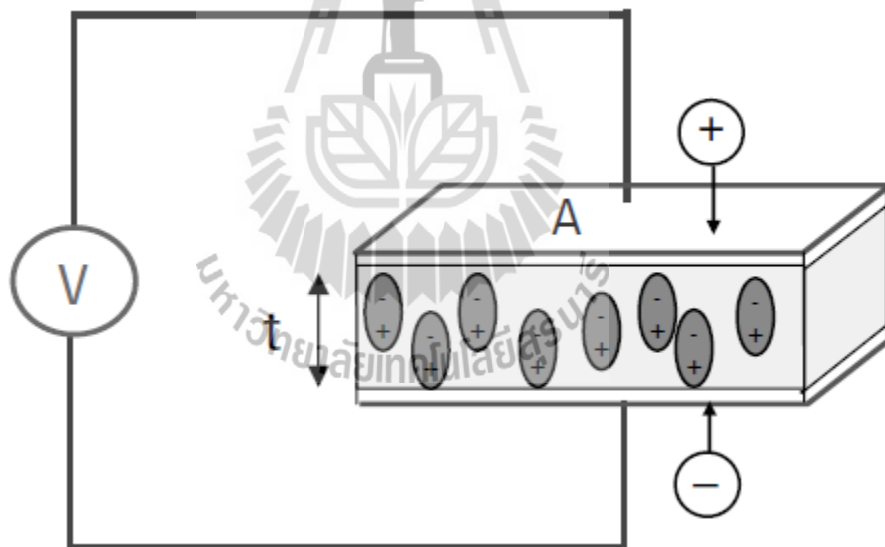


**Figure 3.15** Orientation of charged particles of dielectric in electric field. (Agilent Technologies, 2006).

If a DC voltage source is placed across a parallel plate capacitor, the capacitance of a parallel plate capacitor without a dielectric is $C_0$. When a dielectric

material is placed between the plates, more charge is stored, the capacitance ($C$)
become,

$$C = \kappa C_0 \tag{3.25}$$

$$\kappa = \varepsilon_r = \frac{C}{C_0} \tag{3.26}$$

$$C_0 = \varepsilon_0 \frac{A}{d} \tag{3.27}$$

where $\varepsilon_r$ is the relative permittivity, $\varepsilon_0 = 8.854 \times 10^{-12}$ F / m is the permittivity

of free space, $A$ and $d$ are area and distance between capacitor's plates, respectively.

Equation (3.26) shows that the dielectric constant $\kappa$ is the relative permittivity

($\kappa = \varepsilon_r$) and is the real dielectric constant. If an AC source with frequency $\omega = 2\pi f$

is applied across the same capacitor, the dielectric constant becomes complex number

and as a function of frequency.

$$\kappa^*(\omega) = \varepsilon_r^*(\omega) = \varepsilon_r'(\omega) + i\varepsilon_r''(\omega) \tag{3.28}$$

The complex dielectric constant consists of a real part $\varepsilon_r'$ which represents

how much energy from an external electric field is stored in a material. The imaginary

part $\varepsilon_r''$ is called the dielectric loss factor and is a measure of how dissipative or lossy

a material is to an external electric field. The imaginary part of dielectric constant

($\varepsilon_r''$) is always greater than zero and is usually much smaller than $\varepsilon_r'$ (Agilent

Technologies, 2006).

The complex dielectric constant can be drawn as a simple vector diagram (Figure 3.16), the real and imaginary components are 90° out of phase. The vector sum forms an angle $\delta$ with the real axis ($\varepsilon'_r$).
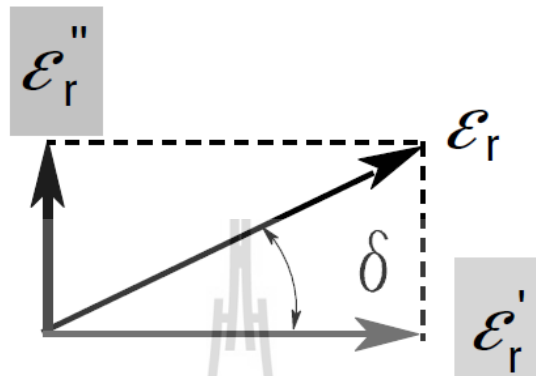


**Figure 3.16** Loss tangent vector diagram. (Agilent Technologies, 2006).

$$\tan\delta = \frac{\varepsilon''_r}{\varepsilon'_r} = D = \frac{\text{Energy Lost per Cycle}}{\text{Energy Stored per Cycle}} \qquad (3.29)$$

The loss tangent or $\tan\delta$ is defined as the ratio of the imaginary part of the dielectric constant to the real part. $D$ denotes a dissipation factor.

A material may have several dielectric mechanisms or polarization mechanisms that depend on applied frequency (Figure 3.17). The electronic polarization arises from electric field displacing the electrons cloud that surrounds the nucleus of an atom. The atomic polarization occurs when adjacent cation (positive) and anion (negative) relatively move under an applied electric field. Orientation (dipolar) polarization is formed by the rotation of molecular dipole to align with the electric field. The ionic polarization occurs because of the mobile charge or space charge carriers can move under applied fields (Newnham, 2005).
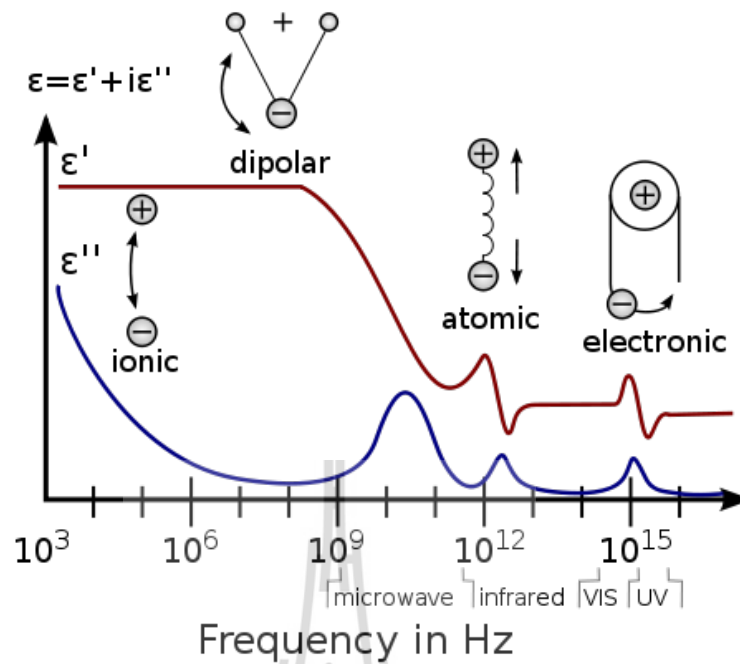
**Figure 3.17** A dielectric permittivity spectrum over a wide range of frequencies. (Available: http://en.wikipedia.org/wiki/Dielectric_spectroscopy).

Measurement of dielectric properties in this work was carried out by using the Agilent E4980A precision LCR meter with 16451B dielectric test fixture as shown in Figure 3.18. The measurement method used is a parallel plate technique and the frequencies used from 20 Hz to 2 MHz. Measured parameters are capacitance ($C$) and dissipation factor ($D$). The dielectric constant and dielectric loss can be derived from equations (3.30) and (3.31), respectively.

$$\varepsilon'_r = \frac{Cd}{\varepsilon_0 A} \qquad (3.30)$$

$$\varepsilon''_r = \varepsilon'_r D \qquad (3.31)$$

**Figure 3.18** Dielectric test fixture. (Available: http://www.home.agilent.com/
agilent/product.jspx?nid=−34051.536879640.00&cc=TH&lc=eng).

## 3.8 References

Agilent Technologies. (2006). Agilent Basics of Measuring the Dielectric Properties
of Materials.

Åmand, L. E. and Tullin, C. J. **The Theory Behind FTIR analysis**. Chalmers
University of Technology. Sweden, Göteborg.

Barton(II), F. E. (2002). **Theory and principles of near infrared spectroscopy**.
Spectroscopy Europe. (P. 12–18).

Bassani, F. and Pastori Parravicini, G. (1975). **Electronic States and Optical
Transitions in Solids.** (1st ed., P. 149–176). Oxford: Pergamon Press.

Callister, W. D. Jr. and Rethwisch, D. G. (2010). **Materials science and engineering:
an introduction**. (8th ed.). USA: John Wiley & Sons.

Dresselhaus, M. S. **Solid State Physics part II Optical Properties of Solids**. [On–
line]. Available: http://web.mit.edu/course/6/6.732/www/6.732-pt2.pdf.

Fox, M. (2007). **Optical Properties of Solids**. (6th ed.) Great Britain, Wiltshire: Oxford University Press.

Guy, A. G. and Hren, J. J. (1974). **Elements of Physical Metallurgy**. (3rd ed., pp. 208) Addison–Wesley.

Justin Raj, C., Dinakaran, S., Krishnan, S., Milton Boaz, B., Robert, R. and Jerome Das, S. (2008). Studies on optical, mechanical and transport properties of NLO active L-alanine formate single crystal grown by modified Sankaranarayanan–Ramasamy (SR) method. **Optics Communications**. 281: 2285–2290.

Karan, S., Sen Gupta, S. and Sen Gupta, S. P. (2001). Microhardness and its related physical constants in solution-grown ammonium sulphate single crystals. **Materials Chemistry and Physics**. 69: 143–147.

Lal, B., Bamzai, K.K. and Kotru, P.N. (2002). Mechanical characteristics of melt grown doped $KMgF_3$ crystals. **Materials Chemistry and Physics**. 78: 202–207.

Miller, A. (1995). **Handbook of optics.** (2nd ed., P. 9.1–9.33). USA: McGraw-Hill.

Newnham, R. E. (2005). **Properties of Materials Anisotropy, Symmetry, Structure.** (1st ed.) Great Britain: Oxford University Press.

On–line edition for students of organic chemistry lab courses at the University of Colorado, Boulder, Dept of Chem and Biochem. (2002).

PerkinElmer, Inc. FT–IR Spectroscopy : Attenuated Total Reflectance (ATR) Available: www.perkinelmer.com.

PIKE Technologies. ATR–Theory and Applications. Available: www.piketech.com.

59

Robert, R., Justin Raj, C., Krishnan, S. and Jerome Das, S. (2010). Growth, theoretical and optical studies on potassium dihydrogen phosphate (KDP) single crystals by modified Sankaranarayanan–Ramasamy (mSR) method**. Physica B**. 405: 20–24.

Santhanaraghavan, P. and Ramasamy, P. (2000). **Crystal Growth Process and Methods.** Kumbakonam, India: KRU publications.

Scintag, Inc. (1999). **Basics of X-ray Diffraction**. (P.7.1–7.25) Cupertino, CA.

Serway, R. A. and Jewett, J. W. (2004). **Physics for Scientists and Engineers**. (6th ed.)  USA: Thomson Brooks/Cole.

Shmueli, U. (2007) **Theories and Techniques of Crystal Structure Determination**. (6th ed.)   Great Britain, Wiltshire: Oxford University Press.

Tilley, R. J. D. (2004). **Understanding solids : the science of materials**. England, West Sussex: John Wiley & Sons.

# CHAPTER IV

# GROWTH OF KDP SINGLE CRYSTALS BY

# CONVENTIONAL SLOW EVAPORATION

# AND SR METHODS

## 4.1 Introduction

Potassium dihydrogen phosphate (KDP) has gained considerable interesting applications due to its electro-optic, nonlinear optical and ferroelectric properties. Doping KDP with some additives is interesting because some dopants may improve the nonlinear properties. Solution growth technique has been widely used for the growth of KDP single crystal. In the present investigation, pure and thiourea doped KPD single crystals were grown by slow evaporation and Sankaranarayanan – Ramasamy methods. Investigations on the basic parameters of grown crystal such as solubility curve and crystal parameters were studied.

## 4.2 Solubility Study

Solubility study has been carried out by using pure KDP. Solubility of pure KDP was determined at four different temperatures: 30, 35, 40 and 45°C. Solubility at a given temperature was determined by dissolving pure KDP with deionized (DI) water in 2,000 ml on hotplate–stirrer maintained at the same temperature with continuous stirring for 4 hours to ensure solution homogeneity and saturation

concentration through out the volume of the solution. Then 200 ml saturation solution was separated into 200 ml beaker to let evaporate at room temperature, after which weight of remaining crystals was determined. The same procedure was repeated to estimate the solubility at different temperatures. The solubility curve of pure KDP is shown in Figure 4.1. The solubility is seen to increase linearly with increasing of temperature.
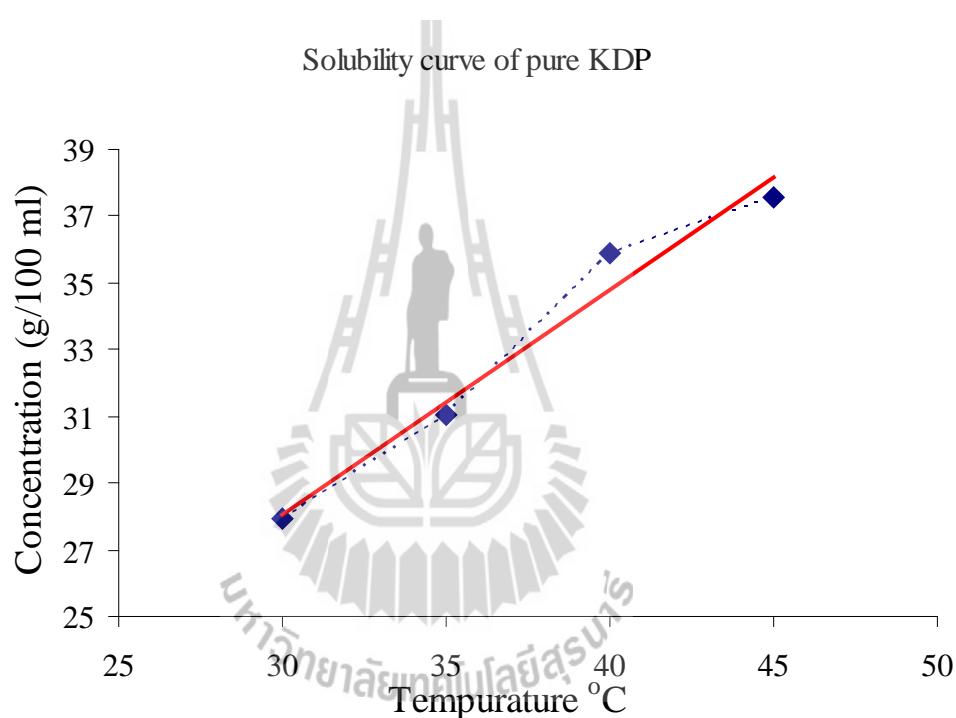


**Figure 4.1** Solubility curve of pure KDP.

## 4.3 Solution Growth by Conventional Slow Evaporation Method

### 4.3.1 Growth of Pure KDP Single Crystal

The GR grade of KDP and DI type I quality water of resistivity 18.2 $M\Omega - cm$ were used. For the growth of pure KDP single crystal by slow evaporation technique, the 2 moles (272.172 g) KDP with molar mass 136.1086 g/mol were dissolved in 2,000 ml beaker with DI water. The solution was prepared in a slightly

undersaturated condition and stirred well for about 3 hours using a magnetic stirrer to obtain a homogeneous mixture at room temperature. The completely dissolved solution was filtered using filter paper Whatman no.1 to remove the suspended impurities and dust into plastic container with $34 \times 26 \times 5 \ \mathrm{cm}^3$ size. The clean net cloth was used to cover the container for protecting dust or insect falling into the solution and to allow crystallization by slow evaporation of water at room temperature. After $7 - 10$ days, the small single crystals of KDP were observed. Figure 4.2 shows several single crystals in various sizes after about 30 days. The single crystals of good size and quality were harvested after the growth period of $45 - 60$ days. Both of the prismatic face and pyramidal face are seen clearly on the grown crystals. For example, a bulk crystal with dimension up to $2.3 \times 1.5 \times 0.9 \ \mathrm{cm}^3$ with well–defined facets is shown in Figure 4.3. Morphology of the KDP crystal (Figure 4.4) shows that the growth rate along c–direction is larger when compared with the other two directions, hence KDP crystal is elongated well along c–axis. The grown crystal has (100) and (010) of prismatic face and (101), $(10\bar{1})$, $(0\bar{1}\bar{1})$ and $(01\bar{1})$ of pyramidal face. The grown crystals were subjected to structural, mechanical, electrical studies and were used as seed crystals for SR method.

**Figure 4.2** Small crystals of KDP and solution in a plastic container.
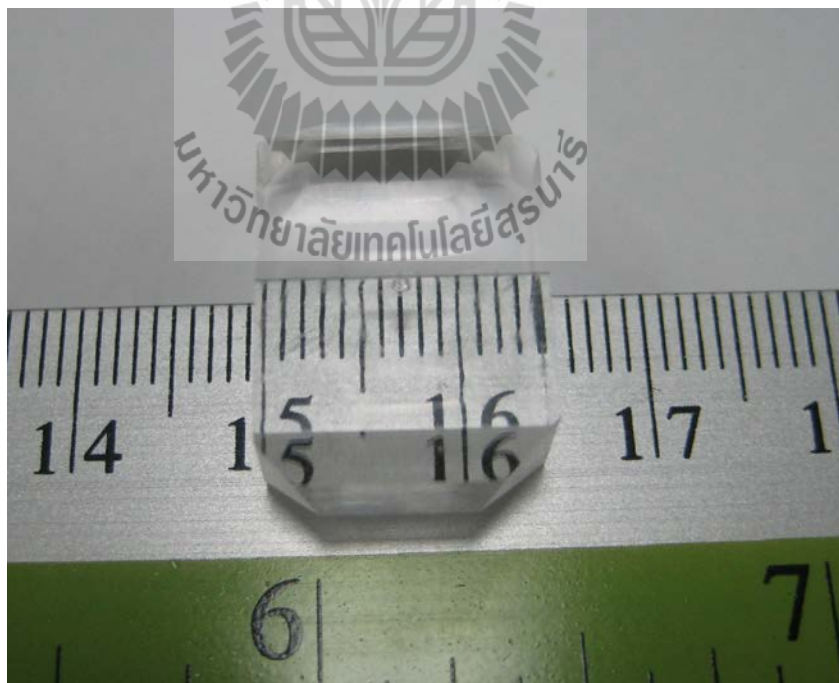


**Figure 4.3** The grown crystal of pure KDP.

C-direction <001>
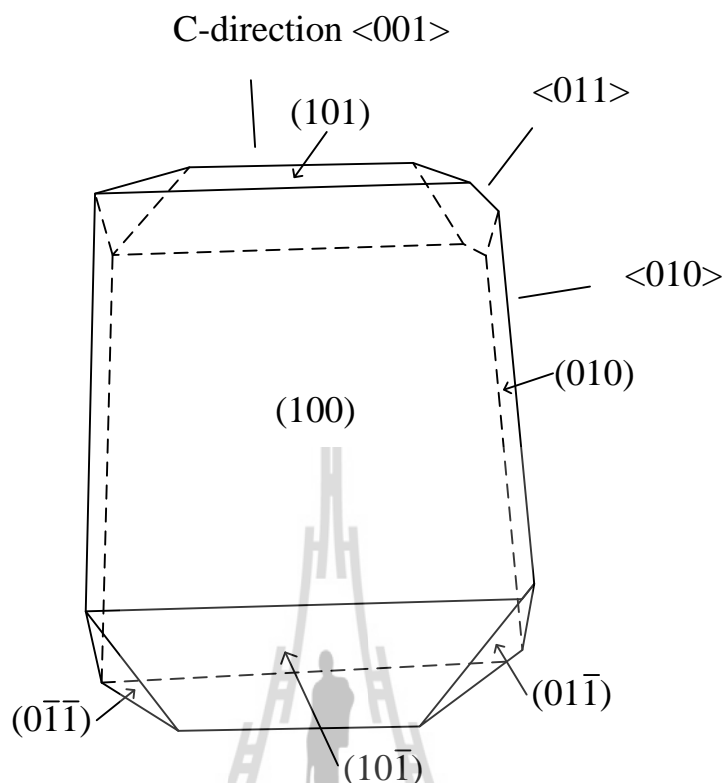


**Figure 4.4** Morphology of as grown pure KDP single crystal.

## 4.3.2 Growth of Thiourea–Doped–KDP Crystals

Thiourea (Thiocarbamide) is an organic compound with the formula $SC(NH_2)_2$ or $CH_4N_2S$. It is structurally similar to urea($CO(NH_2)_2$), except that the oxygen atom is replaced by a sulfur atom. Thiourea is a reagent in organic synthesis. Figure 4.5 gives the structural formula of thiourea. It is a white solid with molar mass of 76.12 g/mol.
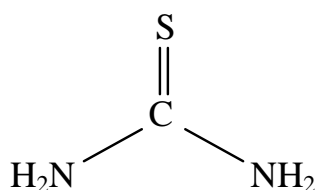


**Figure 4.5** Structural formula of thiourea.

To prepare solution of doped KDP with the impurity concentration of 1, 2, 3, 4 and 5 mol% of thiourea, 1.522 g, 3.045 g, 4.573 g, 6.090 g and 7.612 g of thiourea was each mixed to 2 moles of pure KDP in a given concentration. For all solutions, DI type I water was used and the same procedure of growing pure KDP single crystal as mentioned above was employed. Examples of grown single crystals of 2 mol% and 3 mol% thiourea doped–KDP are shown in Figure 4.6. Again, morphology of the thiourea doped–KDP crystals shows that the growth rate along c–direction is larger than the other two directions. The transparent and clear grown crystals were also studied and used as seed crystals for SR method.



**Figure 4.6** The grown crystals of 2 mol% and 3 mol% thiourea doped KDP.

## 4.4 Crystal Growth by Sankaranarayanan – Ramasamy Method

Sankaranarayanan and Ramasamy discovered the unidirectional crystal growth from solution and designed the container for unidirectional growth and have successfully grown several single crystals with different orientations, such as benzophenone, ammonium dihydrogen orthophosphate (ADP), L–lysine monohydrochloride dihydrate (L–LMHCl) etc. This method is called Sankaranarayanan and Ramasamy (SR) method. (Sankaranarayanan and Ramasamy,

2006; Sankaranarayanan, 2005; and Sethuraman, Ramesh Babu, Gopalakrishnan and Ramasamy, 2006).

### 4.4.1 Seed Crystal Preparation

Seed crystals for growing single crystal by SR method were chosen from crystallization by slow evaporation technique. The orientations of $\langle 010 \rangle$ a– or b– direction, $\langle 001 \rangle$ c–direction and $\langle 011 \rangle$ pyramidal face were selected to study. The crystal was cut very carefully by small saw at given direction about 1 cm thick and was ground into a cone shape for mounting at the bottom of ampoule and then washed by acetone solution. A cone shape seed crystal for SR method is shown in Figure 4.7.
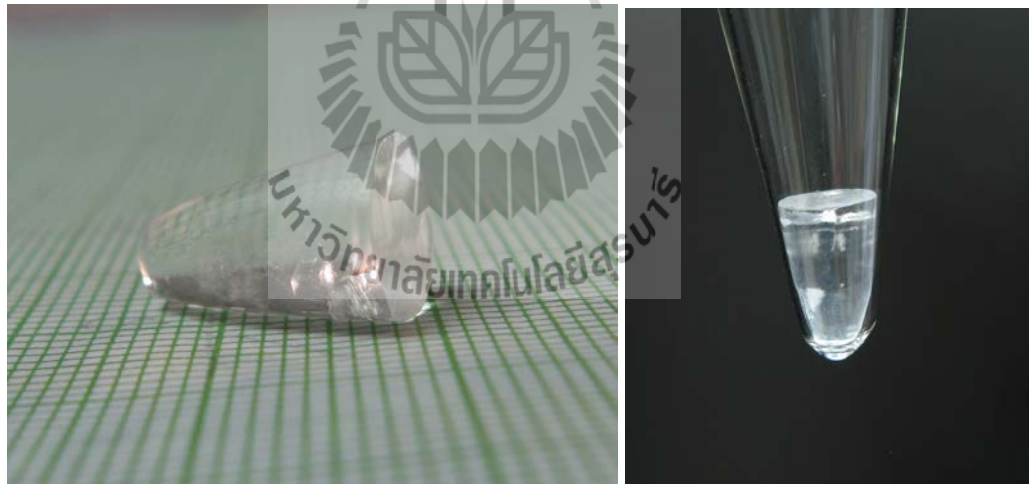


(a)                                      (b)

**Figure 4.7**    (a) A seed crystal for SR method and (b) seed was mounted in the ampoule.

**4.4.2 Apparatus Modifications and Experiment Setup**

In the original SR method, the ampoule glass has the same size as cylinder, as seen in Figure 2.3. In the new modification, the top of the ampoule has bigger diameter than the middle to provide more volume to keep solution and the surface of solution with more evaporation rate. The size of the top of an ampoule is 55 mm in diameter and 80 mm long and the middle part is 20 mm in diameter and 200 mm long. The modified SR ampoule is shown in Figure 4.8. The orientated seed crystal is mounted at the bottom tip of the ampoule. The top portion of the ampoule is covered by a plastic sheet with a hole of size about $1\,cm^2$ for control of evaporation rate of solution.



**Figure 4.8** The modified ampoule glass.

The ampoule with seed is kept in a glass water container to observe the grown crystal and to avoid the daily variation of ambient temperature. To reduce the evaporation of water in the container, it was covered by foam and a hole is made for fixing and floating of the glass ampoule. The ring heater was connected to the temperature controller and fixed on the neck of the ampoule. The AC current (about 1 A with 24 V) was applied to the ring heater. The current can be detected by analog ammeter. The ring heater is made from a resistant wire. The power of ring heater is, from Ampere's law, $P = IV = 24$ W. Type J thermocouple was used as a sensor for measuring temperature to the controller. An alcohol thermometer shows the temperature of water near the ring heater. The ruler was placed outside the ampoule to measure the size of crystal grown in each day. The temperature around the growth ampoule was selected based on the solvent used. In this study, the temperature around the ampoule was $35\,^{\circ}\mathrm{C}$ used for all crystal growth. The modified SR method setup is shown in Figure 4.9 (Balamurugan, Lenin, Bhagavannarayana and Ramasamy, 2007; Balamurugan, Lenin and Ramasamy, 2007).

(a)

(b)
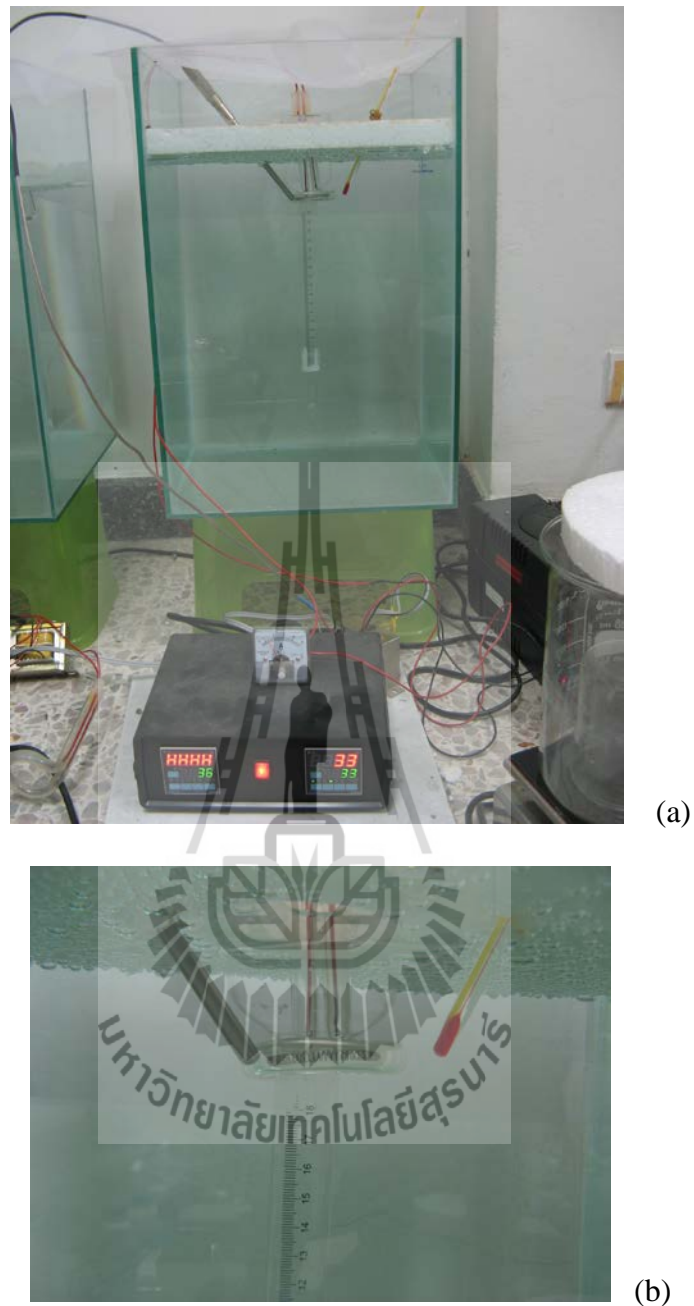
**Figure 4.9** (a) The modified SR method setup system.

(b) The ring heater placed in the neck of an ampoule.

### 4.4.3 The Grown Crystals by SR Method

Before starting the crystal growth experiment, the glass ampoule was cleaned

and washed by type III DI water to prevent any surface contamination from the wall

of the ampoule. Seed crystals along different crystallographic directions of $\langle 010 \rangle$, $\langle 001 \rangle$ and $\langle 011 \rangle$ were used for crystal growth of pure and 5 mol% thiourea–doped KDP. The crystals with concentration of $1 - 4$ mol% thiourea doped KDP were grown only in c– direction $\langle 001 \rangle$.

The glass ampoules were carefully mounted with individual seed crystals in the bottom. The ampoules were slowly filled with saturated solution of KDP, with the same solutions prepared for conventional slow evaporation method. Then, they were placed in a glass water container mentioned above. The temperature of a ring heater was set at $35\,^{\circ}\text{C}$. This has provided hot water for achieving a uniform solvent evaporation throughout the crystal growth experiment. The temperature gradient creates a concentration gradient along the glass ampoule, having a maximum concentration at the bottom of the ampoule and minimum at the top of the ampoule. The excess supersaturation solution by evaporation is driven down the ampoule by the gravity, thus the growth of crystal is initiated from the seed mounted at the bottom growing up to the top. After $2 - 3$ days the seed started to grow and expanded to fill cylindrical glass in about 2 weeks, and finally grew up. The average growth rate was $1 - 2$ mm/day. Figure 4.10 gives the growing crystals from the seed in different orientations of $\langle 010 \rangle$, $\langle 001 \rangle$ and $\langle 011 \rangle$.

The growth rate by SR method depended on the solubility of the material, evaporation rate, size of the growth ampoule and the density of the material, which can be obtained by

$$R_{(T)} = \frac{0.318 kSE}{r^2 d} \qquad \text{cm / day} \qquad\qquad (4.1)$$

where $k$ is the proportionality constant, $S$ is the solubility of the material (g/mL of solvent), $E$ is the evaporation rate of solvent (mL/day), $r$ is the radius of the ampoule (cm), $d$ is the density of the material ($g/cm^3$), and $T$ is the temperature (K) (Balamurugan and Ramasamy, 2006).



(a)



(b)
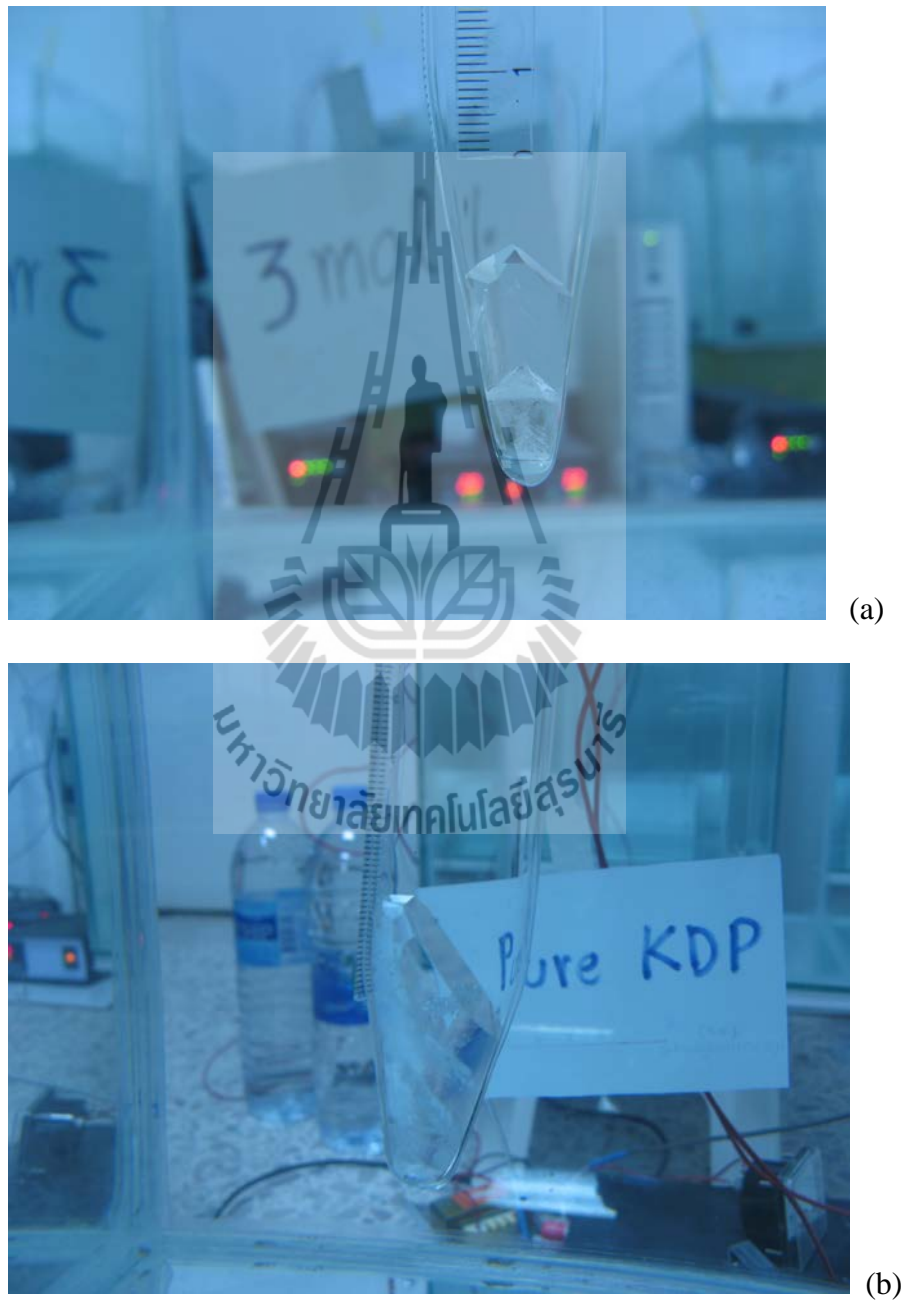
**Figure 4.10** The growing seed crystals in different orientation of (a) $\langle 001 \rangle$–direction, (b) $\langle 011 \rangle$–direction and (c) $\langle 010 \rangle$–direction.

(c)
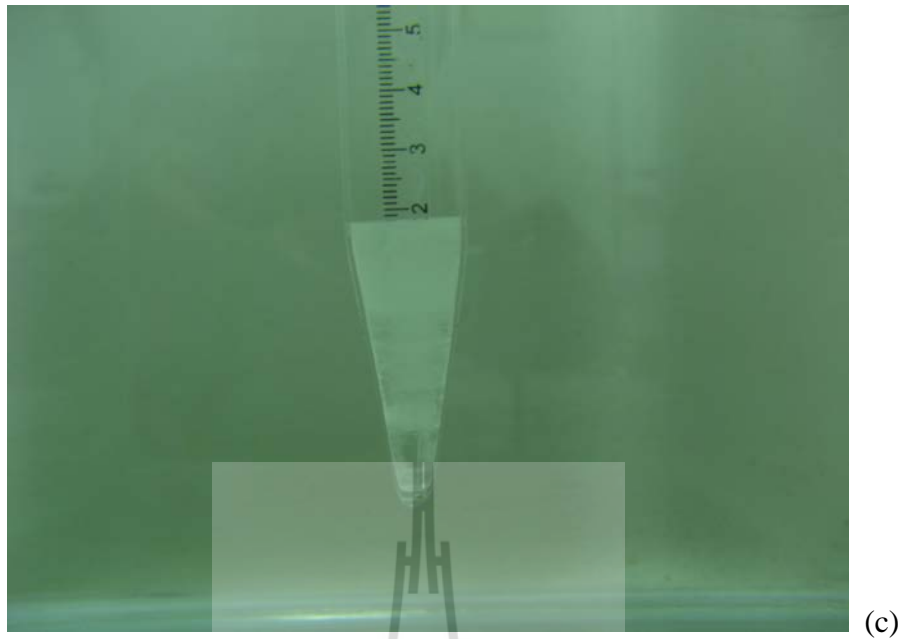
**Figure 4.10** (Continued) The growing seed crystals in different orientation of (a) $\langle 001 \rangle$–direction, (b) $\langle 011 \rangle$–direction and (c) $\langle 010 \rangle$–direction.

According to the evaporation rate of the solvent, the prepared solution was added at about 10 – 15 drops everyday. The addition of just a few drops did not seriously disturb the supersaturation or evaporation rate.

The good transparency of growing seed crystals is observed in $\langle 001 \rangle$ and $\langle 011 \rangle$–directions and poor transparency in $\langle 010 \rangle$–direction. After 2 months, the growth experiments were finished. The grown 5 mol% thiourea doped KDP crystal by SR method in glass ampoule is shown in Figure 4.11.

To take the grown crystal out of the ampoule, the diamond wheel cutter was used to carefully and slowly cut the glass (and softly broke it). The grown crystals in different orientations after taking from ampoule are displayed in Figure 4.12.

**Figure 4.11** The 5 mol% thiourea doped KDP crystals, c–direction by SR method in

glass ampoule.
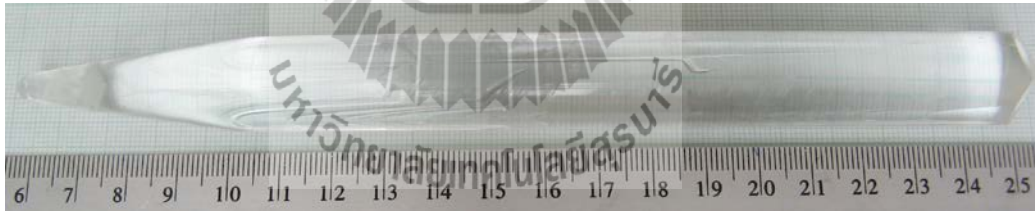


(a)
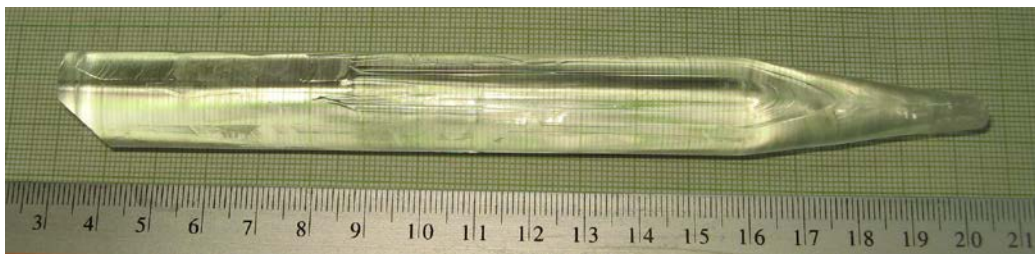


(b)

**Figure 4.12** The grown crystals by SR method in (a) $\langle 001 \rangle$–direction, (b) $\langle 011 \rangle$–

direction and (c) $\langle 010 \rangle$–direction.
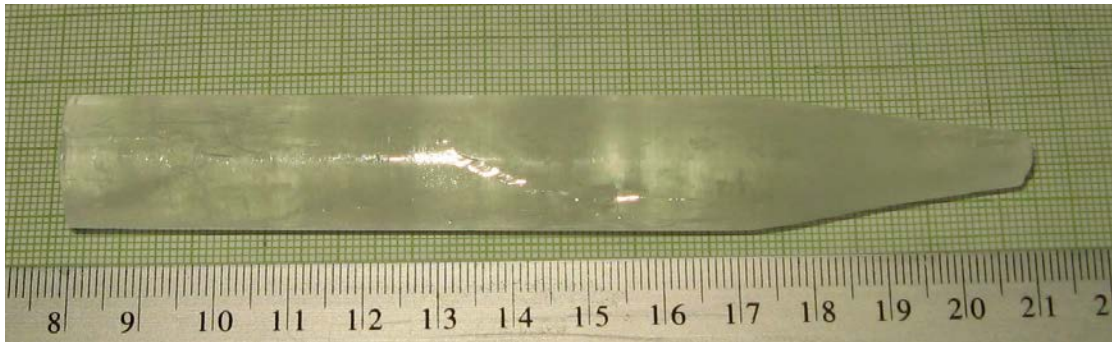
(c)

**Figure 4.12** (Continued) The grown crystals by SR method in (a) $\langle 001 \rangle$–direction,

(b) $\langle 011 \rangle$–direction and (c) $\langle 010 \rangle$–direction.

Figure 4.13 shows the ground and polished crystals by SR method with $\langle 010 \rangle$,

$\langle 001 \rangle$ and $\langle 011 \rangle$ growth directions. The good transparent crystals were observed in

$\langle 001 \rangle$ and $\langle 011 \rangle$–directions and poor transparent and fragile crystal was obtained in

$\langle 010 \rangle$–direction.
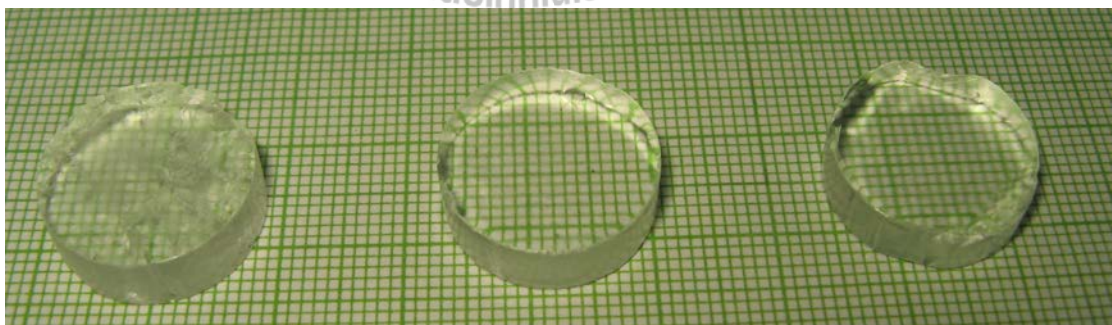


(a)                                    (b)                                    (c)

**Figure 4.13** The ground and polished crystals by SR method with (a) $\langle 010 \rangle$–direction,

(b) $\langle 001 \rangle$–direction and (c) $\langle 011 \rangle$–direction.

**Table 4.**1 the growth rate of crystal in SR method.

| Sample | Period (day) | Length (mm) | Growth rate (mm/day) |
|---|---|---|---|
| Pure KDP $\langle 001 \rangle$ | 118 | 205 | 1.74 |
| Pure KDP $\langle 010 \rangle$ | 129 | 150 | 1.16 |
| Pure KDP $\langle 011 \rangle$ | 119 | 105 | 0.88 |
| KDP + 1 mol% Thiourea | 147 | 195 | 1.33 |
| KDP + 2 mol% Thiourea | 141 | 170 | 1.21 |
| KDP + 3 mol% Thiourea | 128 | 148 | 1.15 |
| KDP + 4 mol% Thiourea | 164 | 182 | 1.11 |
| KDP + 5 mol% Thiourea $\langle 001 \rangle$ | 128 | 175 | 1.37 |
| KDP + 5 mol% Thiourea $\langle 010 \rangle$ | 122 | 130 | 1.07 |
| KDP + 5 mol% Thiourea $\langle 011 \rangle$ | 143 | 160 | 1.12 |

## 4.5 Conclusions

The bulk crystals of pure and 1 – 5 mol% thiourea doped KDP were grown by slow evaporation method and unidirectional SR method. Crystals in $\langle 001 \rangle$–direction of all concentrations and pure and 5 mol% thiourea doped KDP crystals in $\langle 011 \rangle$ and $\langle 010 \rangle$–directions were grown. The good transparent crystals grown by slow evaporation method were used as seed crystals for SR method. The average growth rate by SR method was 0.88 – 1.74 mm/day. The good transparent crystals by SR method were grown in $\langle 001 \rangle$ and $\langle 011 \rangle$–directions and the poor transparent crystals were obtained in $\langle 010 \rangle$–direction.

## 4.6 References

Balamurugan, N. and Ramasamy, P. (2006). Investigation of the Growth Rate Formula and Bulk Laser Damage Threshold KDP Crystal Growth from Aqueous Solution by the Sankaranarayanan-Ramasamy (SR) Method. **Crystal Growth and Design**. 6(7): 1642–1644.

Balamurugan, N., Lenin, M. and Ramasamy, P. (2007). Growth of potassium acid phthalate crystal by Sankaranarayanan–Ramasamy (SR) method and its optical characterization. **Materials letters**. 61: 1896–1898.

Balamurugan, N., Lenin, M., Bhagavannarayana, G. and Ramasamy, P. (2007). Growth TGS crystal using uniaxially solution-crystallization method of Sankaranarayanan–Ramasamy. **Crystal Research and Technology**. 42(2): 151–156.

Sankaranarayanan, K. (2005). Growth of large size $\langle 1\,1\,0 \rangle$ benzophenone crystal using uniaxially solution-crystallization method of Sankaranarayanan–Ramasamy (SR). **Journal of Crystal Growth**. 284(1-2): 203–208.

Sankaranarayanan, K. and Ramasamy, P. (2005). Unidirectional seeded single crystal growth from solution of benzophenone. **Journal of Crystal Growth**. 280(3–4): 467–473.

Sethuraman, K., Ramesh Babu, R., Gopalakrishnan, R. and Ramasamy, P. (2006). Unidirectional growth of $\langle 1\,1\,0 \rangle$ ammonium dihydrogen orthophosphate single crystal by Sankaranarayanan–Ramasamy method. **Journal of Crystal Growth**. 294(2): 349–352.

# CHAPTER V

# CHARACTERISATION AND COMPARISON OF PURE AND THIOUREA-DOPED KDP SINGLE CRYSTALS GROWN BY CONVENTIONAL SLOW EVAPORATION AND SR METHODS

## 5.1 Introduction

In this chapter, pure and thiourea doped KDP crystals grown by slow evaporation solution and SR growth techniques were reported. The grown crystals had been analyzed by different characterization techniques. The results were elaborated in the coming sections.

## 5.2 X–Ray Powder Diffraction Studies

### 5.2.1 Sample Preparations

X–ray powder diffraction pattern was recorded by a BRUKER AXS D5005 system from The Center for Scientific and Technological Equipment, Suranaree University of Technology. The X–ray system with $CuK_\alpha$ $(\lambda = 1.5406 \overset{\circ}{A})$ using a voltage and current of 40 kV and 40 mA, respectively. The X–ray powder diffraction patterns of pure and thiourea–doped KDP crystals grown from conventional slow evaporation and SR methods were investigated. The samples were collected from the

individual grown crystals and ground using a mortar and pestle in order to determine the crystal phases by XRD. The sample was scanned over the range $10^{\circ} - 70^{\circ}$ at a rate of $0.02^{\circ}$ per step with step time 0.2 s. The $2\theta : \theta$ type of goniometer was used.

### 5.2.2 Results and discussions

The powder diffraction patterns of pure and thiourea doped KDP crystals are shown in Figure 5.1.
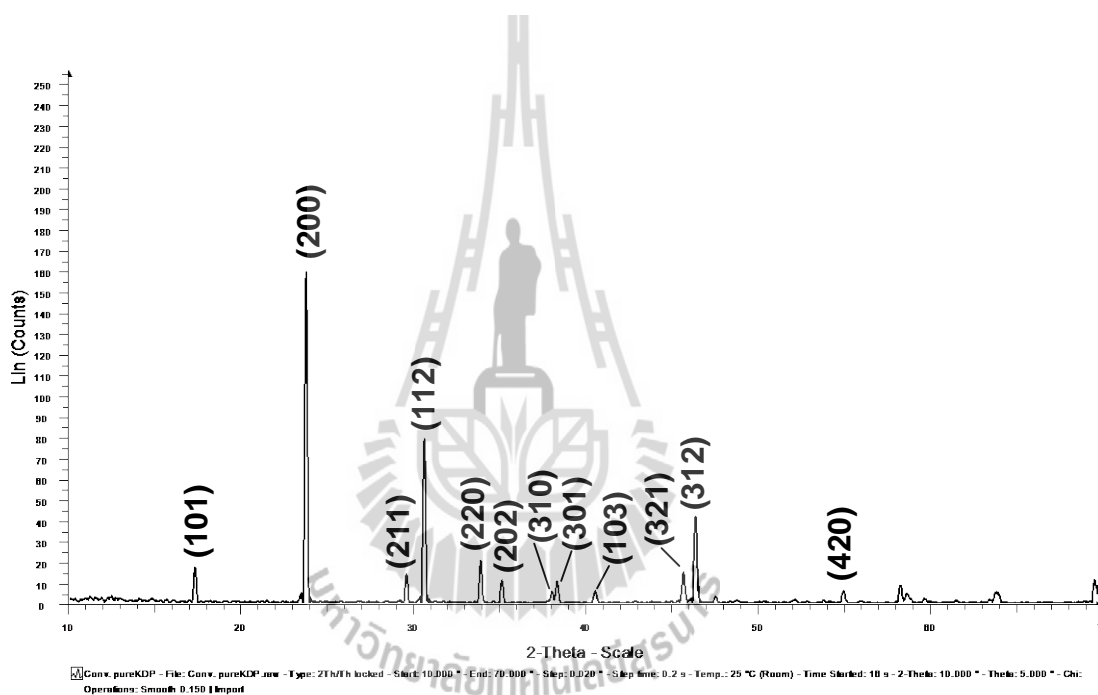


(a) XRD pattern of pure KDP grown by conventional slow evaporation method.

**Figure 5.1** The X–ray powder diffraction patterns of the grown crystals (a) – (l).
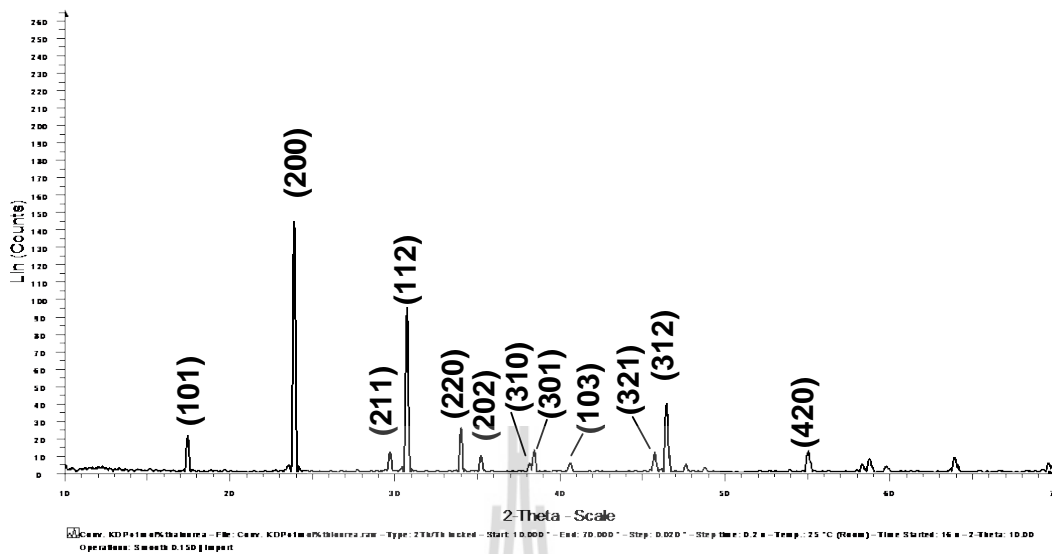
(b) XRD pattern of pure KDP + 1 mol% thiourea grown by conventional slow

evaporation method.
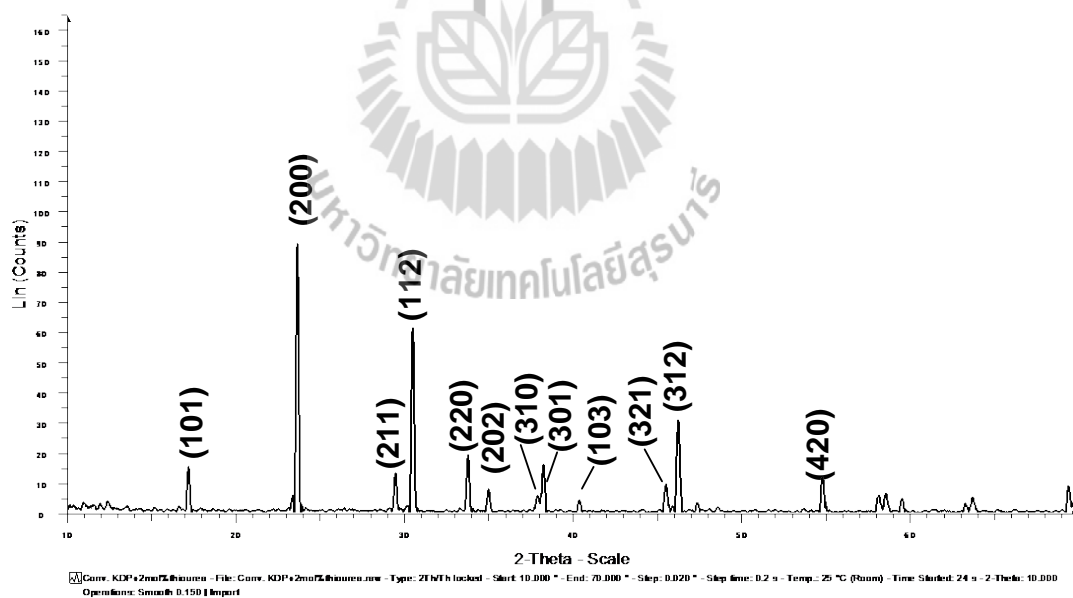


(c) XRD pattern of KDP + 2 mol% thiourea grown by conventional slow

evaporation method.

**Figure 5.1** (Continued) The X–ray powder diffraction patterns of the grown crystals

(a) – (l).
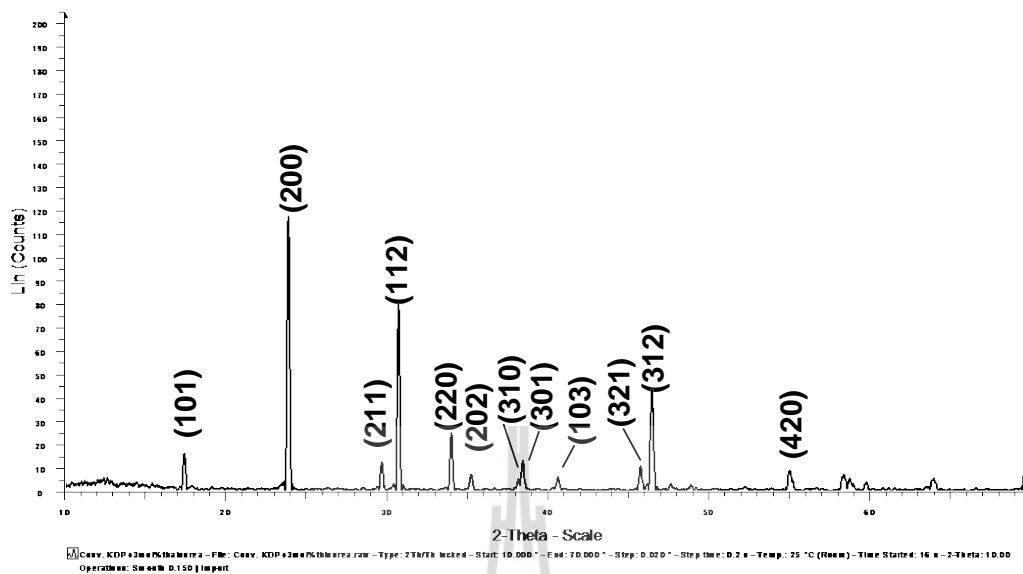
(d) XRD pattern of KDP + 3 mol% thiourea grown by conventional slow evaporation method.
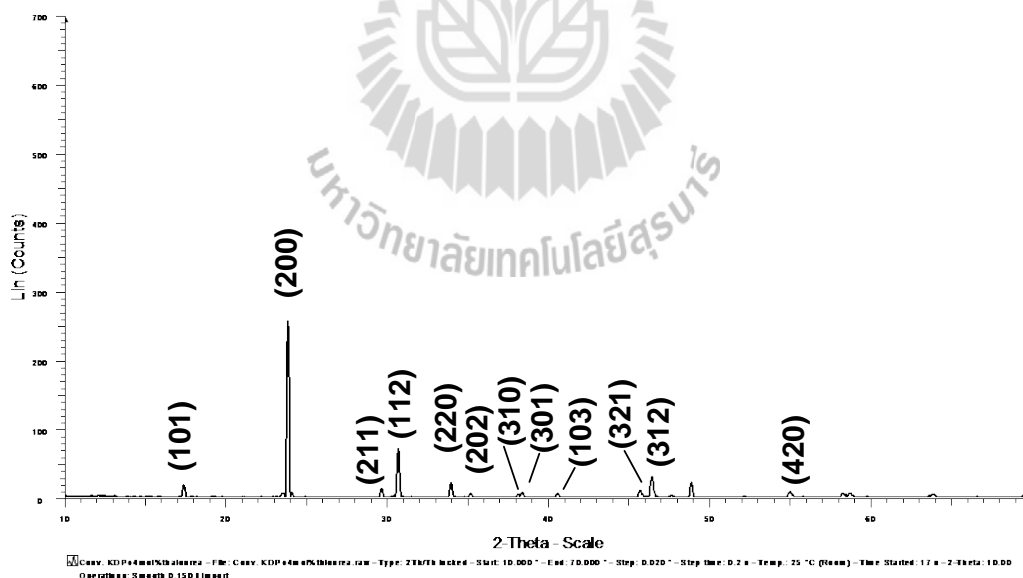


(e) XRD pattern of KDP + 4 mol% thiourea grown by conventional slow evaporation method.

**Figure 5.1** (Continued) The X–ray powder diffraction patterns of the grown crystals (a) – (l).
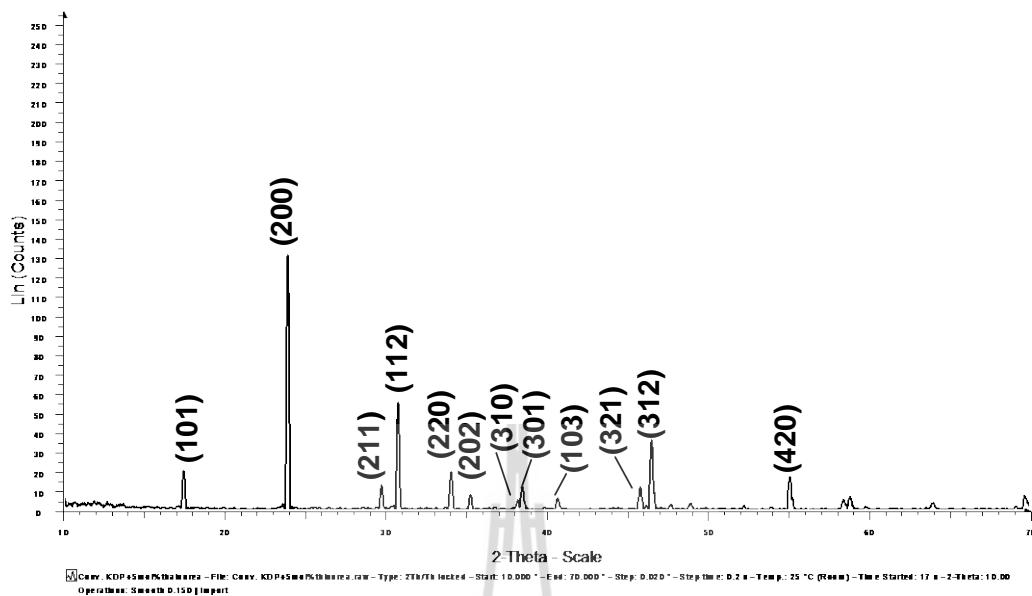
(f) XRD pattern of KDP + 5 mol% thiourea grown by conventional slow
evaporation method.
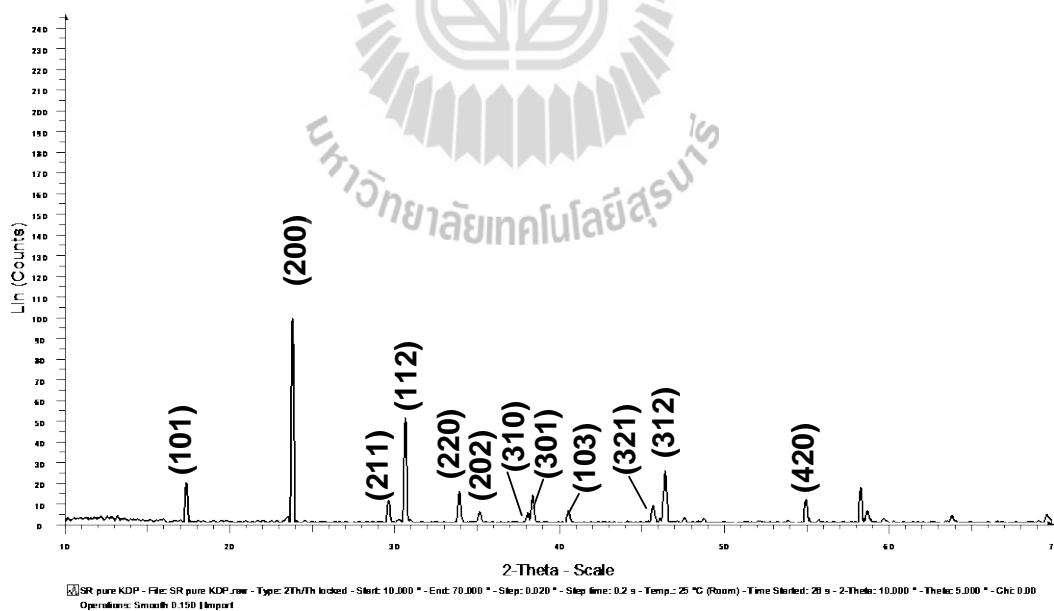


(g) XRD pattern of pure KDP grown by SR method.

**Figure 5.1** (Continued) The X–ray powder diffraction patterns of the grown crystals

(a) – (l).
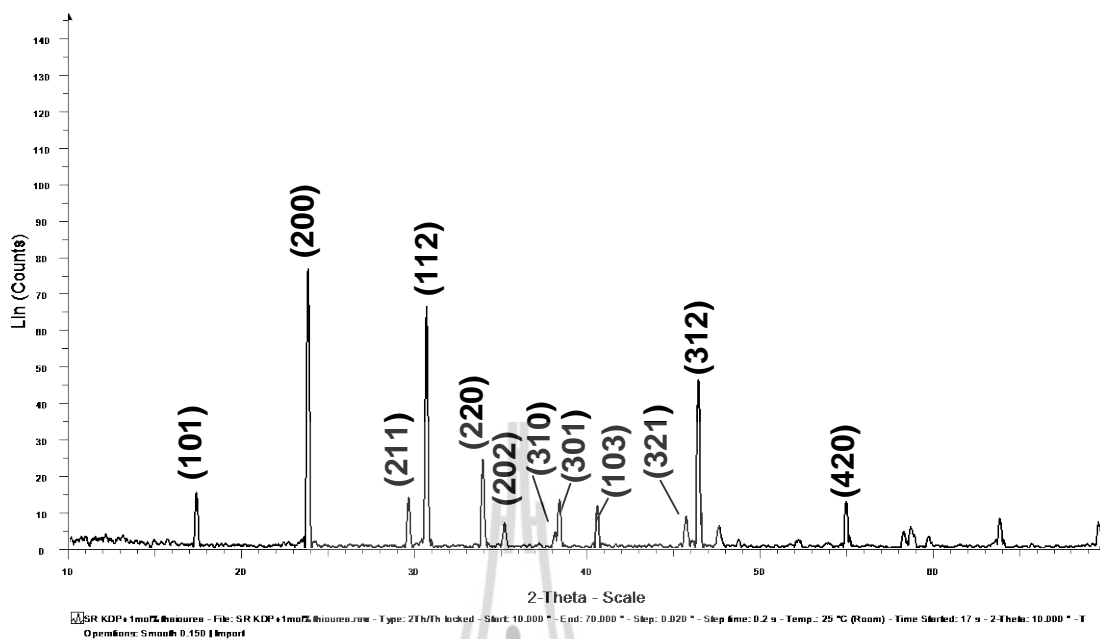
(h) XRD pattern of KDP + 1 mol% thiourea grown by SR method.
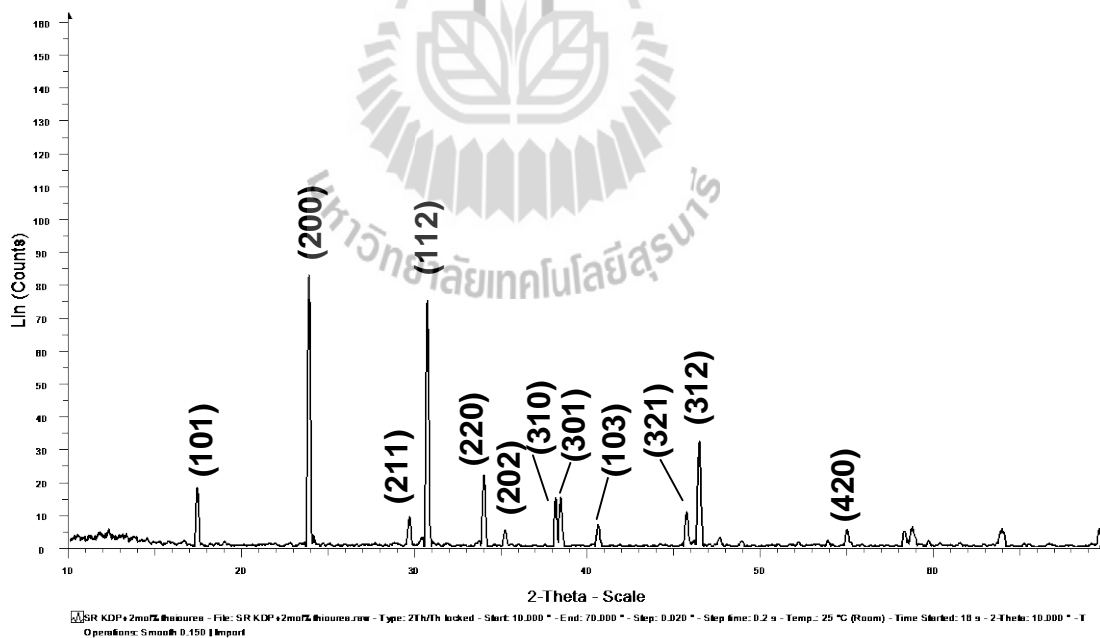


(i) XRD pattern of KDP + 2 mol% thiourea grown by SR method.

**Figure 5.1** (Continued) The X–ray powder diffraction patterns of the grown crystals

(a) – (l).
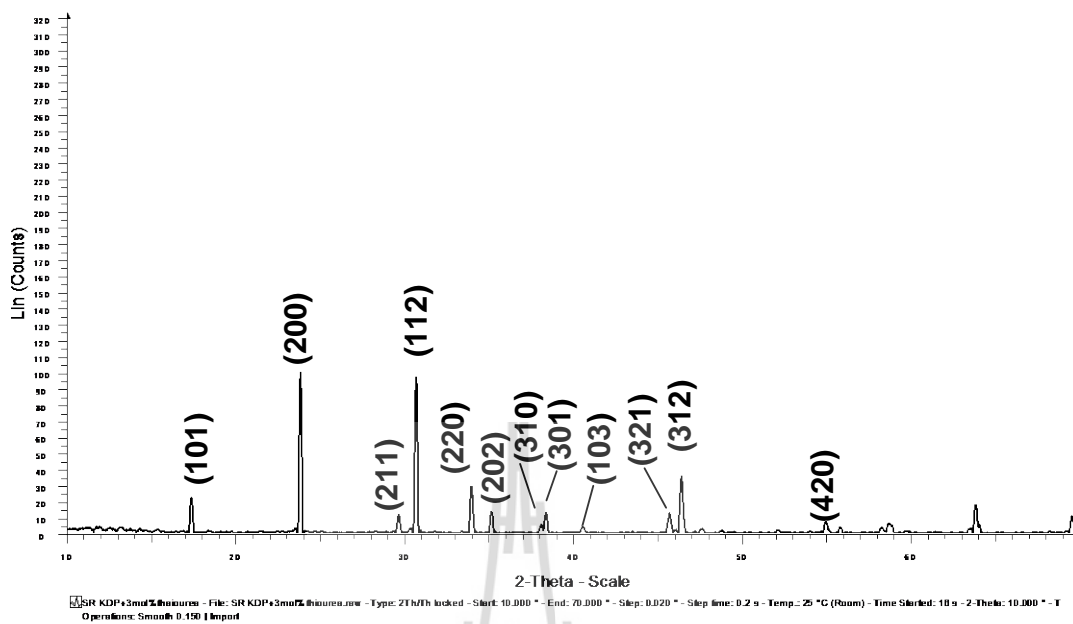
(j) XRD pattern of KDP + 3 mol% thiourea grown by SR method.
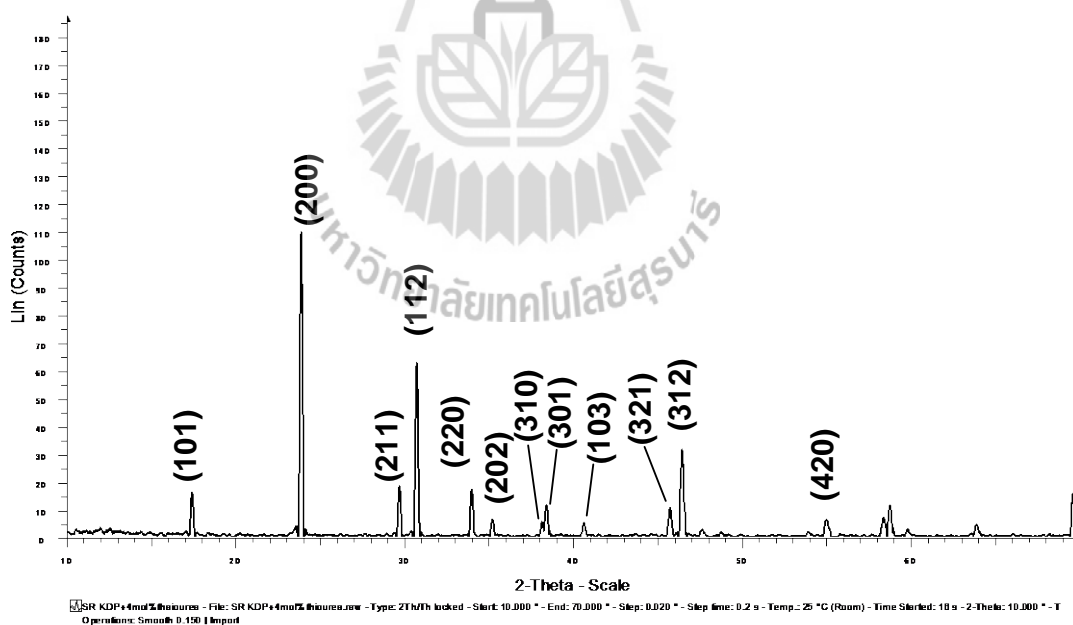


(k) XRD pattern of KDP + 4 mol% thiourea grown by SR method.

**Figure 5.1** (Continued) The X–ray powder diffraction patterns of the grown crystals

(a) – (l).
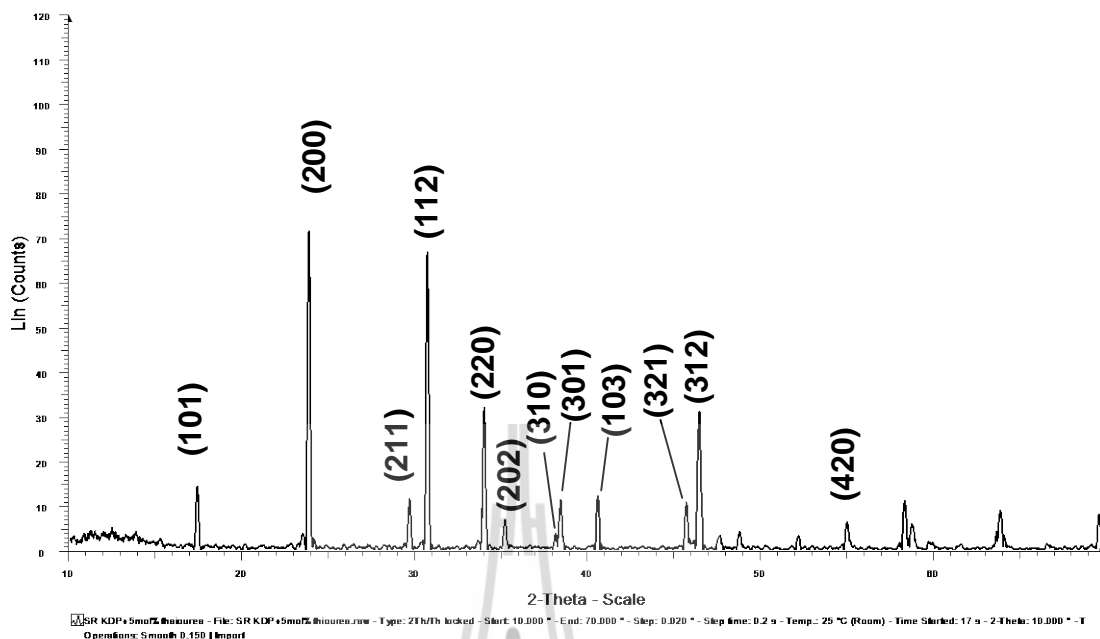
(l) XRD pattern of KDP + 5 mol% thiourea grown by SR method.

**Figure 5.1** (Continued) The X–ray powder diffraction patterns of the grown crystals

(a) – (l).

All of the powder diffraction patterns of pure and thiourea doped KDP crystals correspond to the standard peaks of KDP from ICSD, ("inorganic crystal structures database") as shown in Figure 5.1(a) – (l). The unit cell dimensions of standard ICSD collection code no. 201119 are $a = b = 7.45240 \overset{\circ}{A}$ and $c = 6.97500 \overset{\circ}{A}$. No peaks of thiourea were observed because the amount of thiourea was very small.

The unit cell parameters of pure and doped crystals were determined by comparisons with standard peaks data. The unit cell parameters are listed in Table 5.1

Since the lattice structure of KDP is a body–centered tetragonal system, the unit cell parameters or lattice parameters could be calculated from equation (3.1) $2d_{hkl}\sin\theta = n\lambda$. Let $n=1$, it becomes,

$$\frac{1}{d_{hkl}^2} = \frac{4\sin^2\theta}{\lambda^2} \tag{5.1}$$

The crystal parameters of tetragonal system are according to table 3.1,

$$\frac{1}{d_{hkl}^2} = \frac{h^2+k^2}{a^2} + \frac{l^2}{c^2} \tag{5.2}$$

The 12 peaks were used for calculation of the unit cell parameters and unit cell volume in this work. The parameter $a$ found from $h\,k\,0$ indices of 200, 220, 310 and 420, then equation (5.2) becomes,

$$\frac{1}{d_{hk0}^2} = \frac{h^2+k^2}{a^2}$$

Then

$$a = d_{hk0}\sqrt{(h^2+k^2)} \tag{5.3}$$

The parameter $a$ was calculated from given peaks and then averaged to be used for calculating parameter $c$. The parameter $c$ obtained from equation (5.2) with 8 peaks of 101, 211, 112, 202, 301, 103, 321and 312. The unit cell volume was obtained from $a^2 \cdot c$. The lattice parameters and unit cell volume of grown single crystals are given in Table 5.1.

The obtained lattice parameters values are in good agreement with the reported values from ICSD.

**Table 5.1** The lattice parameters and unit cell volume of grown single crystal**.**

| Growth method | Crystal | Lattice parameters | | unit cell Volume ($\mathring{A}^3$) |
|---|---|---|---|---|
| | | a = b ($\mathring{A}$) | c ($\mathring{A}$) | |
| Conventional slow evaporation method | Pure KDP | 7.4790 | 6.9802 | 390.4449 |
| | KDP + 1 mol% Thiourea | 7.4561 | 6.9871 | 388.4360 |
| | KDP + 2 mol% Thiourea | 7.5047 | 6.9940 | 393.8988 |
| | KDP + 3 mol% Thiourea | 7.4566 | 6.9832 | 388.2795 |
| | KDP + 4 mol% Thiourea | 7.4654 | 6.9976 | 389.9893 |
| | KDP + 5 mol% Thiourea | 7.4528 | 6.9888 | 388.1841 |
| S R method | Pure KDP | 7.4736 | 6.9819 | 389.9723 |
| | KDP + 1 mol% Thiourea | 7.4654 | 6.9920 | 389.6860 |
| | KDP + 2 mol% Thiourea | 7.4534 | 6.9855 | 388.0723 |
| | KDP + 3 mol% Thiourea | 7.4616 | 6.9934 | 390.4044 |
| | KDP + 4 mol% Thiourea | 7.4616 | 6.9841 | 388.8481 |
| | KDP + 5 mol% Thiourea | 7.4523 | 6.9786 | 387.5678 |

## 5.3 High–Resolution X–Ray Diffraction studies

### 5.3.1 Sample preparations

High–Resolution X–Ray Diffraction (HRXRD) was also employed to investigate the pure and 5 mol% thiourea doped KDP crystals grown by SR method. The samples for HRXRD were cut of the tip of single crystals with the size of $0.5 \times 0.5 \times 0.5 \ cm^3$.

### 5.3.2 Results and discussions

#### 5.3.2.1 Pure KDP single crystal

Figure 5.2 shows the high-resolution diffraction/rocking curve (RC) recorded for a typical SR–grown undoped KDP single crystal specimen using (200) diffracting planes in symmetrical Bragg geometry by employing the multicrystal X–ray diffractometer described above with $MoK_{\alpha1}$ radiation. As seen in the figure, the RC is quite sharp without any satellite peaks which may otherwise be observed either due to internal structural grain boundaries (Bhagavannarayana, Ananthamurthy, Budakoti, Kumar and Bartwal, 2005) or due to epitaxial layer which may sometimes form in crystals grown from solution (Bhagavannarayana, Parthiban and Subbiah Meenakshisundaram, 2006). The full width at half maximum (FWHM) of the diffraction curve is 6 arc sec, which is close to that expected from the plane wave theory of dynamical X–ray diffraction (Betterman and Cole, 1964). The single sharp diffraction curve with very low FWHM indicates that the crystalline perfection is quite good. The specimen is a nearly perfect single crystal without having any internal structural grain boundaries.
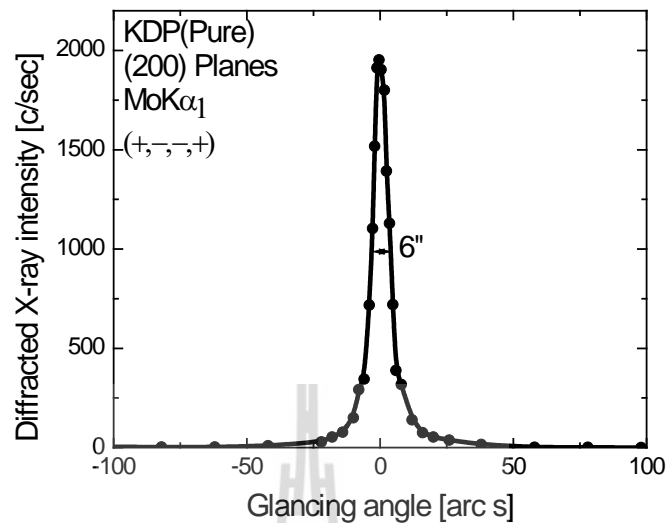
**Figure 5.2** High–resolution X–ray diffraction curve recorded for a SR–grown pure

KDP single crystal specimen using (200) diffracting planes.

**5.3.2.2 Thiourea doped KDP single crystal**

Figure 5.3 shows the RC of the SR-grown thiourea doped KDP specimen

recorded under identical experimental conditions as that of Figure 5.2. As seen in the

Figure, the RC contains a single sharp peak and indicates that the specimen is free

from structural grain boundaries. The FWHM (full width at half maximum) of the

curve is 27 arc sec which is somewhat more than that expected from the plane wave

theory of dynamical X–ray diffraction (Battermanand Cole, 1964) for an ideally

perfect crystal. The broadening of rocking curve without the presence of any splitting

can be attributed to variety of defects like randomly oriented mosaic blocks,

dislocations, point defects or Frankel defects (simultaneous existence of vacancies as

well as interstitial defects) etc. But depending upon the nature of asymmetry, as

investigated in the earlier as well as recent articles, one can expect predominant

occupation of vacancy or interstitial defects (Lal and Bhagavannarayana, 1989; Bhagavannarayana, Choubey, Shubin and Krishan Lal, 2005; Bhagavannarayana, Parthiban and Meenakshisundaram, 2008; Bhagavannarayana, Rajesh and Ramasamy, 2010; Bhagavannarayana, Kushwaha, Shakir, Mohd and Maurya, 2011; Senthilkumar, MoorthyBabu and Bhagavannarayana, 2011) which can be realized in the following way. As seen in Figure 5.3, for a particular angular deviation ($\Delta\theta$) of glancing angle with respect to the peak position, the scattered intensity is much more in the positive direction in comparison to that of the negative direction. This feature clearly indicates that the crystal contains predominantly interstitial type of defects than that of vacancy defects. This can be well understood by the fact that due to interstitial defects, as shown schematically in the inset, the lattice around these defects undergo tensile stress and the lattice parameter $d$ (interplanar spacing) increases and leads to give more scattered (also known as diffuse X–ray scattering) intensity at slightly higher Bragg angles ($\theta_B$) as d and $\sin \theta_B$ are inversely proportional to each other in the Bragg equation ($2d \sin \theta_B = n\lambda$; $n$ and $\lambda$ being the order of reflection and wavelength respectively which are fixed). However, these point defects with much lesser density as in the present case hardly give any effect on the performance of the devices based on such crystals. If the concentration is high, the FWHM would be much higher and often lead to structural grain boundaries and deteriorate the important directional dependent physical properties like second harmonic generation efficiency (Bhagavannarayana, Parthiban and Meenakshisundaram, 2008). Therefore, from the above discussion based on experimental observation of asymmetry in the RC, one can conclude that some amount of thiourea is incorporated inside the crystal

matrix. A detailed investigation of FT–IR on urea doped ZTS crystal confirmed such

incorporation (Bhagavannarayana and Kushwaha, 2010).
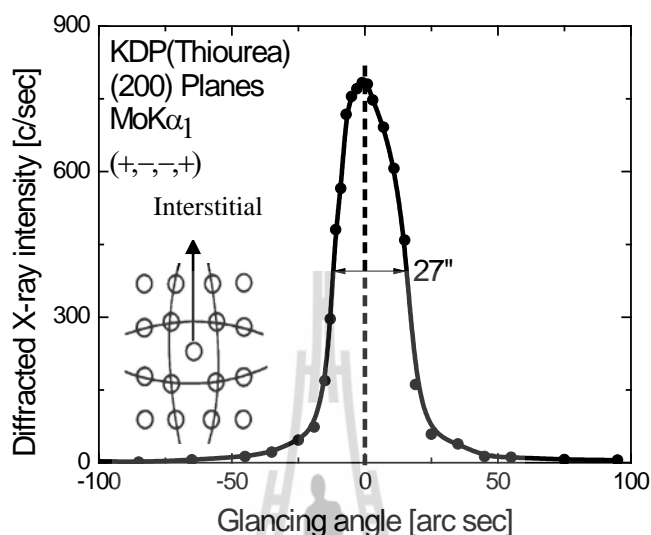


**Figure 5.3** High-resolution X–ray diffraction curve recorded for a typical thiourea–

doped KDP single crystal specimen using (200) diffracting planes.

## 5.4 Fourier transform infrared spectroscopy studies

### 5.4.1 Sample Preparations

Fourier transform infrared (FT–IR) spectrum of grown KDP crystal was

carried out in the middle IR region between the wave number 650 – 4000 $cm^{-1}$ at a

resolution of $\pm 1$ $cm^{-1}$ by using Spectrum 100 PerkinElmer Fourier transform

infrared spectrometer form Faculty of Sciences and Liberal Arts, Rajamangala

University of Technology Isan. The FT–IR spectrometer with attenuated total

reflectance (ATR) technique was used confirm the functional groups. This technique

used small amount of the powder of samples. The samples were collected from the

grown crystals and ground using a mortar and pestle.

**5.4.2 Results and discussions**

The FT–IR spectra of the grown crystals of pure and thiourea doped KDP crystals are shown in Figures 5.4. A strong band occurring at about 1,280 $cm^{-1}$ is due to the P=O stretching vibrations of KDP crystals. A strong band present at about 865 $cm^{-1}$ is assigned to P–O–H stretching vibrations. A strong band occurring at about 1,080 $cm^{-1}$ is contribution of P–stretching vibrations. Wide band occurring at about 1400 – 1800 $cm^{-1}$ is contribution of OP–O–H stretching vibrations. Band of very weak intensity is observed at 3,614 $cm^{-1}$ in the FT–IR spectra which is due to free O–H stretching hydrogen bond of KDP. Weak bands appearing around 2,800 and 2,400 $cm^{-1}$ are due to P–O–H symmetric stretching and bending, respectively (Balamurugan and Ramasamy, 2009; Dhanaraj, Mahadevan, Bhagavannarayana, Ramasamy and Rajesh, 2008). Some FT–IR spectral frequencies of the grown crystals are shown in Table 5.2.
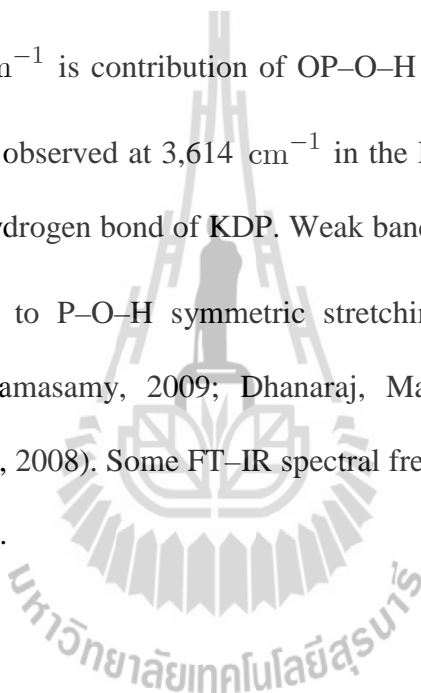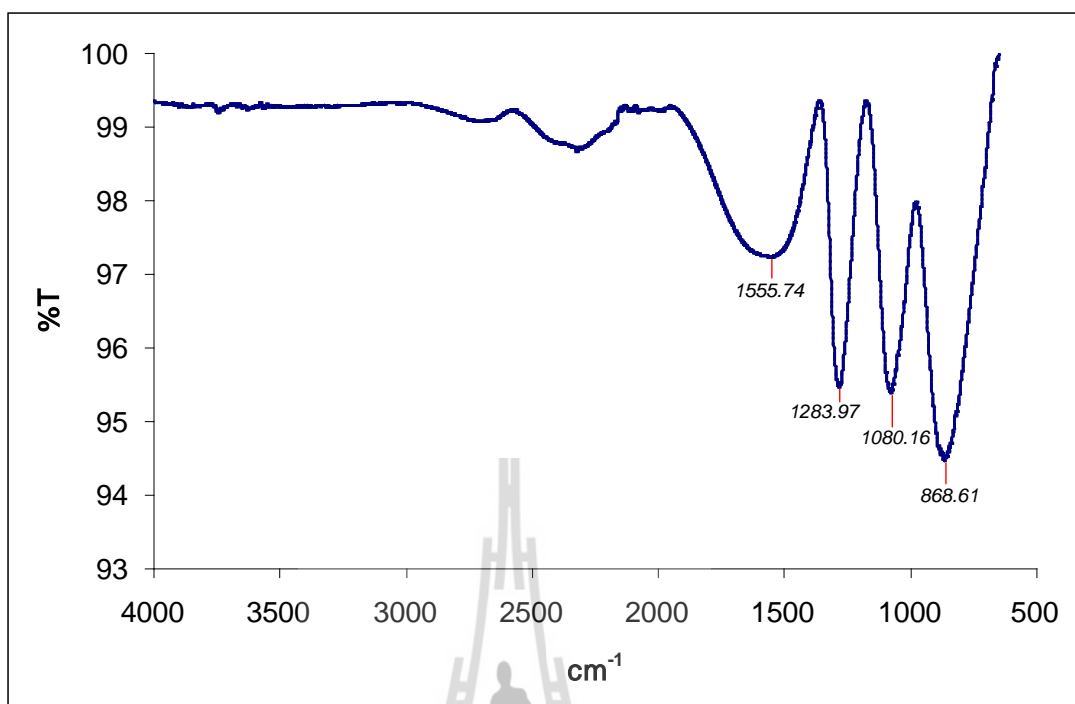
(a) Conventional slow evaporation method of pure KDP.
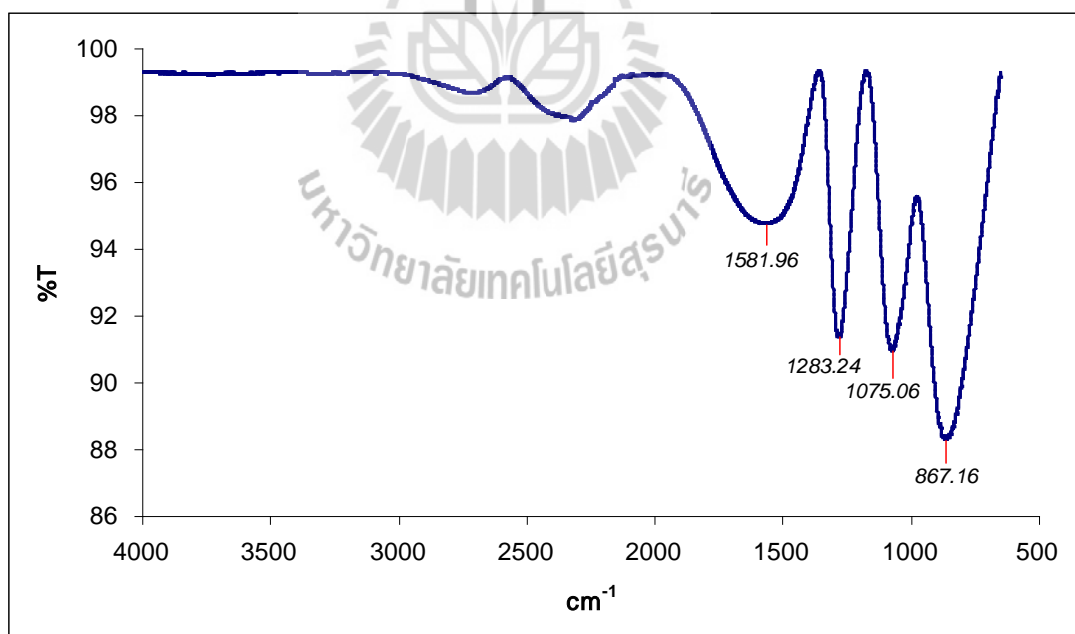


(b) Conventional slow evaporation method of KDP + 1 mol% thiourea.

**Figure 5.4** The FT–IR spectra of the grown crystals (a) – (l).
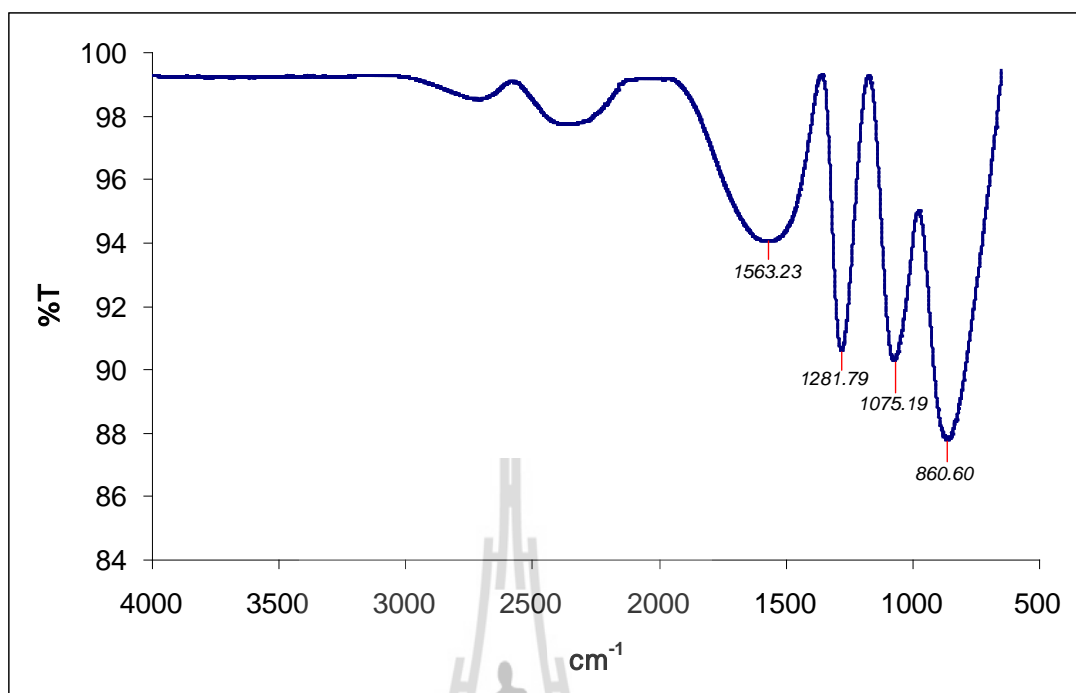
(c) Conventional slow evaporation method of KDP + 2 mol% thiourea.
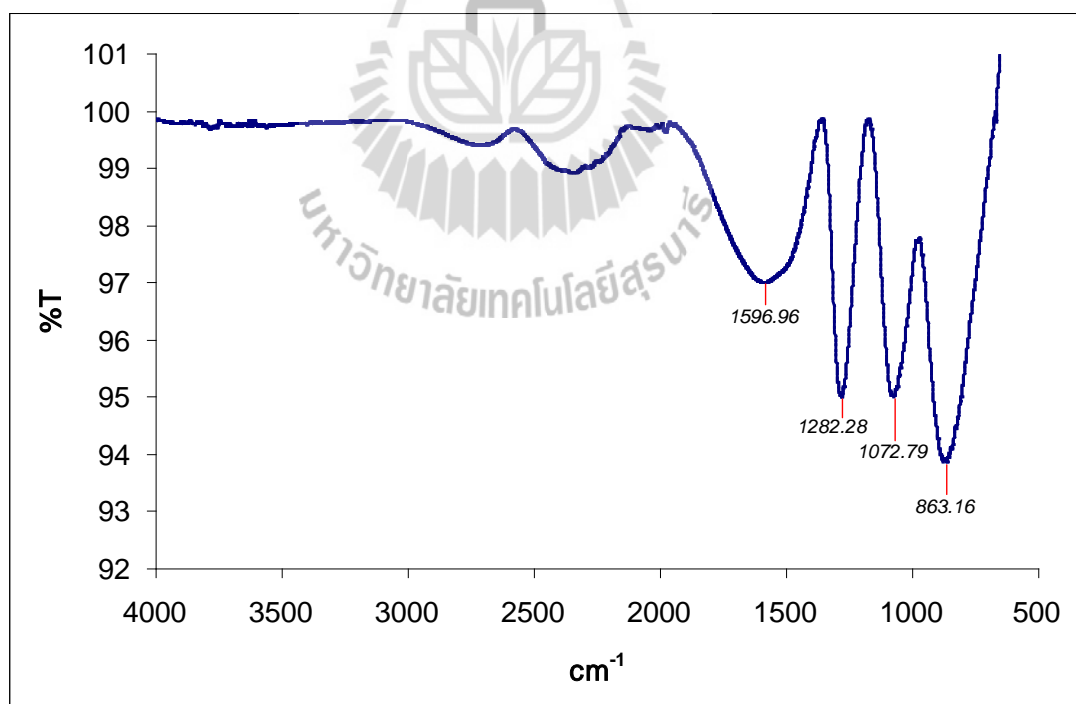


(d) Conventional slow evaporation method of KDP + 3 mol% thiourea.

**Figure 5.4** (Continued) The FT–IR spectra of the grown crystals (a) – (l).
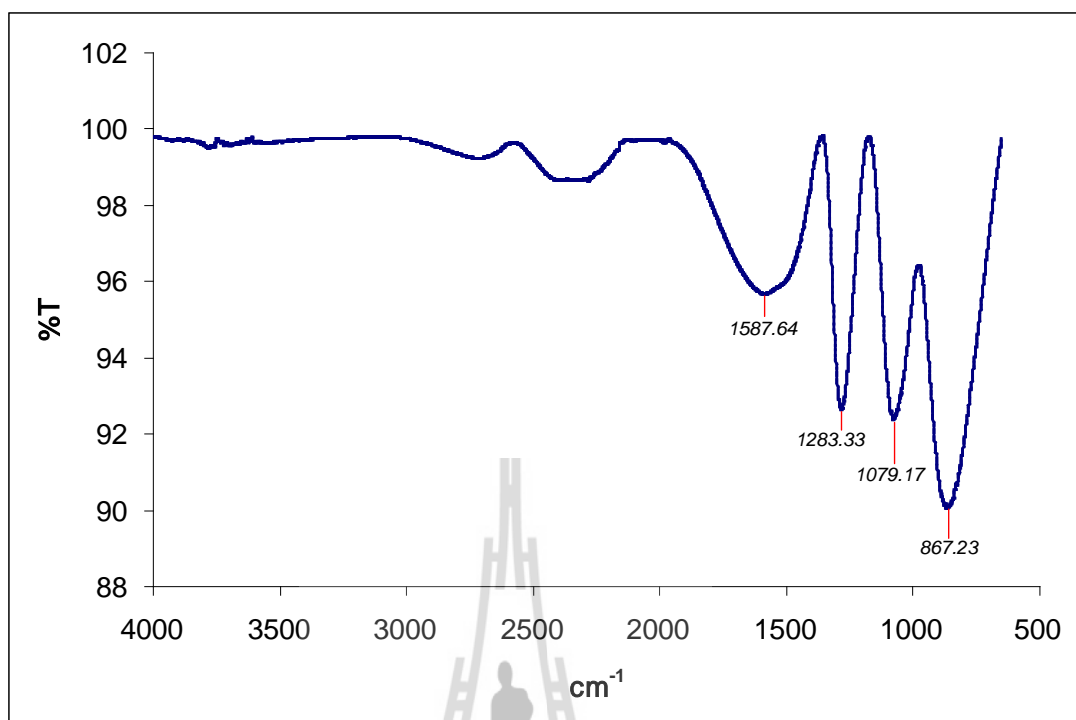
(e) Conventional slow evaporation method of KDP + 4 mol% thiourea.
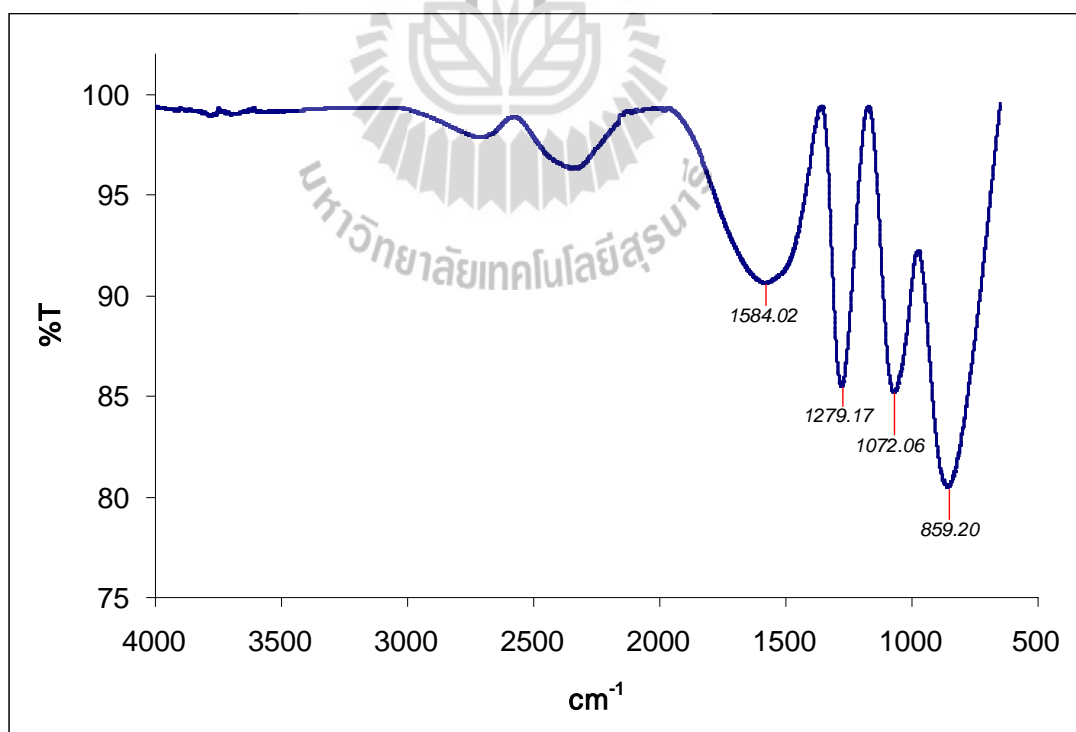


(f) Conventional slow evaporation method of KDP + 5 mol% thiourea.

**Figure 5.4** (Continued) The FT–IR spectra of the grown crystals (a) – (l).
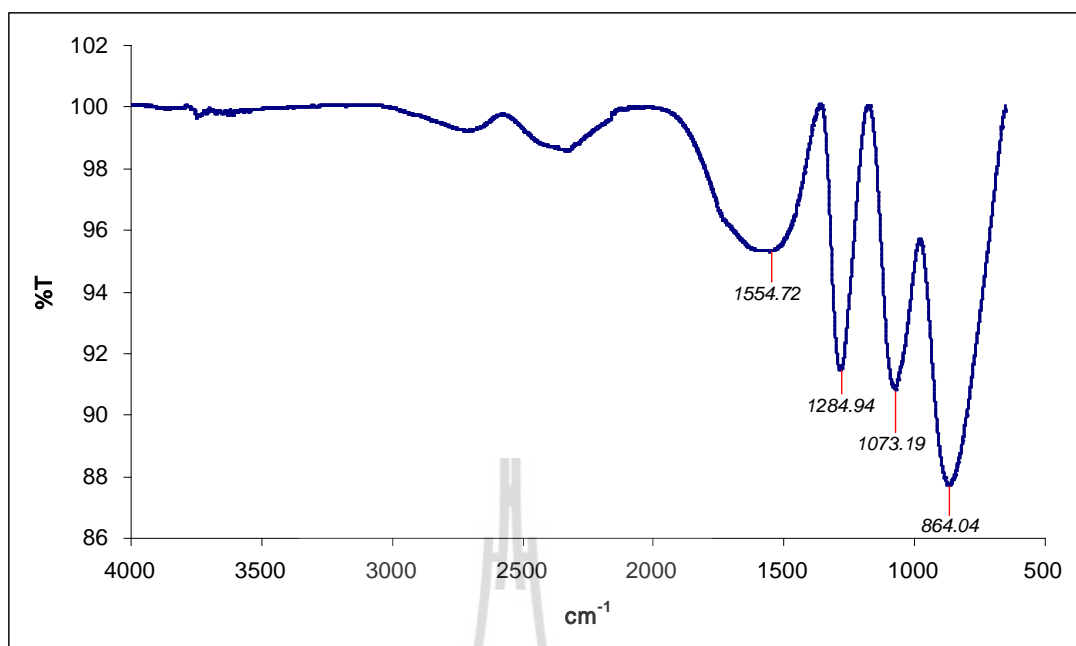
(g) SR method of pure KDP.
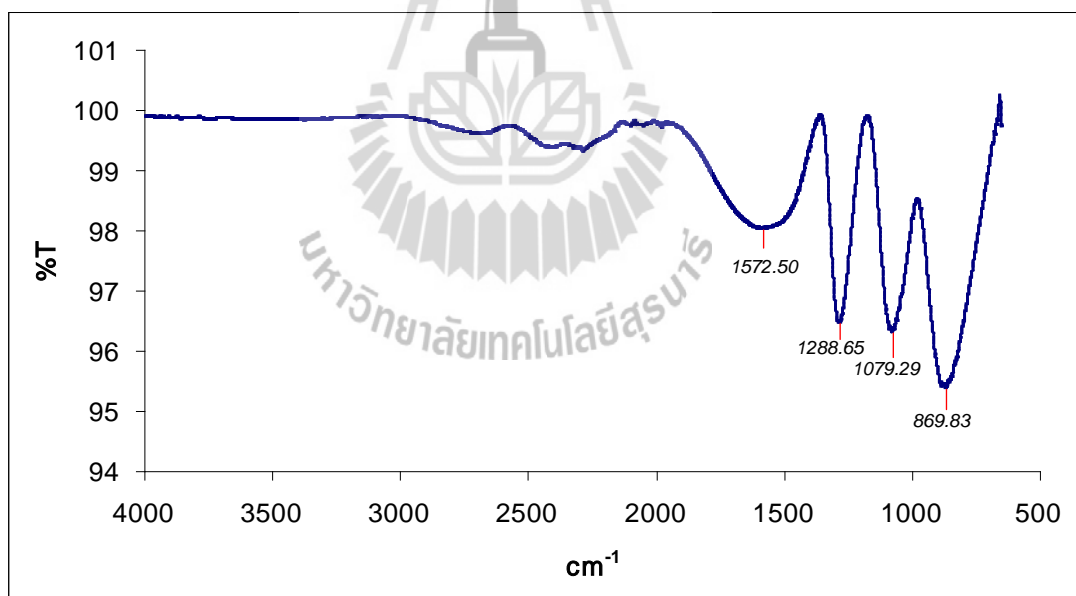


(h) SR method of KDP + 1 mol% thiourea.

**Figure 5.4** (Continued) The FT–IR spectra of the grown crystals (a) – (l).
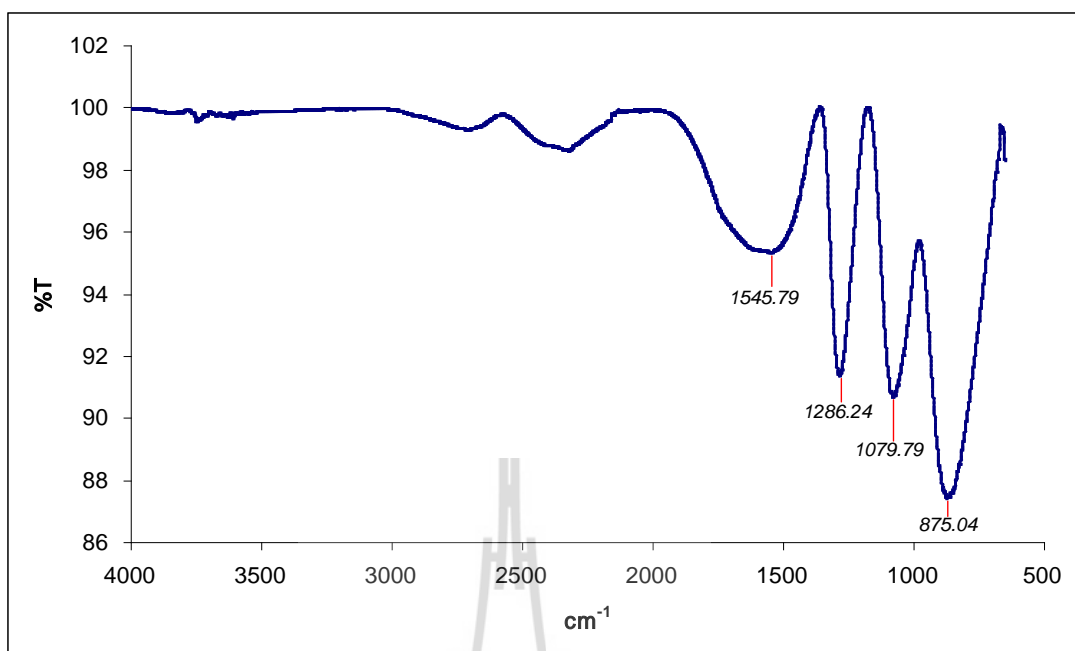
(i) SR method of KDP + 2 mol% thiourea.
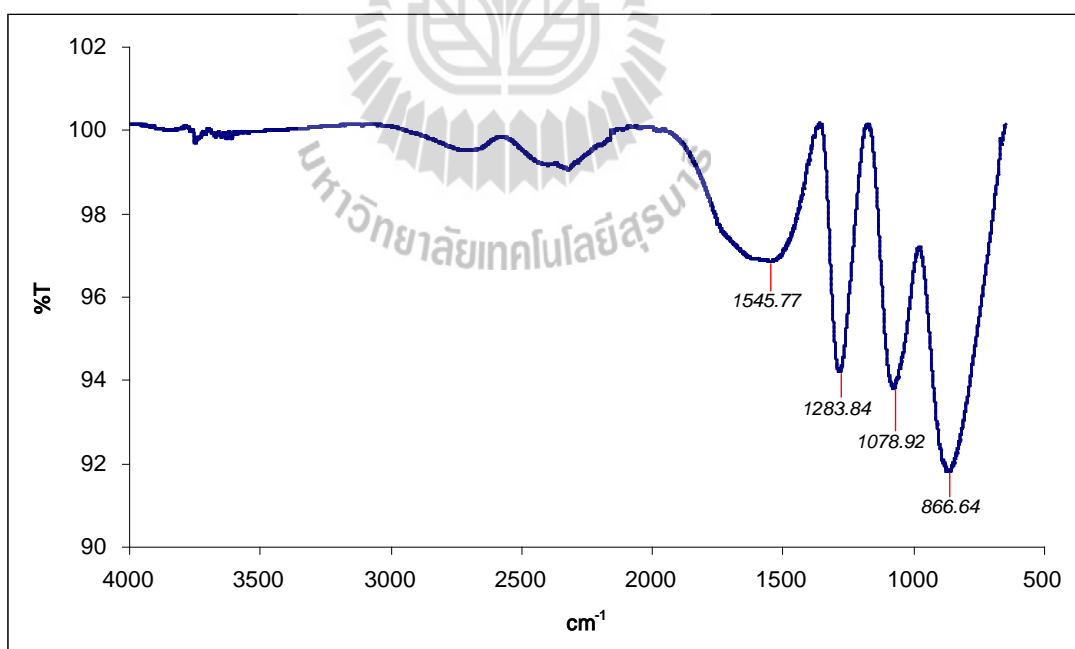


(j) SR method of KDP + 3 mol% thiourea.

**Figure 5.4** (Continued) The FT–IR spectra of the grown crystals (a) – (l).
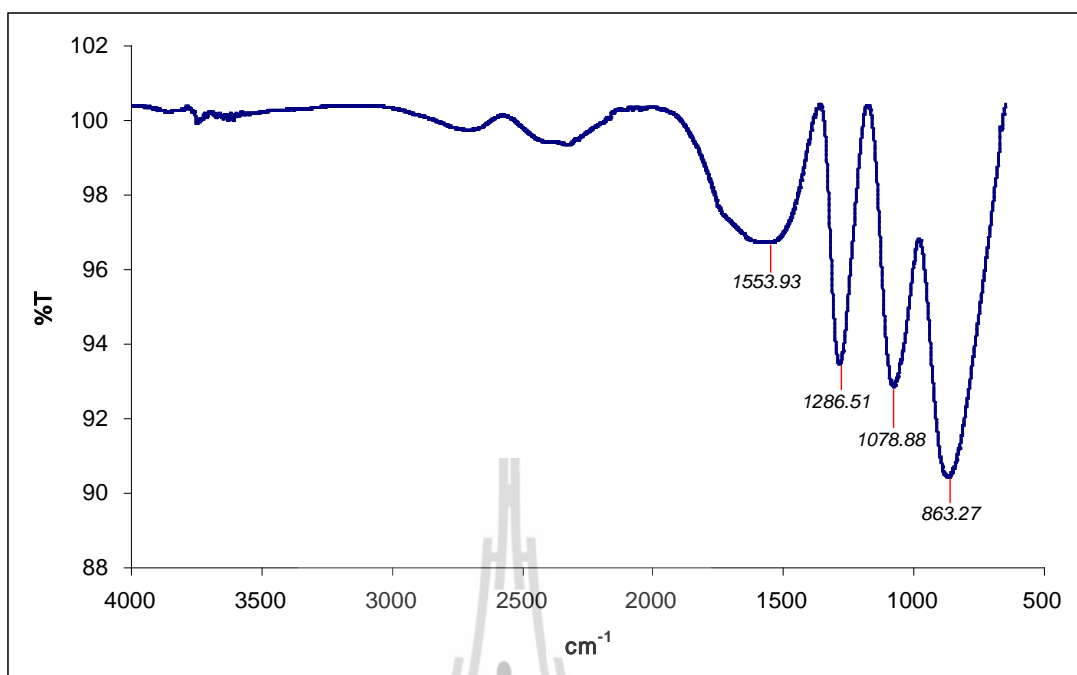
(k) SR method of KDP + 4 mol% thiourea.
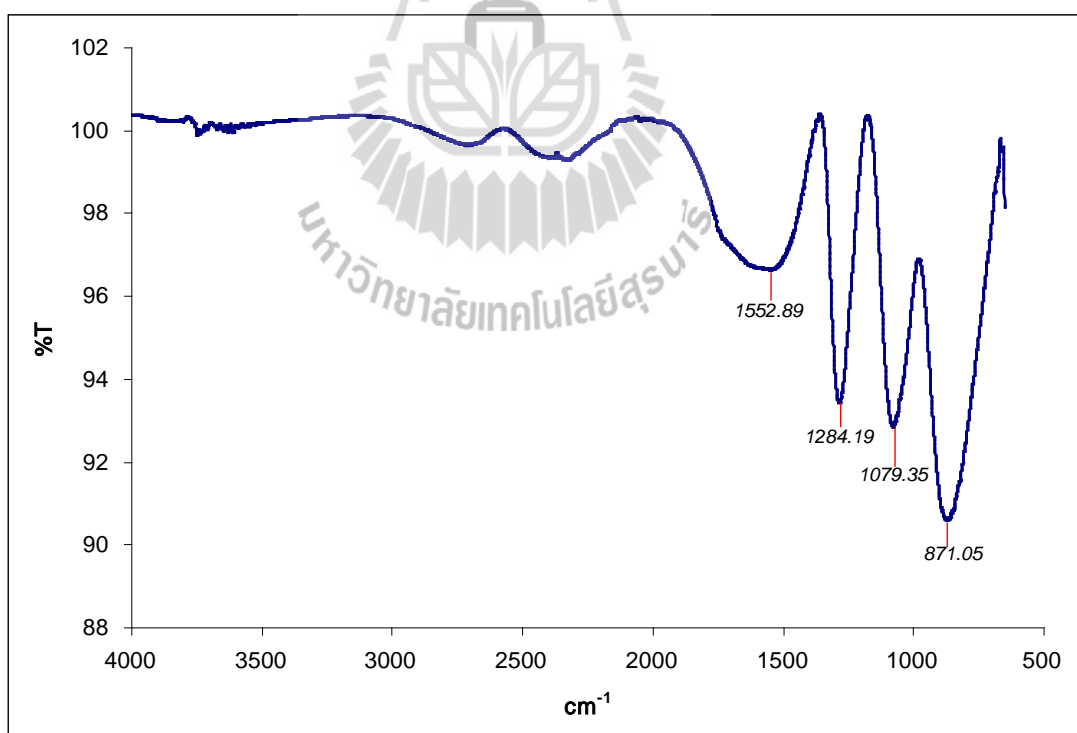


(l) SR method of KDP + 5 mol% thiourea.

**Figure 5.4** (Continued) The FT–IR spectra of the grown crystals (a) – (l).

**Table 5.2** The FT–IR spectra of grown single crystal.

| | Crystal | P–O–H Stretching ($cm^{-1}$) | P– Stretching ($cm^{-1}$) | P=O stretching ($cm^{-1}$) | OP–O–H stretching ($cm^{-1}$) |
|---|---|---|---|---|---|
| | Pure KDP | 868.61 | 1080.16 | 1283.97 | 1555.74 |
| Conventional method | KDP+1 mol% | 867.16 | 1075.06 | 1283.24 | 1581.96 |
| | KDP+2 mol% | 860.60 | 1075.19 | 1281.79 | 1563.23 |
| | KDP+3 mol% | 863.16 | 1072.79 | 1282.28 | 1596.96 |
| | KDP+4 mol% | 867.23 | 1079.17 | 1283.33 | 1587.64 |
| | KDP+5 mol% | 859.20 | 1072.06 | 1279.17 | 1584.02 |
| | Pure KDP | 864.04 | 1073.19 | 1284.94 | 1554.72 |
| S R method | KDP+1 mol% | 869.83 | 1079.29 | 1288.65 | 1572.50 |
| | KDP+2 mol% | 875.04 | 1079.79 | 1286.24 | 1545.79 |
| | KDP+3 mol% | 866.64 | 1078.92 | 1283.84 | 1545.77 |
| | KDP+4 mol% | 863.27 | 1078.88 | 1286.51 | 1553.93 |
| | KDP+5 mol% | 871.05 | 1079.35 | 1284.19 | 1552.89 |

## 5.5 UV-Vis Spectrophotometer Studies

### 5.5.1 Sample preparations

Single crystals are mainly used in optical applications, as the optical transmission spectra and the transparency cut off are important. The good transmission property of the crystal in the visible region promoted its suitability for second harmonic generation applications (Robert, Justin Raj, Krishnan and Jerome Das, 2010). The UV–Vis spectrum gives information about the structure of the molecule because the absorption of UV and visible light involves electron from the ground state to higher energy states. The UV–Vis spectrophotometer studies were

carried out for the optical transmittance of the as-grown crystals, by using Shimadzu UV-1700 spectrophotometer in the range of 200 – 1100 nm with increasing 1 nm/step at Faculty of Sciences and Liberal Arts, Rajamangala University of Technology Isan.

The samples were cut from the as-grown crystals and ground by silicon carbide paper no. 1200, then polished by using diamond abrasive with size $2 – 4$ $\mu$m until the samples' surfaces were clear and smooth and finally cleaned with acetone. The thickness of all samples is 2 mm.

### 5.5.2 Results and discussions

#### 5.5.2.1 The optical studies of KDP crystals with variation of additive

The transmittance of the as–grown crystals by conventional slow evaporation method is shown in Figure 5.5. The pure and thiourea doped KDP as–grown single crystals have a good transmittance in considerable region of wavelength and the lower cut off wavelength of the grown crystals was found to be about 350 nm. Pure KDP crystal has better transmittance than the doped crystals, except for 2 mol% thiourea-doped KDP shows better transmittance than that of pure KDP crystal. The low transmittance of the grown crystals by conventional method is caused by the scattered by small particles or cracks within the crystals.

The transmittance of the as-grown crystals by SR method is shown in Figure 5.6. The crystals grown by SR method have a good transmission when compared with the crystals grown by conventional method. The transmittance of crystals grown by SR method was nearly 90% in wavelength region of 250 to 1,100 and the cut off wavelength of the grown crystals was found to be about 250 nm. This indicates that the crystal growth by SR method is suitable for fabrication of devices used in visible

and IR region. A good optical transmittance in this region is a desirable property in an NLO crystal for SHG laser radiation, Nd-YAG laser with the wavelength 1,064 nm in fundamental and 532 nm in second harmonic, of other application in the blue region (Mary Linet and Jerome Das, 2011).
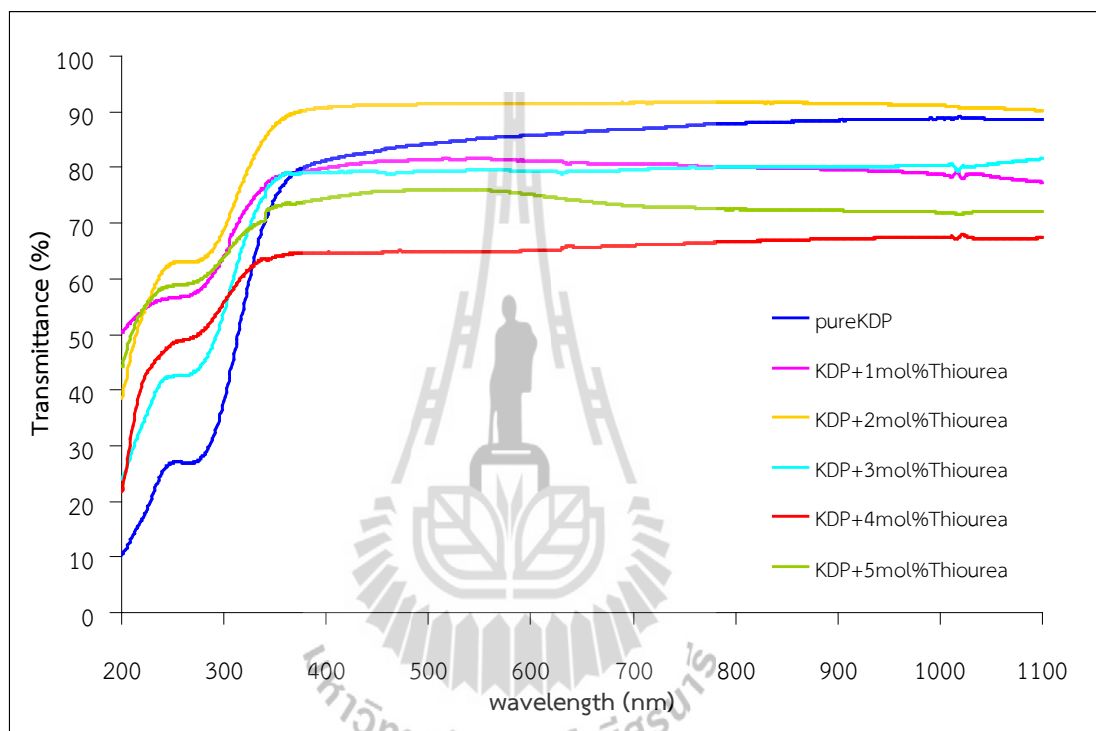


**Figure 5.5**   The UV–Vis spectra of the crystals grown by conventional slow evaporation method.
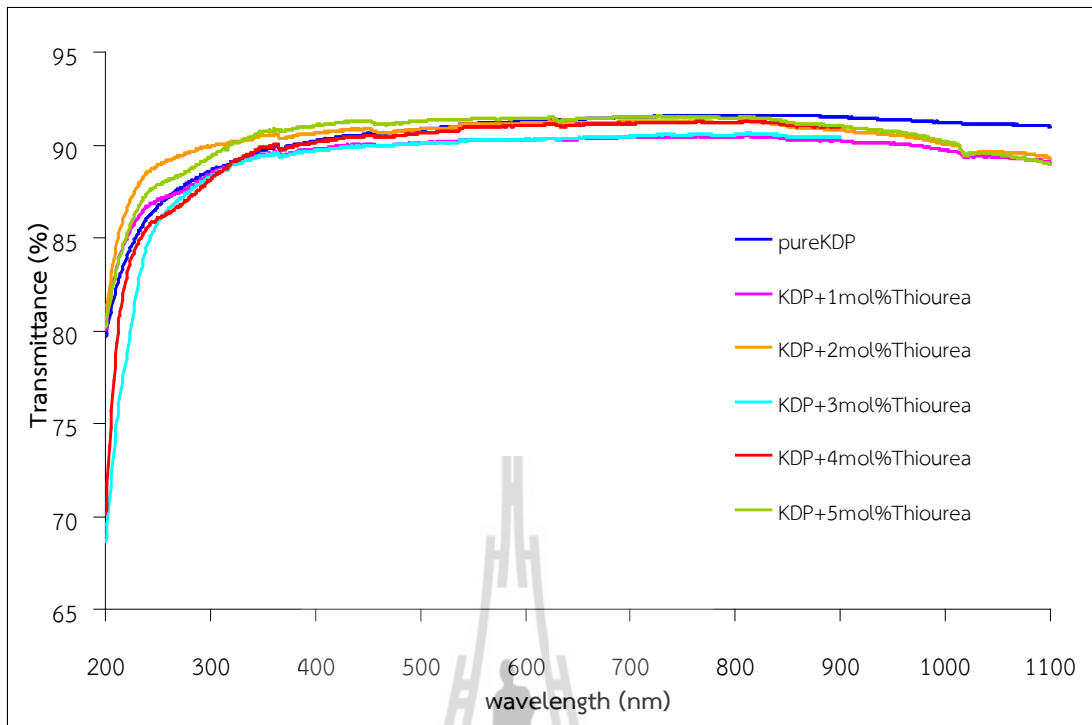
**Figure 5.6** The UV–Vis spectra of the crystals grown by SR method.

The optical absorption coefficient ($\alpha$) for pure and dopped–KDP crystals were calculated from transmittance of the as grown crystals by using Beer–Lambert law as described in Chapter III. By deriving equation 3.10, $A = -\log T = \alpha\ell$, it becomes.

$$\alpha = \frac{1}{\ell}\log\frac{1}{T} \qquad (5.4)$$

where $T$ is the transmittance and $\ell$ is the thickness of the crystal.

Figure 5.7 shows the optical absorption spectrum of crystals grown by conventional slow evaporation method as a function of wavelength. In the visible and infrared regions (400 – 1,100 nm), the optical absorption is low and nearly constant. KDP + 2 mol% thiourea shows the lowest absorption coefficient of (39.33 m$^{-1}$) with

the average from 400 – 1,100 nm and 4 mol% thiourea-added exhibits highest

absorption coefficient (175.50 $m^{-1}$) with the average from 400 – 1,100 nm.
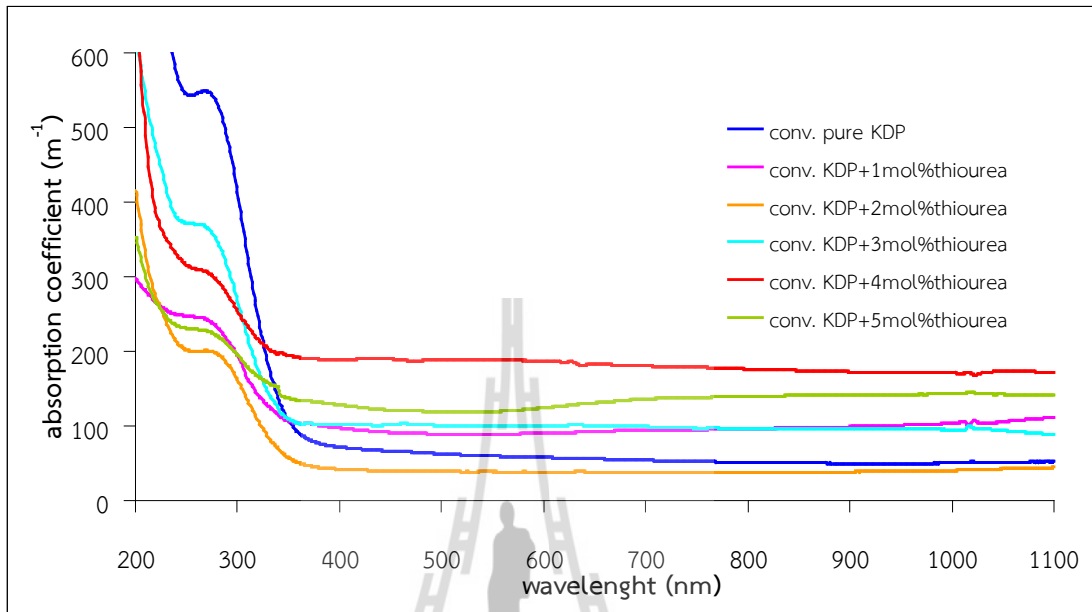


**Figure 5.7** The absorption coefficient of the crystals grown by conventional slow

evaporation method.

Figure 5.8 shows the optical absorption coefficient of crystals grown by SR

method as a function of wavelength. In the visible and infrared regions (400 – 1,100

nm), the optical absorption coefficient of the crystals is around 40 – 50 $m^{-1}$, which is

smaller than that of the crystals grown by the conventional method.
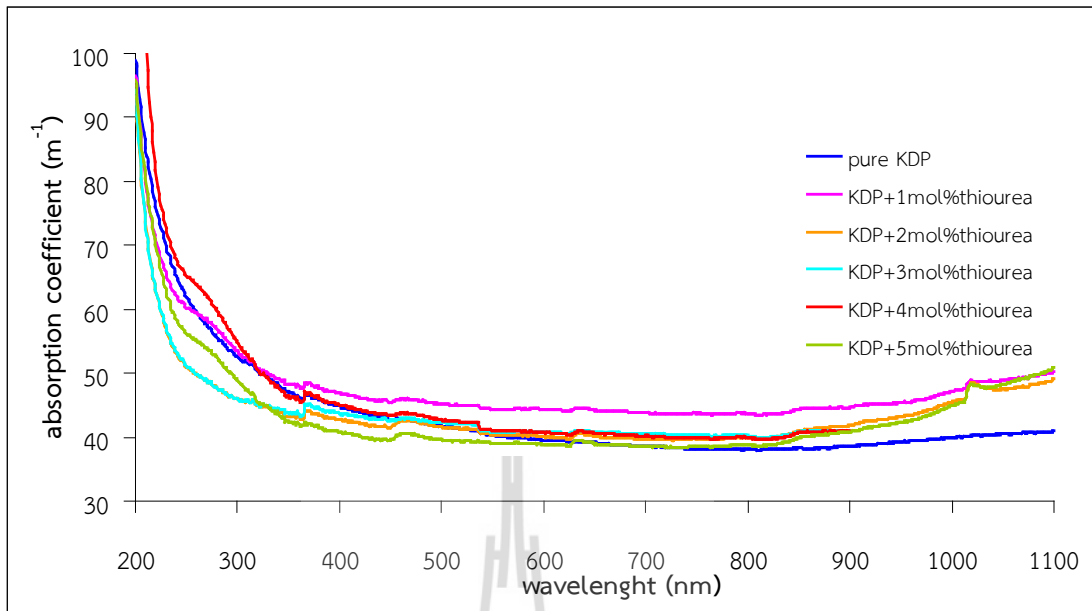
**Figure 5.8** The absorption coefficient of the crystals grown by SR method.

The energy band gap and the absorption coefficient have the relation as follows (from equation 3.11),

$$(\alpha h\nu)^2 = C(h\nu - E_g) \tag{5.5}$$

where $E_g$ is optical band gap of crystal, $C$ is a constant.

The optical band gap is determined from the linear part of plot of $(\alpha h\nu)^2$ versus $h\nu$ ). Figure 5.9 shows a plot of $(\alpha h\nu)^2$ versus $h\nu$ of pure KDP grown by SR method. As a consequence of wide band gap, the grown crystal has large transmittance in the visible region (Robert, Justin Raj, Krishnan and Jerome Das, 2010). The optical band gap of the grown crystals is listed in Table 5.3.
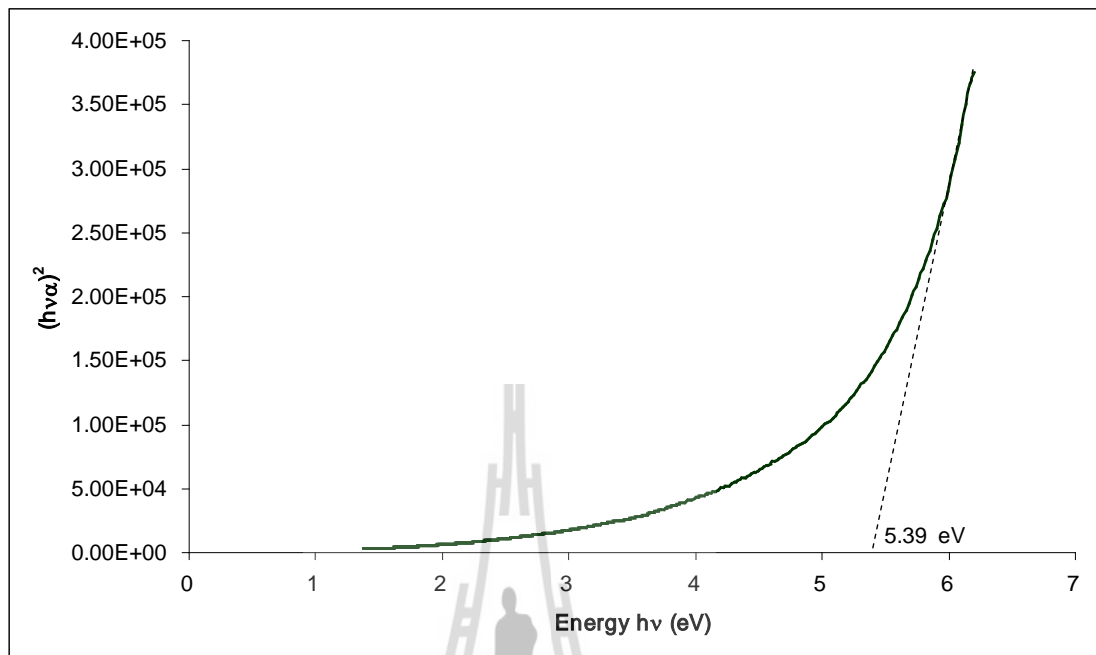
**Figure 5.9** Plot of $(\alpha h\nu)^2$ versus $h\nu$ of pure KDP grown by SR method.

The optical constants of a material such as optical band gap and extinction coefficient are quite essential to examine the material's potential optoelectronic applications. The optical properties may also be closely related to the material's atomic structure, electronic band structure and electrical properties. The optical constants (refractive index, $n$ and extinction coefficient, $k$) are determined from the transmittance ($T$) and reflectance ($R$) spectrum based on the following relations (Robert, Justin Raj, Krishnan and Jerome Das, 2010).

**Table 5.3** The optical band gap of grown single crystal.

| | Crystal | $E_g$ (eV) |
|---|---|---|
| Conventional method | Pure KDP | 5.34 |
| | KDP+1 mol% | 4.49 |
| | KDP+2 mol% | 4.96 |
| | KDP+3 mol% | 4.82 |
| | KDP+4 mol% | 5.30 |
| | KDP+5 mol% | 5.30 |
| S R method | Pure KDP | 5.39 |
| | KDP+1 mol% | 5.41 |
| | KDP+2 mol% | 5.63 |
| | KDP+3 mol% | 5.51 |
| | KDP+4 mol% | 5.61 |
| | KDP+5 mol% | 5.44 |

From equation (3.12), the relationship of the transmittance and reflectance becomes

$$R = 1 \pm \frac{\sqrt{T \exp(-\alpha t)}}{\exp(-\alpha t)} \tag{5.6}$$

This present work uses a minus sign $(-)$, and equation (5.6) becomes.

$$R = 1 - \frac{\sqrt{T \exp(-\alpha t)}}{\exp(-\alpha t)} \tag{5.7}$$

The reflectance is related to $n$ and $k$ by equations (3.15), (3.16) and (3.17) and

$$k = \frac{\alpha\lambda}{4\pi} \tag{5.8}$$

$$n = \frac{-(R+1) \pm \sqrt{4R}}{(R-1)} = \frac{1+\sqrt{R}}{1-\sqrt{R}} \tag{5.9}$$

Thus, for transparent materials, there is a relationship between the index of refraction and the dielectric constant. The phenomenon of refraction is related to electronic polarization at the relatively high frequencies for visible light; thus, the electronic component of the dielectric constant may be determined from index of refraction measurements using (Callister and Rethwisch, 2010).

$$n \cong \sqrt{\varepsilon_r} \tag{5.10}$$

The extinction coefficient of conventional and SR grown crystals determined from equation (5.8) are shown in Figure 5.10 and 5.11, respectively.
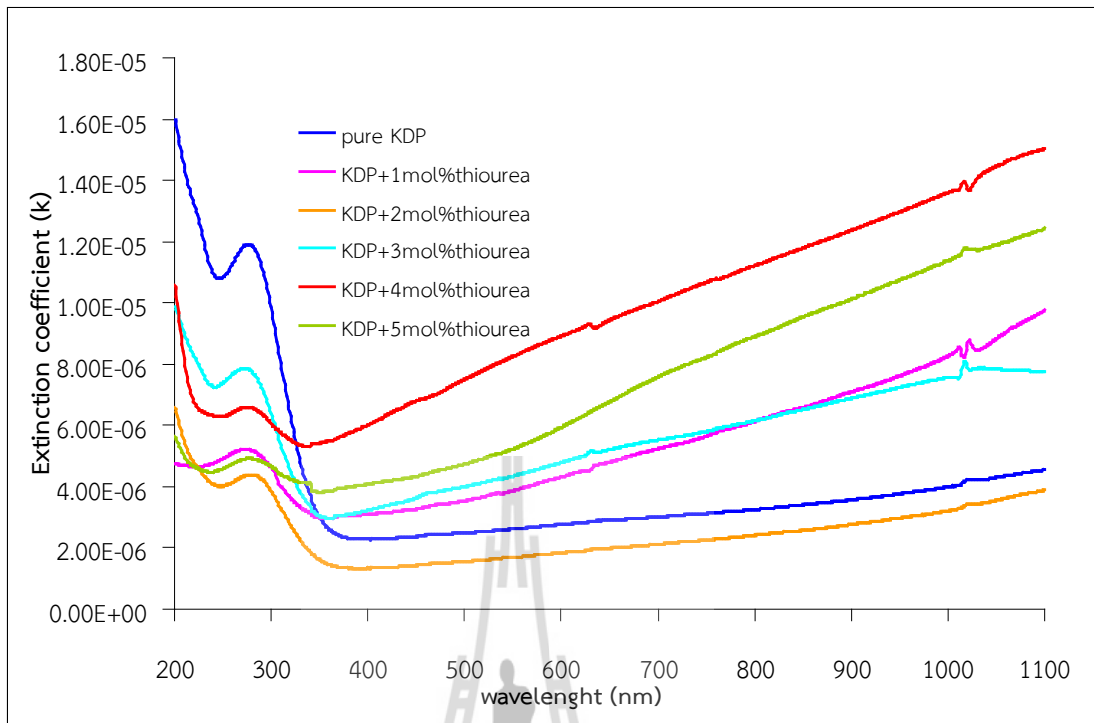
**Figure 5.10** The extinction coefficient of conventional grown crystals.
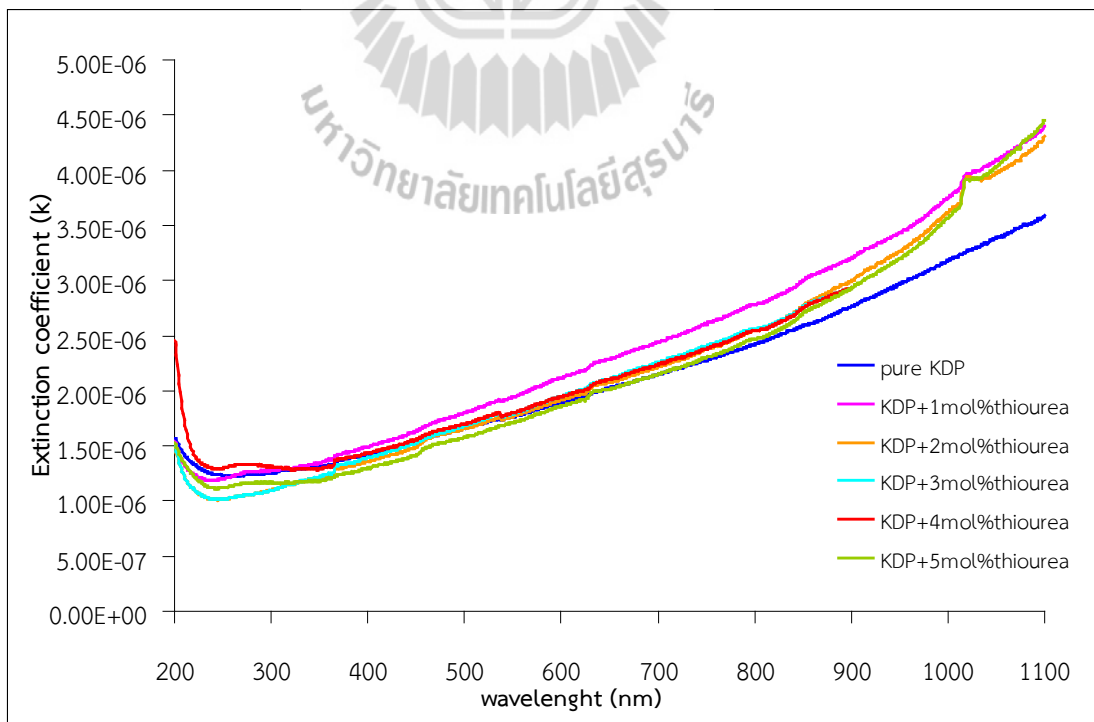


**Figure 5.11** The extinction coefficient of SR grown crystals.

The extinction coefficient is linearly increasing from the wavelength in range of 400 – 1,100 nm in the order of $1.0 \times 10^{-6} - 1.5 \times 10^{-5}$ and $1.0 \times 10^{-6} - 1.45 \times 10^{-6}$ for the conventional grown and SR grown crystals, respectively. In the case of good transparent material, $k$ is very low, then neglected.

Refractive index of the conventional grown and SR grown crystals are shown in Figure 5.12 and Figure 5.13 respectively. The refractive index in visible region to IR region at frequency of 400, 700, 1,064 nm and average from 400 – 700 nm of grown crystal and dielectric constant derived from equation (5.9) of average from 400 – 700 nm are given in Table 5.4, with a comparison to standard value of KDP from Refractive index database (available: http://refractiveindex.info).
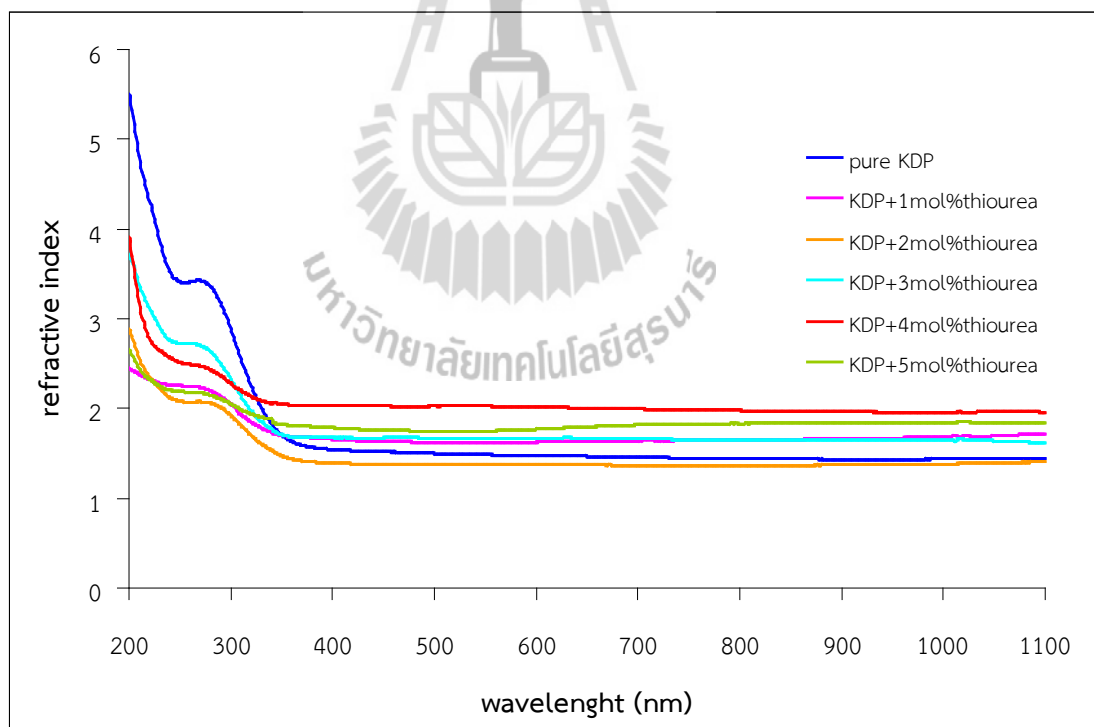


**Figure 5.12** Refractive index of the conventional grown crystals.
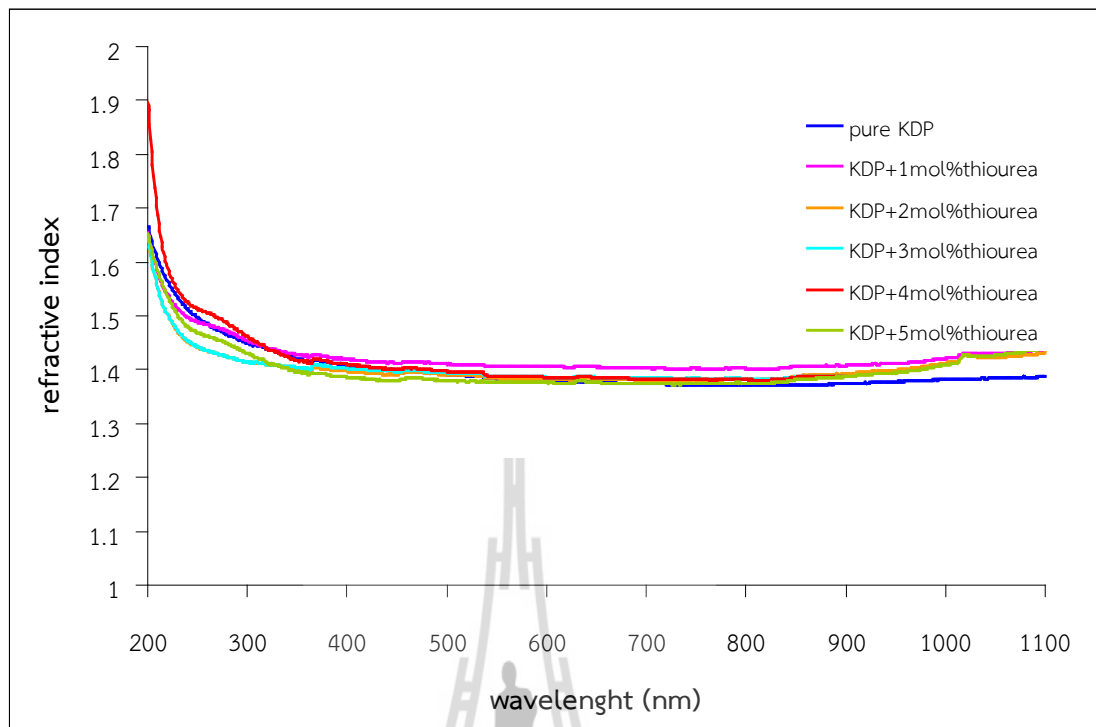
**Figure 5.13** Refractive index of the SR grown crystals.
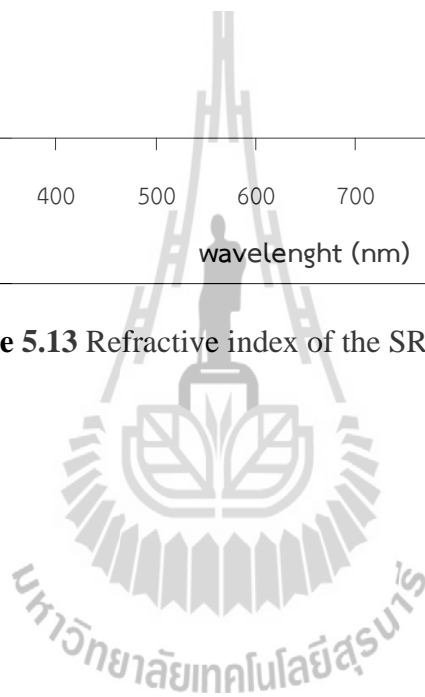
**Table 5.4** Refractive index and dielectric constant of grown single crystal.

| | Crystal | $n$ (400 nm) | $n$ (700 nm) | $n$ (1,064 nm) | $\overline{n}$ (400–1,100 nm) | $\varepsilon_r$ |
|---|---|---|---|---|---|---|
| | Pure KDP | 1.543 | 1.457 | 1.445 | 1.463 | 2.140 |
| Conventional method | KDP+1 mol% | 1.659 | 1.644 | 1.705 | 1.654 | 2.736 |
| | KDP+2 mol% | 1.394 | 1.371 | 1.340 | 1.378 | 1.899 |
| | KDP+3 mol% | 1.677 | 1.667 | 1.637 | 1.661 | 2.759 |
| | KDP+4 mol% | 2.032 | 1.998 | 1.971 | 1.995 | 3.980 |
| | KDP+5 mol% | 1.790 | 1.822 | 1.846 | 1.812 | 3.283 |
| | Pure KDP | 1.409 | 1.374 | 1.385 | 1.381 | 1.907 |
| S R method | KDP+1 mol% | 1.419 | 1.403 | 1.432 | 1.411 | 2.076 |
| | KDP+2 mol% | 1.397 | 1.381 | 1.424 | 1.393 | 1.940 |
| | KDP+3 mol% | 1.403 | 1.385 | – | 1.389 | 1.929 |
| | KDP+4 mol% | 1.410 | 1.383 | – | 1.389 | 1.929 |
| | KDP+5 mol% | 1.386 | 1.374 | 1.430 | 1.388 | 1.927 |
| | standard value | 1.524 | 1.505 | 1.494 | 1.515 | |

### 5.5.2.2 The optical studies of KDP crystals grown by SR method in different facets

KDP crystals were grown by SR method in different facets from seed crystals along different crystallographic directions of $\langle 010 \rangle$, $\langle 001 \rangle$ and $\langle 011 \rangle$ for pure and 5 mol% thiourea doped KDP. The samples were cut out along given direction and polished as mentioned above. The samples with good transparency were found in $\langle 001 \rangle$ and $\langle 011 \rangle$ directions but poor transparent samples were obtained in $\langle 010 \rangle$ direction. The transmittance of crystals is shown in Figure 5.14.

From the transmittance, the crystals grown in $\langle 001 \rangle$ direction or c–direction show a very good transmission, nearly 90%, for both pure and thiourea 5 mol% doped KDP. The cut off wavelength is around 230 nm. The crystal grown in $\langle 011 \rangle$ direction shows a good transmission, $\sim 85\%$ for thiourea 5 mol% doped KDP and $\sim 75\%$ for pure KDP crystals. Poor transmission for crystals grown in $\langle 010 \rangle$ direction is likely because it is difficult to grow good crystal in this direction. For each growth direction, the doped crystals show slightly better transparency than that of the pure crystals.
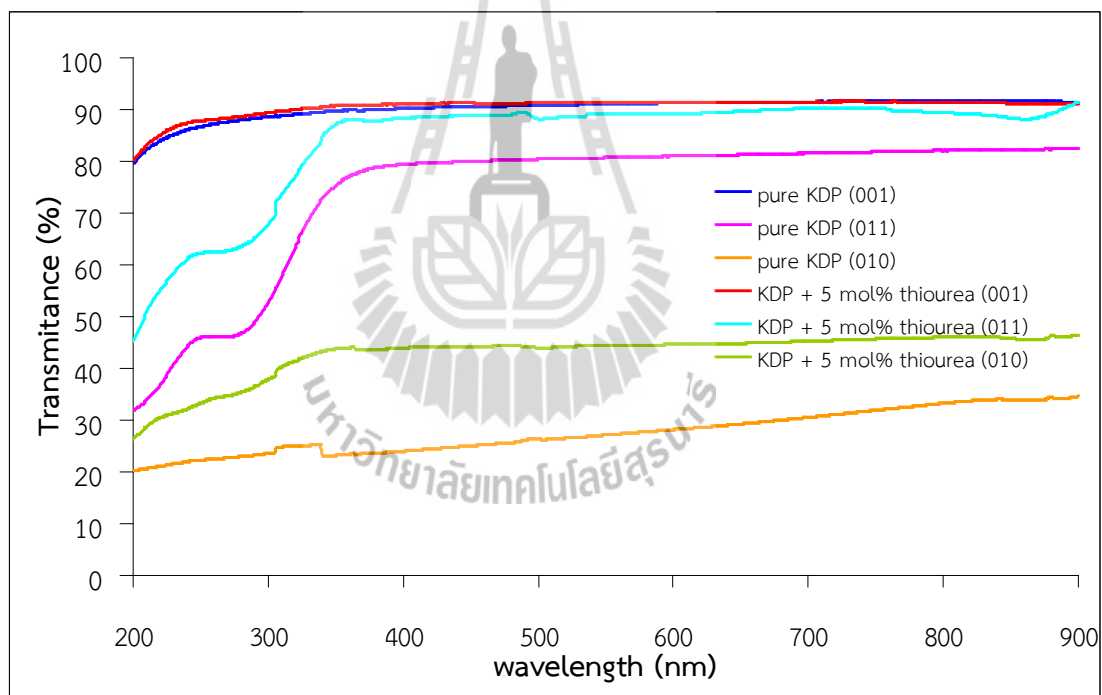


**Figure 5.14** Transmittance of different crystal facets.

The optical absorption coefficient of the grown crystals is shown in Figure 5.15. Clearly, the crystals grown in $\langle 010 \rangle$ direction exhibit high absorption coefficient. Low optical absorption coefficient was found in $\langle 001 \rangle$ and $\langle 011 \rangle$

directions resulting in good transparencies. Optical band gap of the grown crystals is listed in Table 5.5
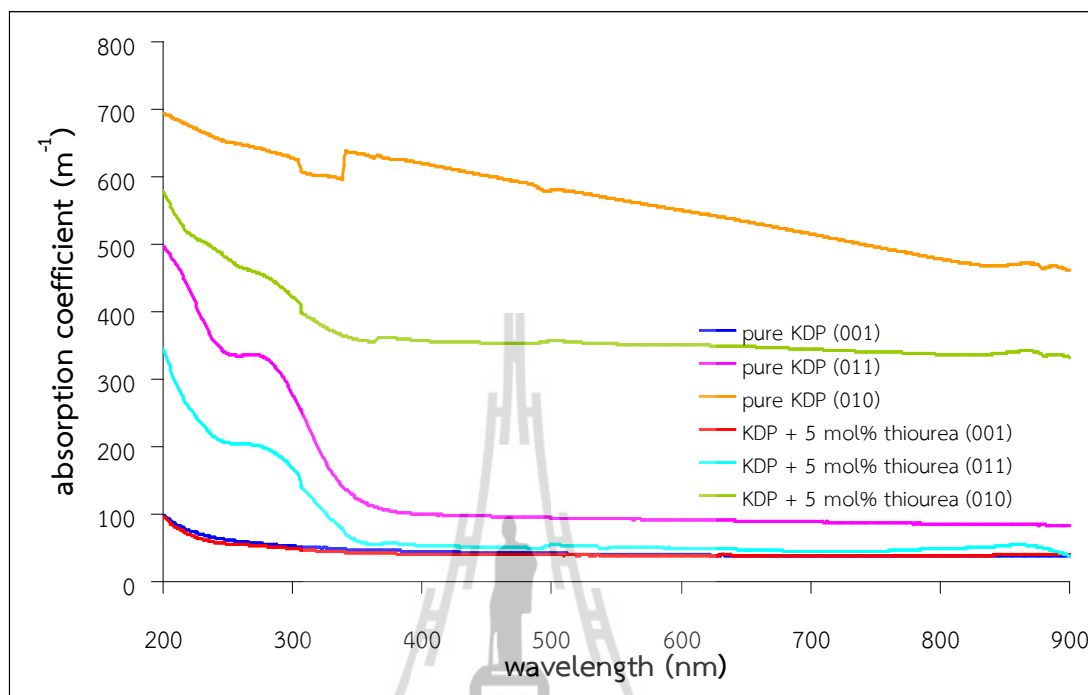


**Figure 5.15** Absorption coefficient of different crystal facets.

**Table 5.5** The optical band gap of grown single crystal in different facets.

| Crystal | $E_g$ ( eV ) |
|---------|-----------|
| Pure KDP (001) | 5.39 |
| Pure KDP (011) | 4.67 |
| Pure KDP (010) | 4.96 |
| KDP+5 mol% thiourea (001) | 5.44 |
| KDP+5 mol% thiourea (011) | 5.23 |
| KDP+5 mol% thiourea (010) | 4.64 |

The grown crystal has a wide band gap, meaning that there is a large transmittance in the visible region (Robert, Justin Raj, Krishnan and Jerome Das, 2010).

Refractive index of the crystals grown by SR method with the different directions are shown in Figure 5.16. The average refractive index in visible region at frequency 400 – 700 nm is listed in Table 5.6. The comparison with standard value of KDP from Refractive index database (available: http://refractiveindex.info) is also listed.

Although, the dielectric constant for crystals grown in $\langle 010 \rangle$ direction are higher than another directions but poor transmission, which indicated that the crystals are unsuitable for optical applications.
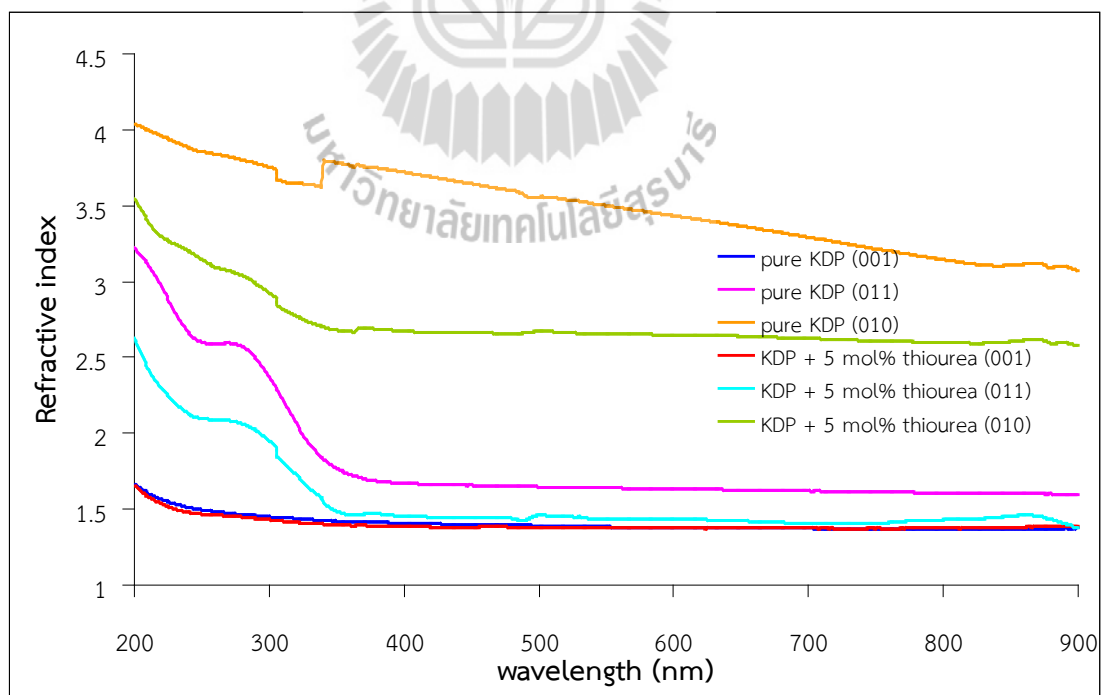


**Figure 5.16** Refractive index of the crystals grown in different crystal facets.

**Table 5.6** Refractive index and dielectric constant of different direction grown crystals.

| Crystal | $n$ (400 nm) | $n$ (700 nm) | $\overline{n}$ (400–700 nm) | $\varepsilon_r$ |
|---|---|---|---|---|
| Pure KDP (001) | 1.409 | 1. 347 | 1.387 | 1.924 |
| Pure KDP (011) | 1.671 | 1.620 | 1.642 | 2.696 |
| Pure KDP (010) | 3.721 | 3.292 | 3.502 | 12.26 |
| KDP+5 mol% thiourea (001) | 1.386 | 1.374 | 1.378 | 1.899 |
| KDP+5 mol% thiourea (011) | 1.457 | 1.408 | 1.436 | 2.062 |
| KDP+5 mol% thiourea (010) | 2.674 | 2.645 | 2.653 | 7.038 |
| standard value | 1.524 | 1.505 | 1.515 | |

## 5.6 Microhardness Studies

### 5.6.1 Sample preparations

Hardness study on pure and various concentrations of thiourea doped KDP crystals was carried out by pyramidal indentation test for applied loads of 10, 25, 50 and 100 g by using Microhardness tester Anton–Paar MHT-10 at National Metal and Material Technology Center (M–tech). The average of diagonal length of indentation for various applied loads with constant indentation period of 10 s. was investigated. The indentation of this experiment is shown in Figure 5.17. The Vicker's microhardness number ( $H_v$ ) was evaluated from equation (3.20).

$$H_v = \frac{1.8544P}{d^2}$$

where $P$ is the applied load and $d$ is the average of diagonal length of indentation.
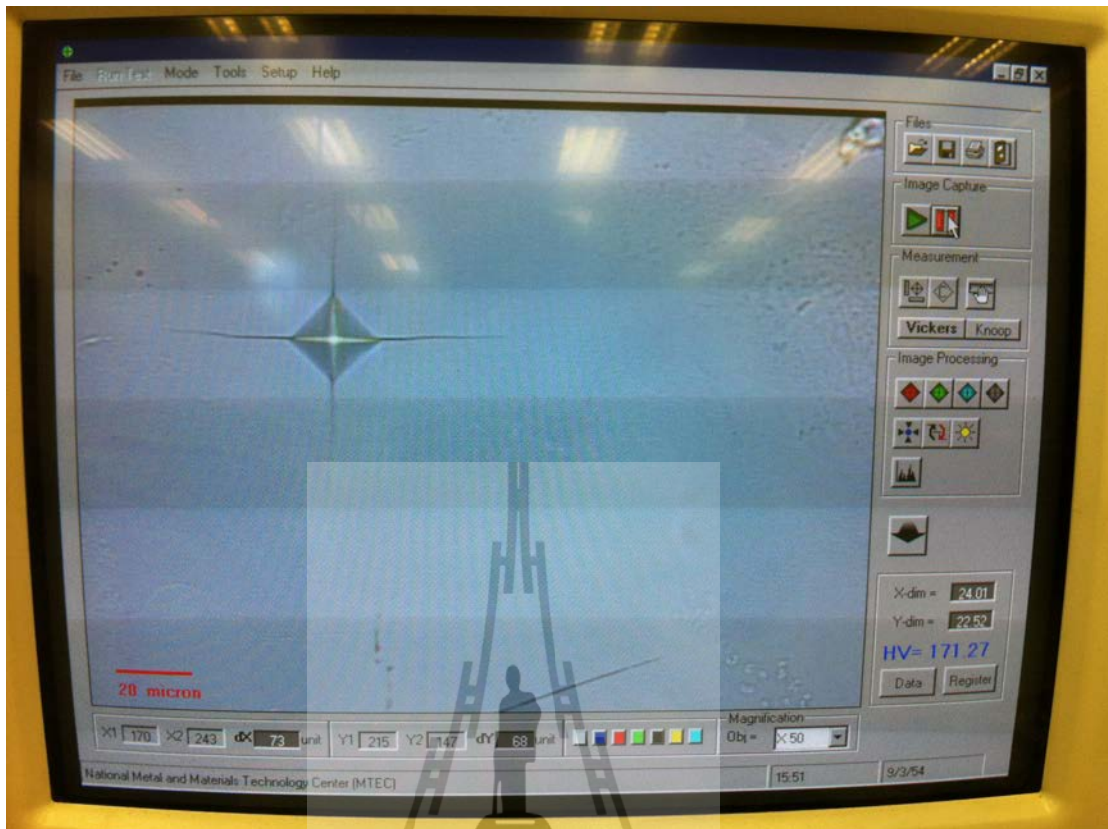
**Figure 5.17** The indentation of KDP crystal.

**5.6.2 Results and discussions**

**5.6.2.1 The microhardness studies of pure and additive added KDP crystals in (001) plane**

Samples for microhardness studies were cut from the grown crystal with size 5 mm thick, then lapping and polishing was done until the surfaces of samples were clear and smooth, and finally cleaned with acetone. Microhardness of single crystals grown by conventional and SR methods is shown in Figures 5.18 and 5.19, respectively. According to the results, the hardness value decreases with increasing load.

The relationship between load and the size of indentation is given by Meyer's law following equation (3.21), $P = k_1 d^n$, where $k_1$ is the standard hardness value, $n$ the Meyer's index (or work-hardening coefficient), $n$ usually lies around the values of 2, the lattice is soft if $n > 2$ and the lattice is hard if $n < 2$. The work-hardening coefficient was calculated from the slope of the plot of $\log P$ versus $\log d$. Since the material takes sometime to revert to the elastic mode after every indentation, a correction $x$ is applied to the $d$ value and the Kick's law is related to equation (3.22), $P = k_2(d + x)^2$. Figure 5.20 shows the plot of $\log P$ versus log $d$ of KDP + 5mol% thiourea grown by SR method in (001) plane. The correction $x$ value determined from the plot of $d^{n/2}$ versus $d$ is related with equation (3.23), and shown in Figure 5.21 (Justin Raj, Dinakaran, Krishnan, Milton Boaz, Robert and Jerome Das, 2008). The evaluated values of $n$, $k_1$, $k_2$ and $x$ are given in Table 5.7
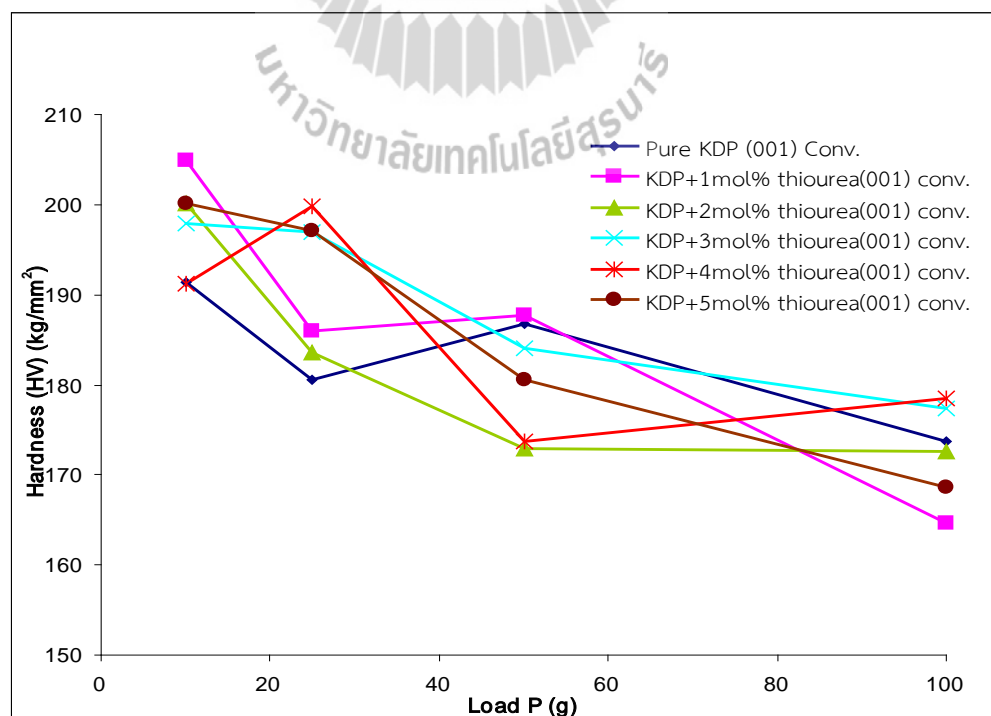


**Figure 5.18** Microhardness of crystals grown by conventional method.
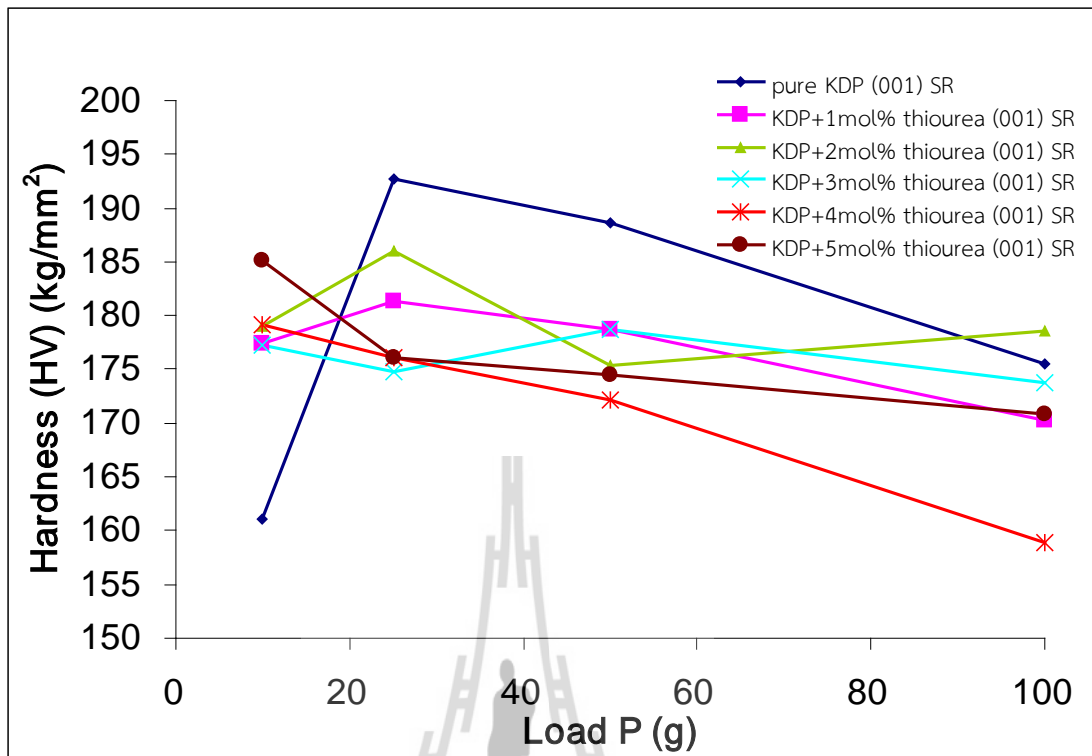
**Figure 5.19** Microhardness of crystals grown by SR method.
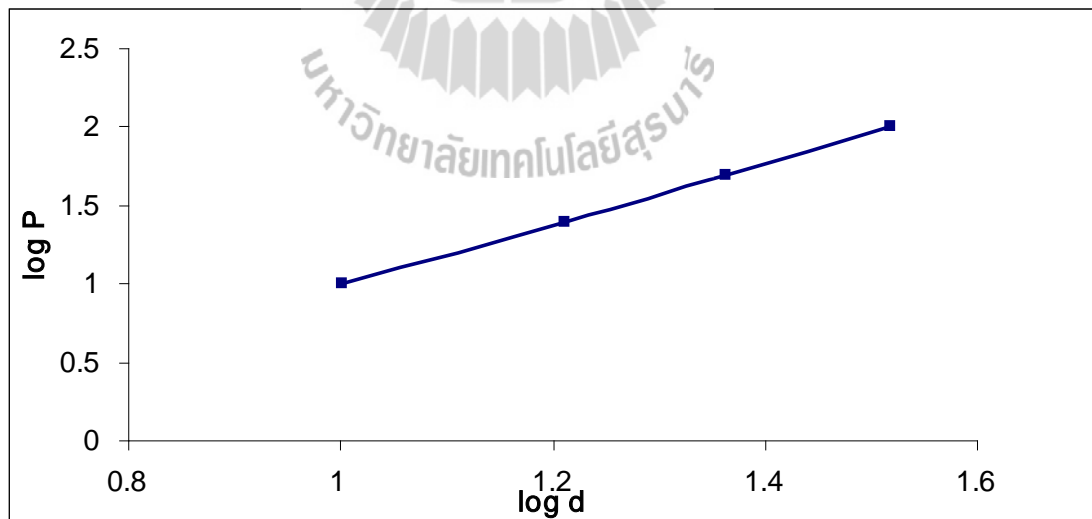


**Figure 5.20** Plot of $\log P$ versus $\log d$ of crystals grown by SR method.
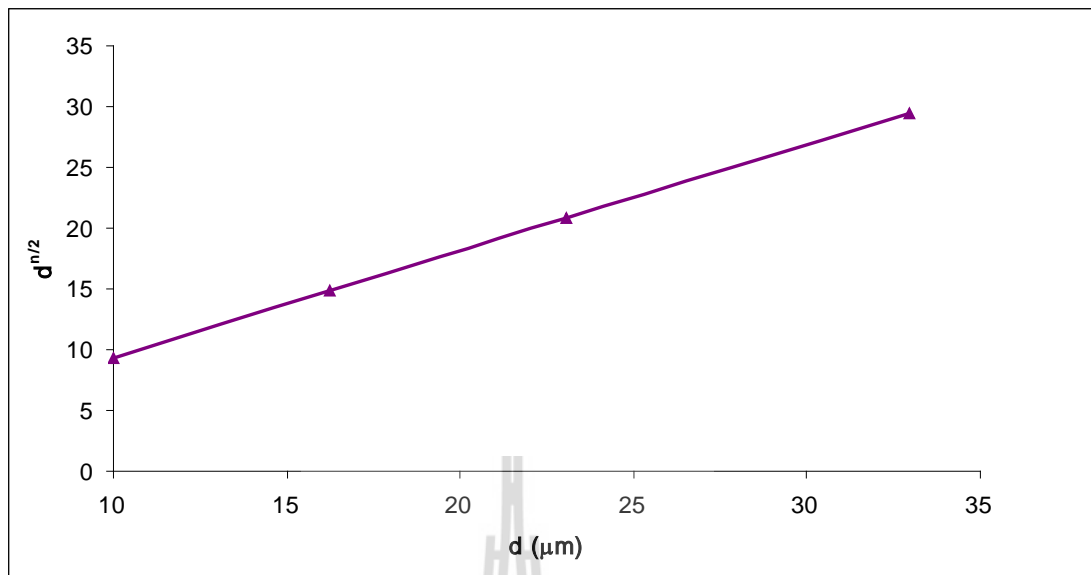
**Figure 5.21** Plot of $d^{n/2}$ versus $d$ of crystals grown by SR method.

**Table 5.7** Microhardness parameters of KDP single crystals.

| | Crystal | $n$ | $k_1$ (kg/mm) | $k_2$ (kg/mm) | $x$ ($\mu$m) |
|---|---|---|---|---|---|
| Conventional method | Pure KDP | 1.9332069 | 0.119881 | 0.090369 | 0.648908 |
| | KDP+1 mol% | 1.8416593 | 0.1583258 | 0.081259 | 1.621876 |
| | KDP+2 mol% | 1.8724995 | 0.1423094 | 0.086875 | 1.26256 |
| | KDP+3 mol% | 1.9021833 | 0.1352136 | 0.090314 | 0.949558 |
| | KDP+4 mol% | 1.9120892 | 0.1291819 | 0.091082 | 0.849205 |
| | KDP+5 mol% | 1.8550377 | 0.1529366 | 0.083524 | 1.462895 |
| S R method | Pure KDP | 2.062815 | 0.0803655 | 0.096653 | −0.58941 |
| | KDP+1 mol% | 1.9664064 | 0.1052412 | 0.089795 | 0.327147 |
| | KDP+2 mol% | 1.9831607 | 0.1017977 | 0.095052 | 0.159363 |
| | KDP+3 mol% | 1.9900076 | 0.0978009 | 0.0932 | 0.095572 |
| | KDP+4 mol% | 1.9058042 | 0.1219719 | 0.081106 | 0.965159 |
| | KDP+5 mol% | 1.9353432 | 0.1150643 | 0.088584 | 0.632699 |

## 5.6.2.2 The microhardness studies of KDP crystal grown by SR method in various planes

The samples were cut from the crystal grown by SR method in directions of $\langle 010 \rangle$, $\langle 001 \rangle$ and $\langle 011 \rangle$ for pure and 5 mol% thiourea-doped KDP with size 5 mm thick, then lapping and polishing was done, as mentioned above. Microhardness of single crystals is shown in Figure 5.22. The comparison of hardness of both pure and additive added KDP crystals show $\langle 001 \rangle > \langle 011 \rangle > \langle 010 \rangle$. The evaluated values of $n$, $k_1$, $k_2$ and $x$ are given in Table 5.8
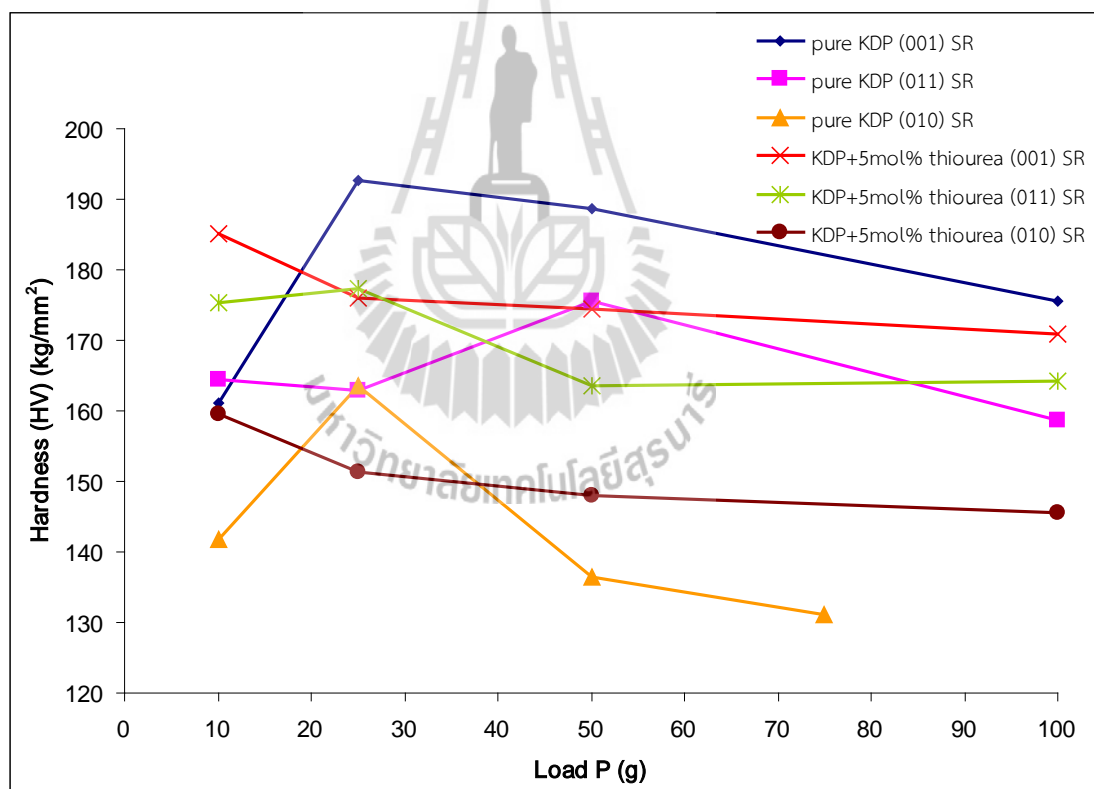


**Figure 5.22** Microhardness of KDP crystals in direction of $\langle 010 \rangle$, $\langle 001 \rangle$ and $\langle 011 \rangle$.

**Table 5.8** Microhardness values of KDP single crystals in different directions.

| Crystal | $n$ | $k_1$ (kg/mm) | $k_2$ (kg/mm) | $x$ ($\mu$m) |
|---|---|---|---|---|
| Pure KDP (001) | 2.062815 | 0.0803655 | 0.096653 | –0.58941 |
| Pure KDP (011) | 1.9889159 | 0.0921036 | 0.084741 | 0.111167 |
| Pure KDP (010) | 1.8870439 | 0.1080158 | 0.064975 | 1.179014 |
| KDP+5 mol% thiourea(001) | 1.9353432 | 0.1150643 | 0.088584 | 0.632699 |
| KDP+5 mol% thiourea(011) | 1.9300127 | 0.1126806 | 0.088584 | 0.700529 |
| KDP+5 mol% thiourea(010) | 1.9242372 | 0.1022815 | 0.075416 | 0.805427 |

## 5.7 Dielectric Properties Studies

### 5.7.1 Sample preparations

The dielectric properties of the material are important to study the SHG of the crystal. The grown KDP single crystals were subjected to dielectric studies using the Agilent E4980A precision LCR meter with 16451B dielectric test fixture from Faculty of Sciences and Liberal Arts, Rajamangala University of Technology Isan. The samples for dielectric studies were cut from pure and thiourea doped KDP single crystals grown in direction of $\langle 001 \rangle, \langle 011 \rangle$ and $\langle 010 \rangle$ by SR method. The cut crystals were ground by grinding paper no. 800 and 1200 and polished using diamond abrasive size $2 - 4$ $\mu$m. The thickness for all samples is 1 mm and diameter is 17 mm. Both surfaces of the samples were painted with silver paste for electrical contact. The experiment was carried out for the frequencies from 100 Hz to 2 MHz at the room temperature.

### 5.7.2 Results and discussions

As seen in Figure 3.17, the dielectric constant is high in the lower frequency region, hence, the experiments were carried out in the lower frequency region only (<2 MHz). The dielectric constant $\varepsilon_r$ was calculated using the relation of equation (3.30), $\varepsilon_r = \varepsilon_r' = \dfrac{Cd}{\varepsilon_0 A}$, where $C$ is the measured capacitance, $d$ is the thickness of the crystal, $\varepsilon_0$ is the vacuum dielectric constant and $A$ is the area of the crystal. The dielectric loss was calculated using equation (3.31), $\varepsilon_r'' = \varepsilon_r D$, where $D$ is the dissipation factor.

Dielectric constant ($\varepsilon_r$) and dielectric loss ($\varepsilon''$) obtained at room temperature in the frequency range of 100 Hz to 2 MHz for KDP crystals grown by SR method in $\langle 001 \rangle$–direction are shown in Figures 5.23 – 5.28.

From the figure, it is seen that the value of $\varepsilon_r$ for pure, 2 mol% and 5 mol% thiourea added KDP remains practically constant at log frequency of 2 – 4.78 (100 – 60,000 Hz) and for 1 mol%, 3 mol% and 4 mol% thiourea added KDP slightly deceases with increase in given frequency. In the range of log frequency of 4.8 - 5.8 (~ 60 – 600 kHz), the $\varepsilon_r$ value is oscillating. This behaviour has occurred in all the samples, it might be due to the resonance of the crystals.

The very high values of $\varepsilon_r$ at low frequencies may be due to the presence of all the four polarizations, namely, space charge, orientation, ionic and electronic polarizations and its low value at high frequencies may be due to the loss of significance of these polarizations gradually. The increase in the dielectric constant at

low frequency is attributed to the space charge polarization (Boomadevi and Dhanasekaran, 2004).



(a)
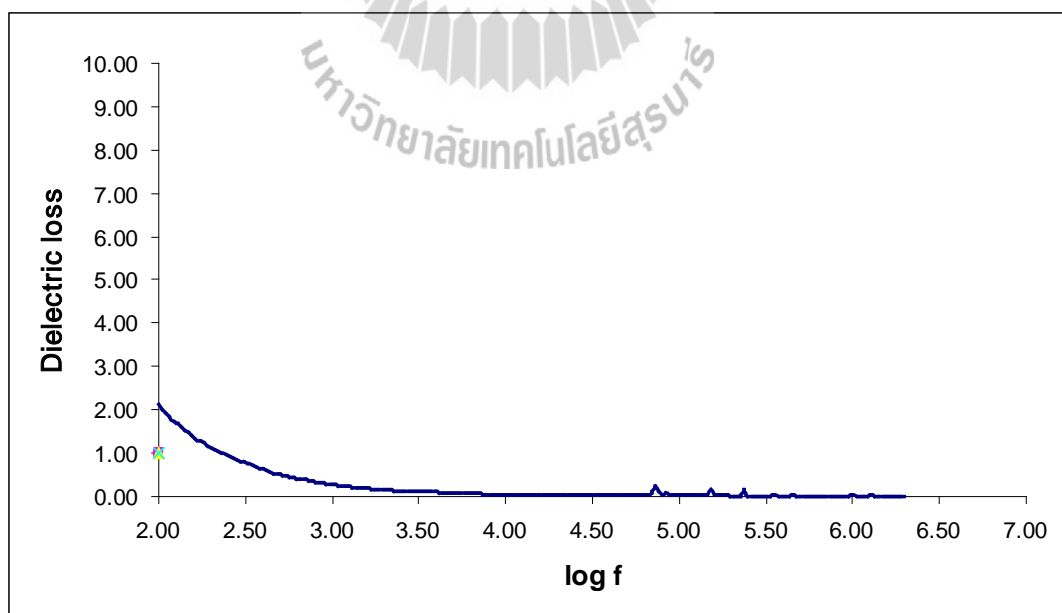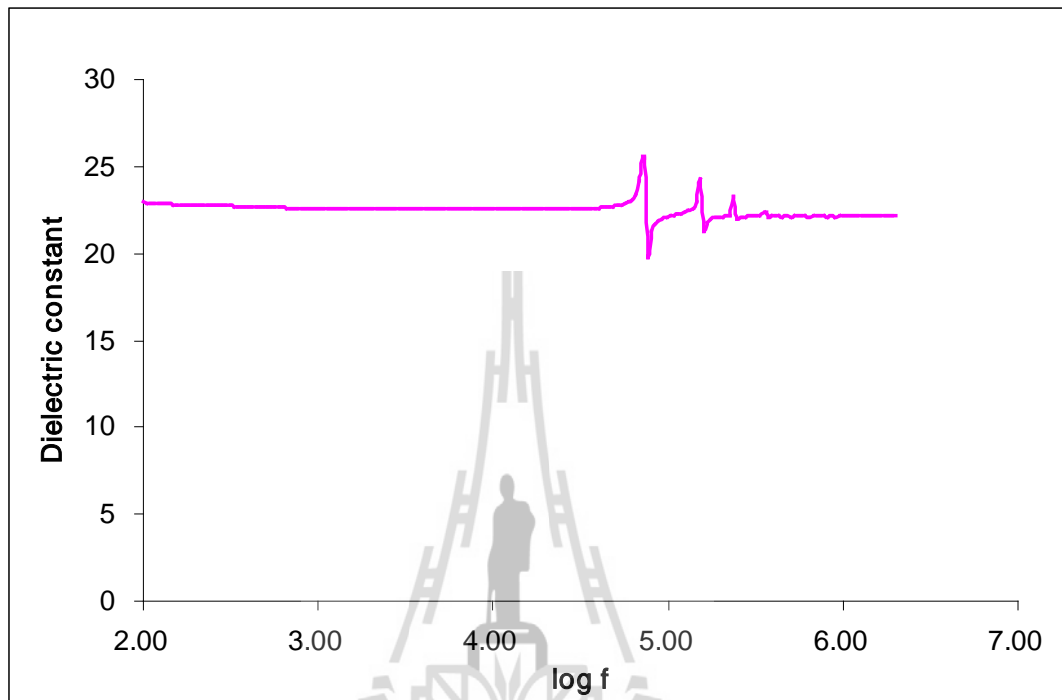


(b)

**Figure 5.23** (a) dielectric constant and (b) dielectric loss of pure KDP in $\langle 001 \rangle$ – direction

(a)



(b)
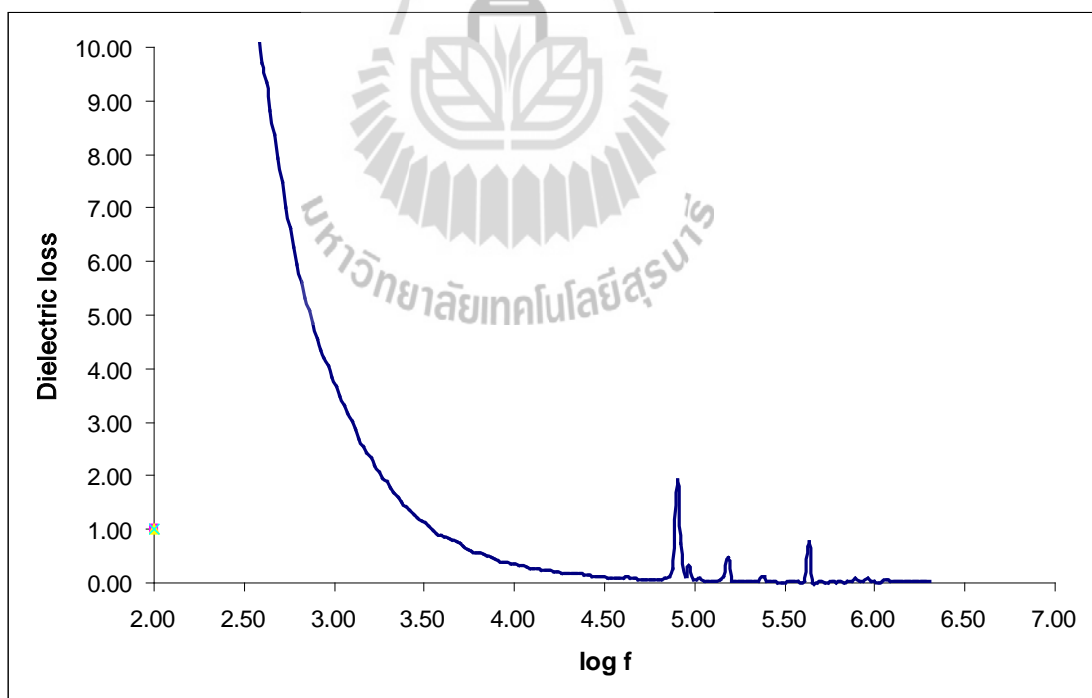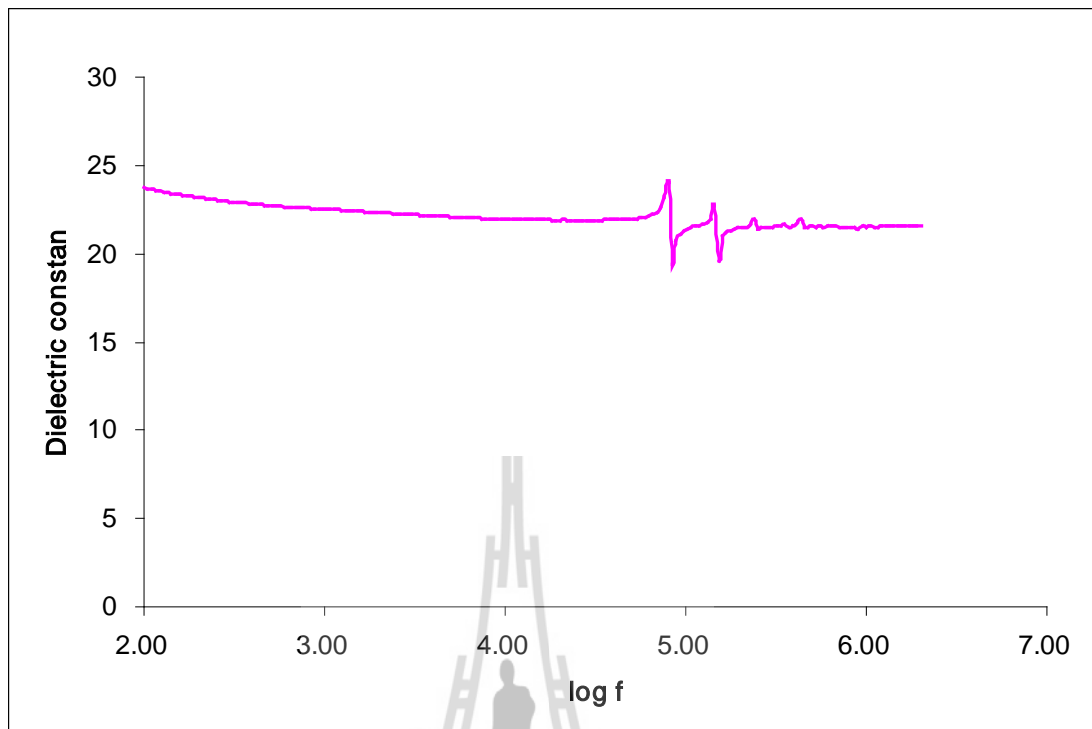
**Figure 5.24** (a) dielectric constant and (b) dielectric loss of KDP + 1 mol% thiourea

in $\langle 001 \rangle$ –direction.
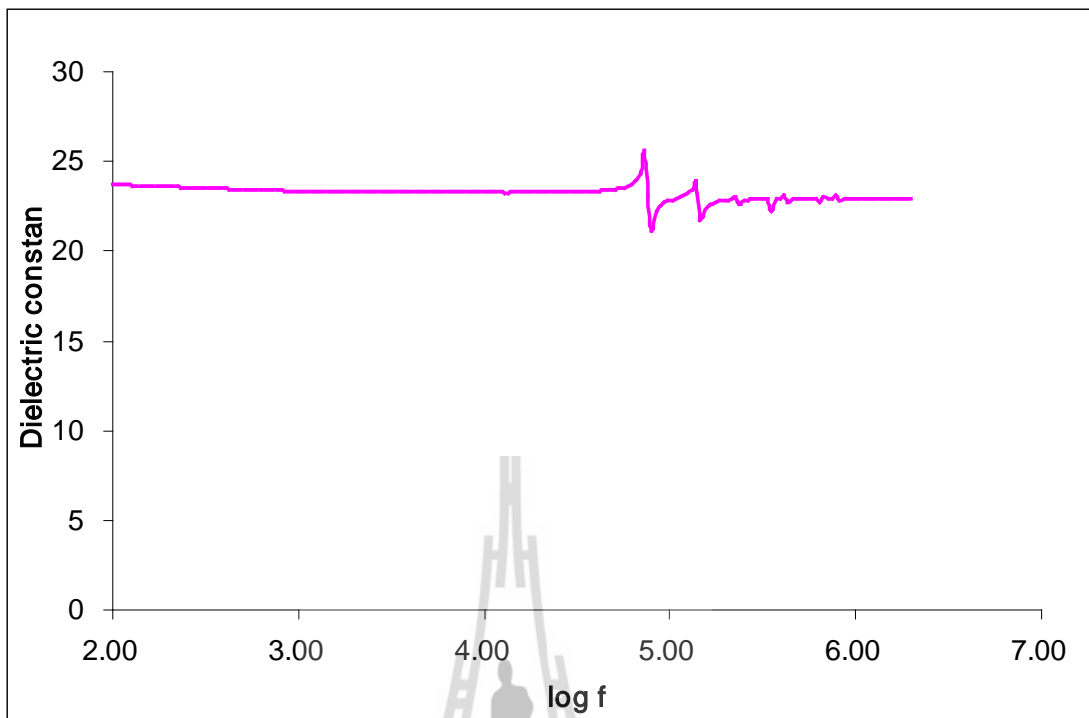
(a)
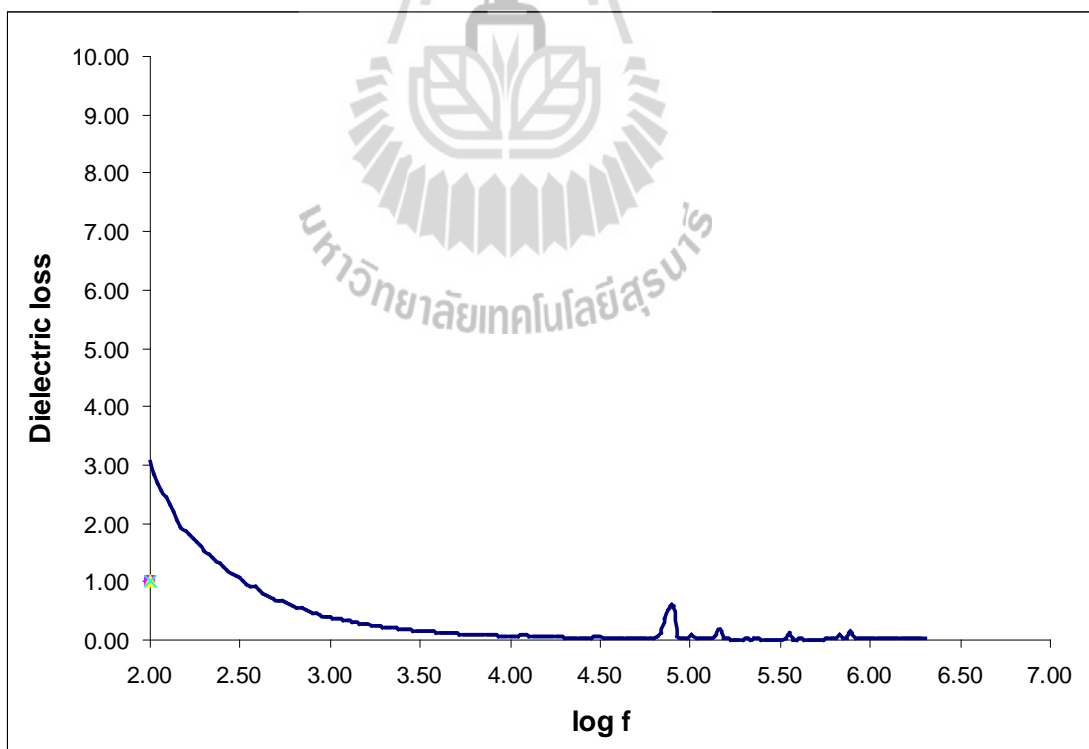


(b)

**Figure 5.25** (a) dielectric constant and (b) dielectric loss of KDP + 2 mol% thiourea

in $\langle 001 \rangle$ –direction.

(a)



(b)
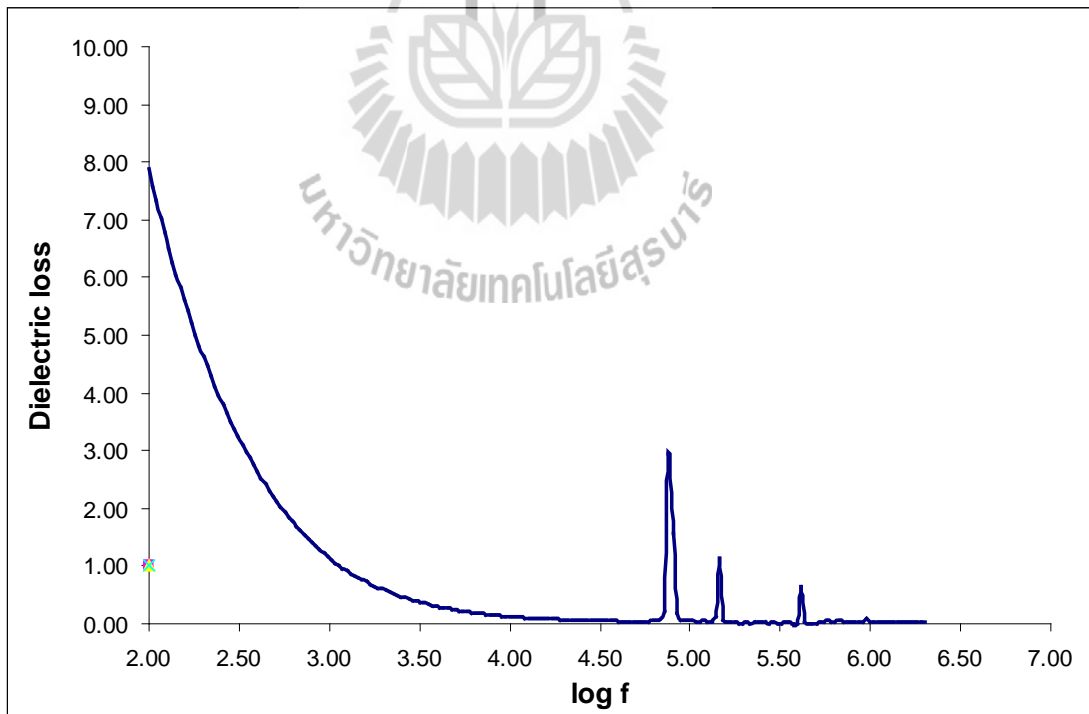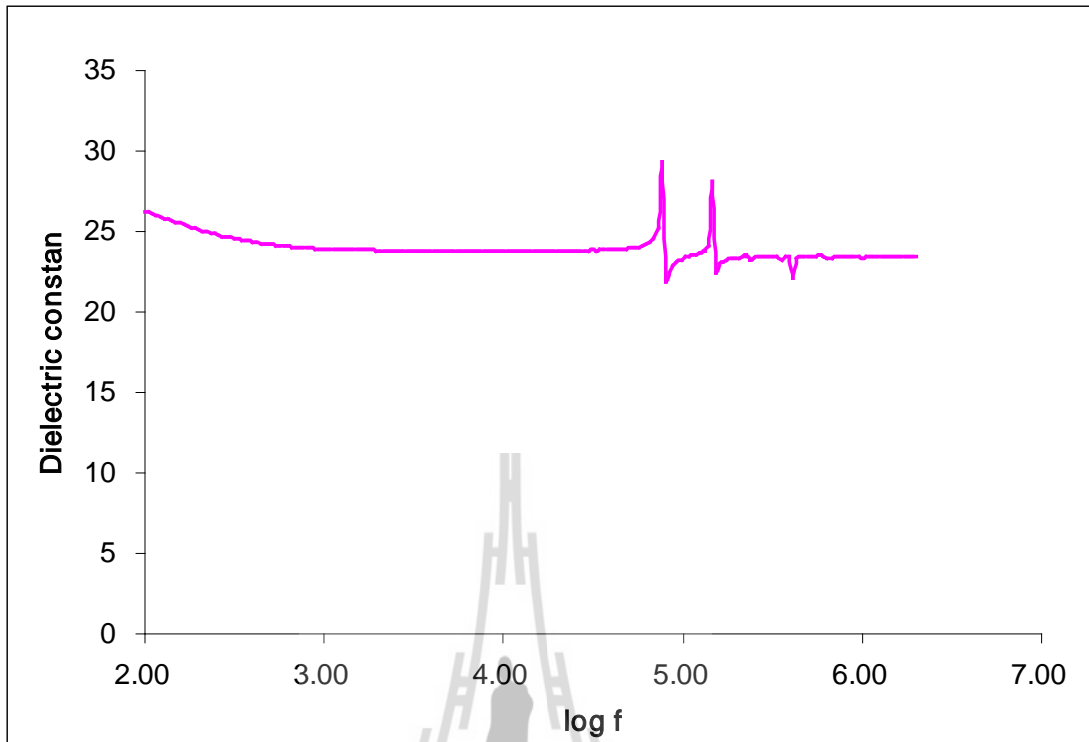
**Figure 5.26** (a) dielectric constant and (b) dielectric loss of KDP + 3 mol% thiourea

in $\langle 001 \rangle$ –direction.

(a)



(b)
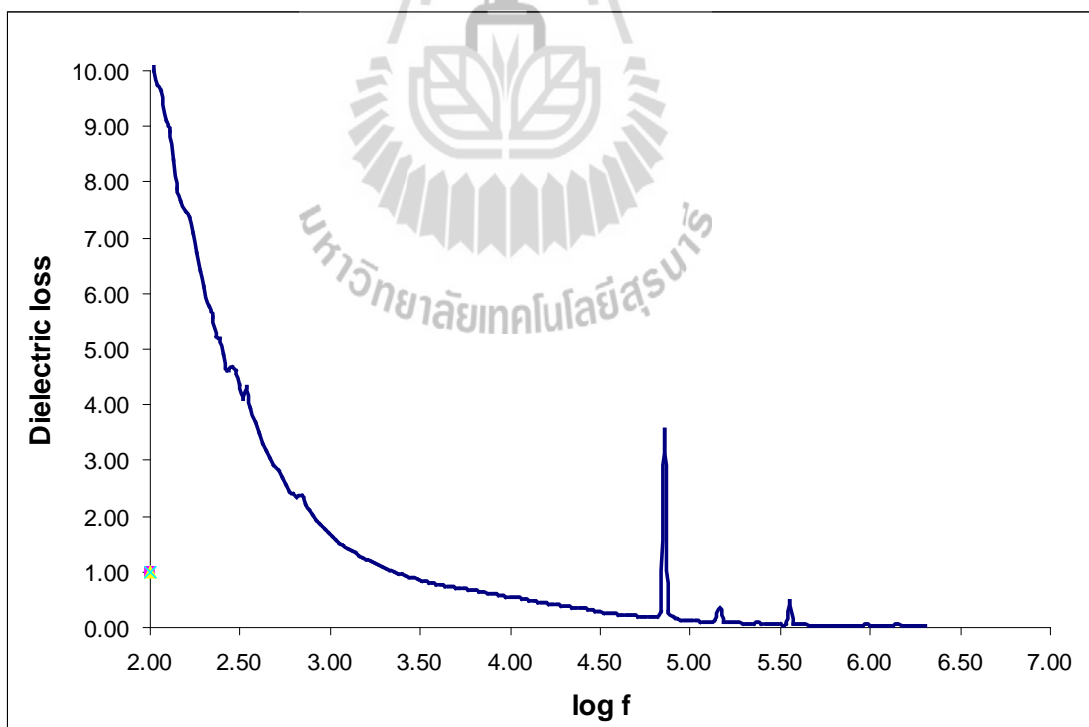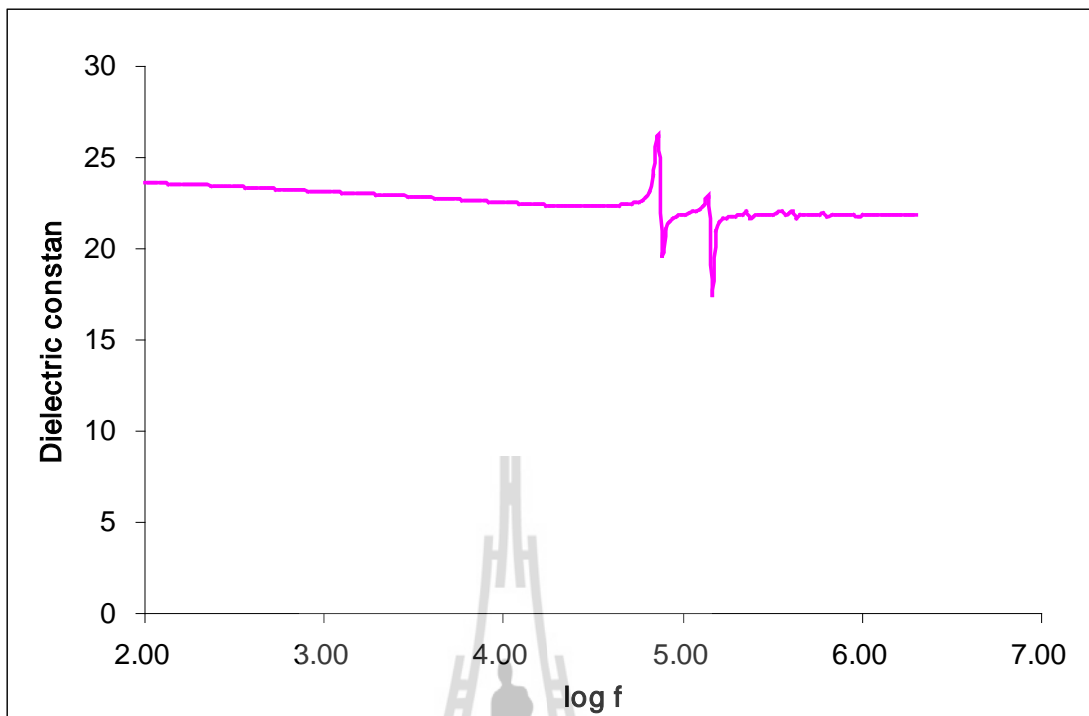
**Figure 5.27** (a) dielectric constant and (b) dielectric loss of KDP + 4 mol% thiourea

in $\langle 001 \rangle$ –direction.
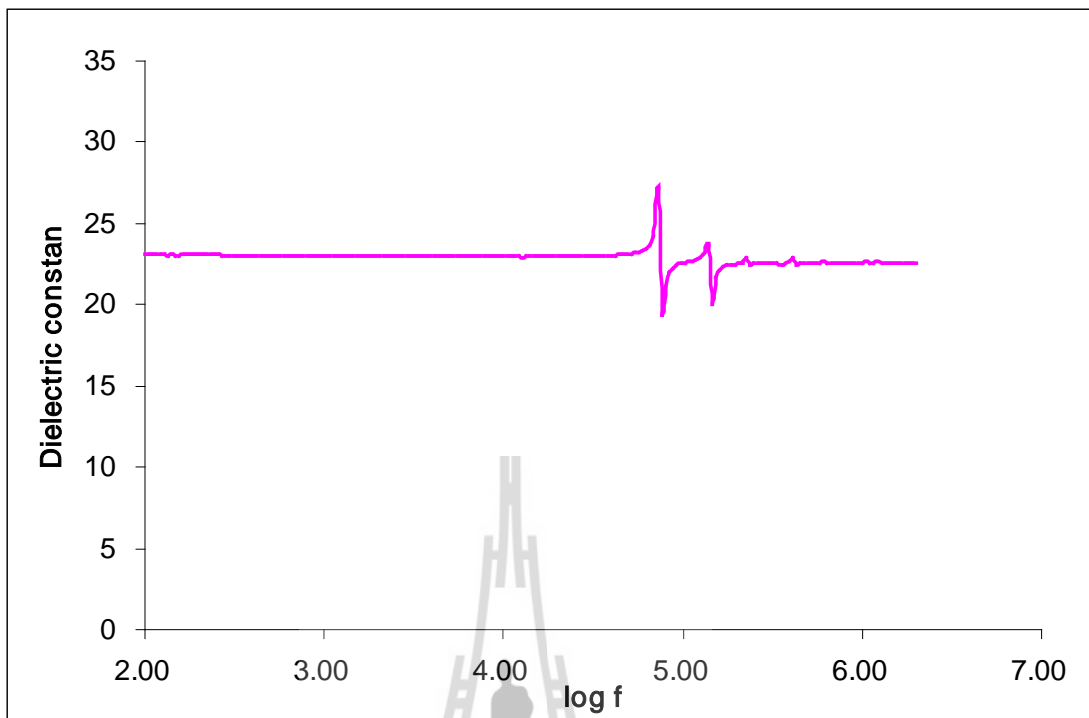
(a)
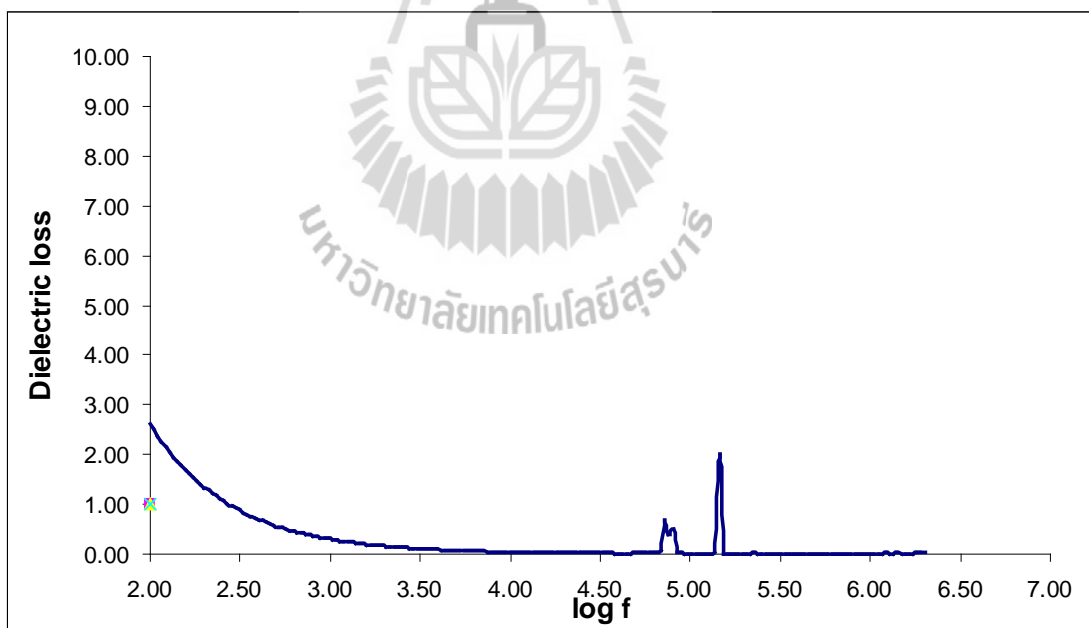


(b)

**Figure 5.28** (a) dielectric constant and (b) dielectric loss of KDP + 5 mol% thiourea

in $\langle 001 \rangle$ –direction.

The dielectric loss is also studied as a function of frequency at room temperature, as shown in Figures 5.23(b) – 5.28(b). The curves of the dielectric loss suggest that it strongly depends on the frequency of the applied field. The dielectric loss decreases as an exponential function with frequency. For the given frequency 1 kHz – 2 MHz, dielectric loss decreases from 0.28 to almost zero (0.01) for pure KDP crystal and decreases from 3.85, 0.39, 1.16, 1.69 and 0.31 to almost zero for 1 – 5 mol% thiourea doped KDP, respectively. The dielectric loss of the crystals was close to zero at around log frequency of ~4.50 (~40 kHz). The characteristic of low dielectric loss with high frequency of samples suggests that the sample possesses good optical quality with lesser defects and this parameter is of vital importance for nonlinear optical materials in their application (Balarew and Duhlew, 1984).

Figure 5.29 shows comparison of the dielectric constant of pure and doped KDP. For the frequency of 1 MHz (log frequency of 6.0), the dielectric constants are 22.2, 21.5, 22.9, 23.4, 21.9 and 22.6 of pure and 1 – 5 mol% thiourea doped KDP, respectively.

Dielectric constant and dielectric loss of pure KDP grown by SR method in different direction are shown in Figure 5.29, it is seen that the dielectric constant and dielectric loss of $\langle 010 \rangle$–direction are higher than $\langle 011 \rangle$ and $\langle 001 \rangle$–direction. High value of dielectric loss in $\langle 010 \rangle$–direction might be caused by defects of crystal.
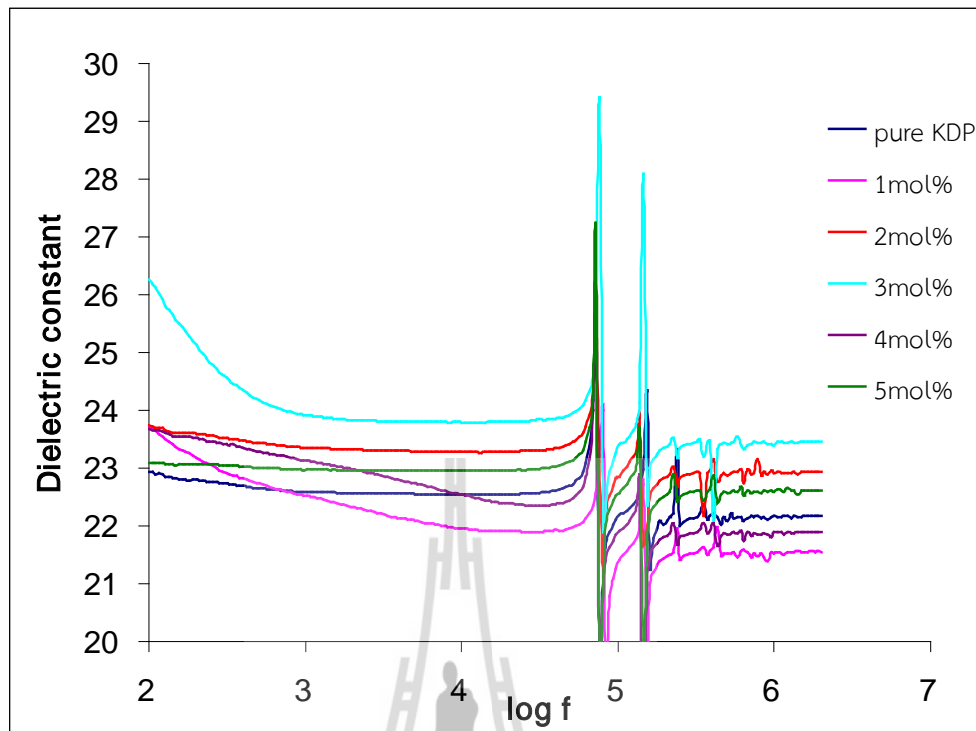
**Figure 5.29** Dielectric constant of pure and thiourea doped KDP crystals

in $\langle 001 \rangle$–direction.
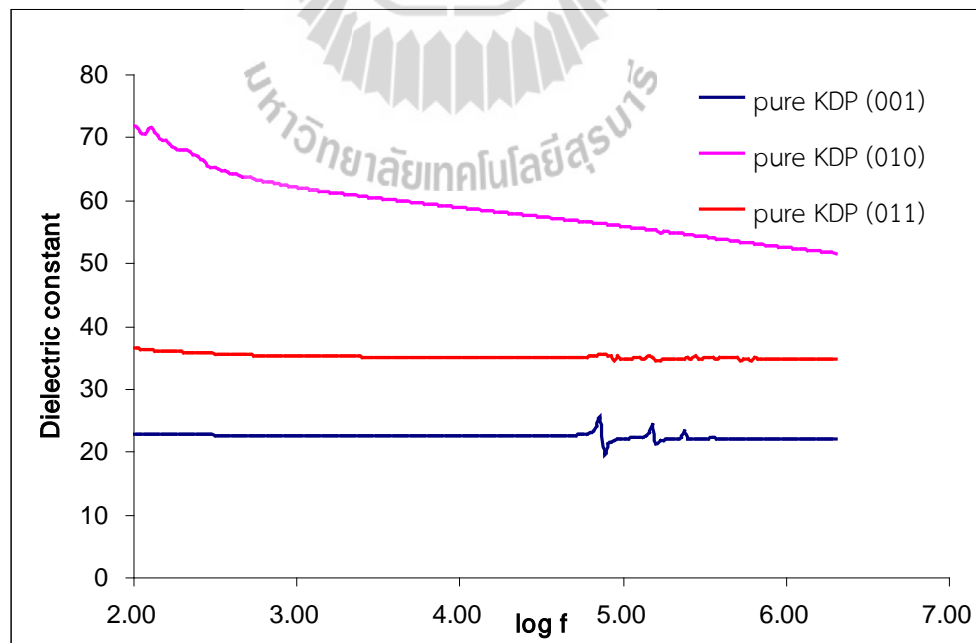


(a)

**Figure 5.30** (a) dielectric constant and (b) dielectric loss of pure KDP crystals grown

by SR method in different directions.

(b)
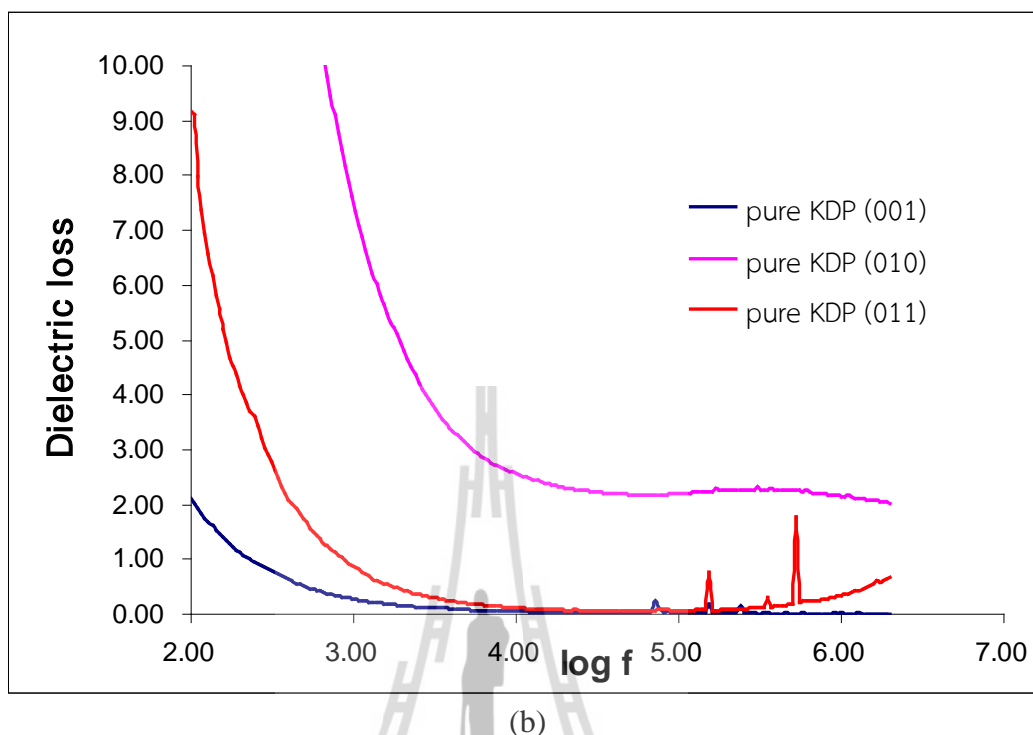
**Figure 5.30** (Continued) (a) dielectric constant and (b) dielectric loss of pure KDP crystals grown by SR method in different directions.

## 5.8 Conclusion

Single crystals of pure and thiourea doped KDP were grown by conventional slow evaporation and SR techniques. The lattice parameters of the grown crystals were found by powder XRD. The perfection of pure and 5 mol% thiourea doped KDP grown by SR technique in $\langle 001 \rangle$–direction was investigated by HRXRD. The FT–IR analysis confirms the functional groups in the crystal lattice. The optical transmission spectrum reveals that the crystals grown by SR technique in $\langle 001 \rangle$ and $\langle 011 \rangle$–direction have good optical transmittance in the visible and IR region but low transmittance in $\langle 010 \rangle$–direction. The cut-off value of grown crystal is lower than 350

nm which makes them promising materials for NLO applications in visible to IR regions. Microhardness measurement reveals that the crystals have a hard lattice. The dielectric studies also reveal the high dielectric constant at low frequency region of 100 Hz – 2MHz. The values of dielectric loss generally decrease exponentially with the given frequency. Low values of dielectric loss indicate that the grown KDP single crystals have very low defects.

## 5.9 Acknowledgment

## 5.10 References

Balamurugan, S. and Ramasamy, P. (2009). Growth and characterization of unidirectional <100> KDP single crystal by Sankaranarayanan–Ramasamy (SR) method. **Spectrochimica Acta Part A: Molecular and Biomolecular Spectroscopy**. 71: 1979–1983.

Balarew, C. and Duhlew, R. (1984). Application of the hard and soft acids and bases concept to explain ligand coordination in double salt structures. **Journal of Solid State Chemistry**. 55: 1–6.

Betterman, B. W. and Cole, H. (1964). Dynamical diffraction of X–rays by perfect crystals. **Reviews of Modern Physics**. 36: 681 – 717.

Bhagavannarayana, G., Ananthamurthy, R.V., Budakoti, G.C., Kumar, B. and Bartwal, K. S. (2005) A study of the effect of annealing on Fe–doped LiNbO$_3$ by HRXRD, XRT and FT–IR. **Journal of Applied Crystallography**. 38: 768–771.

Bhagavannarayana, G., Choubey, A., Shubin, Yu.V. and Lal, K. (2005). Study of point defects in as–grown and annealed bismuth germanate single crystals. **Journal of Applied Crystallography**. 38: 448–454.

Bhagavannarayana, G. and Kushwaha, S. K. (2010). Enhancement of SHG efficiency by urea doping in ZTS single crystals and its correlation with crystalline perfection as revealed by Kurtz powder and high–resolution X–ray diffraction methods. **Journal of Applied Crystallography**. 43: 154–162.

Bhagavannarayana, G., Kushwaha, S. K., Shakir, Mohd. and Maurya, K. K. (2011). Effect of necking on Czochralski–grown LiF crystals and its influence on crystalline perfection and the correlated physical properties. **Journal of Applied Crystallography**. 44: 122–128.

Bhagavannarayana, G., Parthiban, S. and Meenakshisundaram, S. (2006). Enhancement of crystalline perfection by organic dopants in ZTS, ADP and KHP crystals as investigated by high–resolution XRD and SEM. **Journal of Applied Crystallography**. 39: 784–790**.**

Bhagavannarayana, G., Parthiban, S. and Meenakshisundaram, S. (2008). An interesting correlation between crystalline perfection and second harmonic

generation efficiency on KCl– and Oxalic acid–doped ADP Crystals. **Crystal Growth & Design**. 8: 446–451.

Bhagavannarayana, G., Rajesh, P., Ramasamy, P. (2010). Interesting growth features in potassium dihydrogen phosphate: unravelling the origin and dynamics of point defects in single crystals. **Journal of Applied Crystallography**. 43: 1,372–1,376.

Boomadevi, S. and Dhanasekaran, R. (2004)**.** Synthesis, Crystal Growth and Characterization of L–pyrrolidone–2–carboxylic acid (L–PCA) crystals. **Journal of Crystal Growth**. 261: 70–76.

Callister, W. D. Jr. and Rethwisch, D. G. (2010). **Materials science and engineering: an introduction**. (8th ed.). USA: John Wiley & Sons.

Dhanaraj, P.V., Mahadevan, C.K., Bhagavannarayana, G., Ramasamy, P. and Rajesh, N.P. (2008). Growth and characterization of KDP crystals with potassium carbonate as additive. **Journal of Crystal Growth**. 310: 5341–5346.

Lal, K. and Bhagavannarayana, G. (1989). A high-resolution diffuse X–ray scattering study of defects in dislocation-free silicon crystals grown by the float–zone method and comparison with Czochralski–grown crystals. **Journal of Applied Crystallography**. 22 : 209–215.

Mary Linet, J. and Jerome Das, S. (2011). Optical, mechanical and transport properties of unidirectional grown L-tartaric acid bulk single crystal for non–linear optical application. **Materials Chemistry and Physics**. 126: 886–890.

Maunier, C., Bouchut, P., Bouillet, S., Cabane, H., Courchinoux, R., Defossez, P., Poncetta, J.C. and Ferriou-Daurios, N. (2007). Growth and characterization of large KDP crystals for high power lasers. **Optical Materials**. 30: 88–90.

Pritula, I. M., Kolybayeva, M. I., Salo, V. I. and V. M. Puzikov. (2007). Defects of large-size KDP single crystals and their influence on degradation of the optical properties. **Optical Materials**. 30: 98–100.

Robert, R., Justin Raj, C., Krishnan, S. and Jerome Das, S. (2010). Growth, theoretical and optical studies on potassium dihydrogen phosphate (KDP) single crystals by modified Sankaranarayanan–Ramasamy (mSR) method. **Physica B**. 405: 20–24.

Santhanaraghavan, P. and Ramasamy, P. (2000). **Crystal Growth Process and Methods**. Kumbakonam, India: KRU publications.

Senthilkumar, K., MoorthyBabu, S. and Bhagavannarayana, G. (2011). Study of the influence of dopants on the crystalline perfection of ferroelectric glycine phosphite single crystals using high–resolution X–ray diffraction analysis. **Journal of Applied Crystallography**. 44: 313–318.
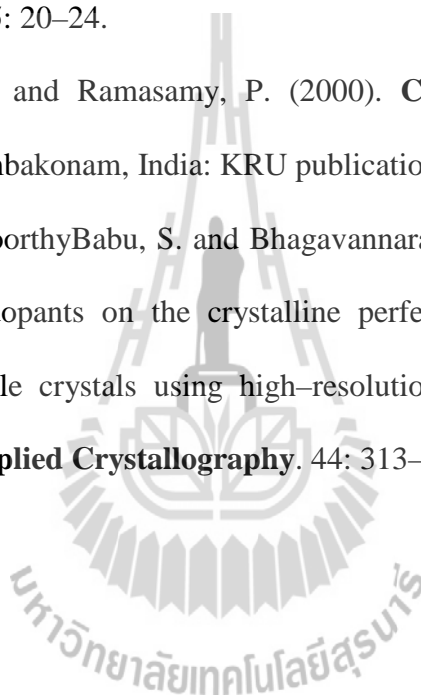
# CHAPTER VI

# SUMMARY

In this present work, crystals of pure and thiourea doped KDP were grown from slow evaporation solution growth technique at room temperature and SR technique. The good and transparent crystals grown by slow evaporation technique were chosen as seed crystals of SR technique. The growth rate of crystals grown by SR technique was shown in Table 4.1. The lattice parameters and unit cell volume of the grown crystals were found by powder XRD, given in Table 5.1.

The perfection of grown crystals was investigated by HRXRD. The pure KDP crystal has the crystalline perfection quite good and it is nearly perfect single crystal without having any internal structural grain boundaries. The single crystal of 5 mol% thiourea doped KDP is found to contain interstitial defects.

The FT–IR analysis confirms the functional groups in the crystal lattice. The results show strong peaks of the P=O stretching, P–O–H stretching, OP–O–H stretching vibrations.

The optical transmission spectrum reveals that the crystals grown by SR technique have better optical transmittance than the crystals grown from slow evaporation solution technique. The crystals grown by SR technique in $\langle 001 \rangle$ and $\langle 011 \rangle$–direction have good optical transmittance in the visible–IR region but low transmittance in $\langle 010 \rangle$–direction. The cut-off value of grown crystal is lower than 350

nm which makes them promising material for NLO applications in visible to IR regions. The optical parameters such as absorption coefficient ($\alpha$), optical band gap ($E_g$), extinction coefficient ($k$) and refractive index ($n$) were determined from the transmittance ($T$) and shown in Figures 5.7–5.8, Table 5.3, Figures 5.11–5.12, and Table 5.4, respectively.

Microhardness measurement reveals that the Vicker's microhardness number ($H_v$) of pure and thiourea doped KDP crystals decreases with increased load, given in Figures 5.18–5.19. The Meyer's index or work–hardening coefficient, ($n$) show the crystals have a hard lattice (n < 2), given in Table 5.7.

The dielectric studies also reveal the high dielectric constant at low frequency region of 100 Hz – 2MHz. The dielectric constant of crystals grown by SR method in $\langle 001 \rangle$–direction slightly decrease with increase in frequency. The values of dielectric loss generally decrease exponentially with the given frequency. Low values of dielectric loss indicate that the grown KDP single crystals have very low defects. Dielectric constant of pure KDP grown by SR method of $\langle 010 \rangle$–direction has shown higher value than $\langle 011 \rangle$ and $\langle 001 \rangle$–directions. Dielectric loss, also, in $\langle 010 \rangle$–direction has shown higher value than $\langle 011 \rangle$ and $\langle 001 \rangle$–directions. High value of dielectric loss in $\langle 010 \rangle$–direction might be caused by defects of crystal.
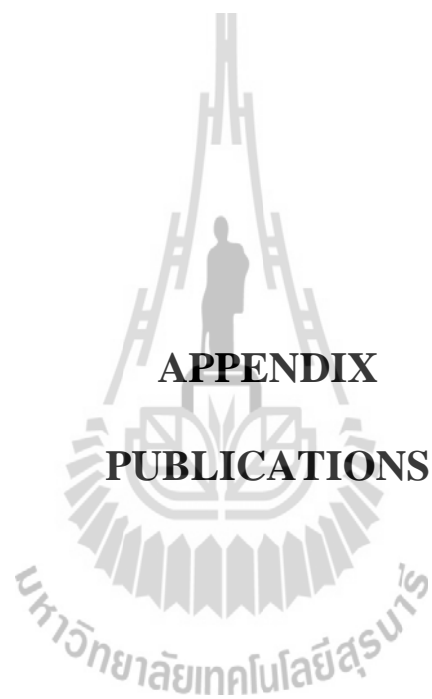
**APPENDIX**

**PUBLICATIONS**
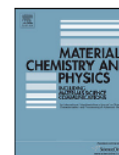
# Effect of KCl on the bulk growth KDP crystals by Sankaranarayanan-Ramasamy method

S. Balamurugan[a], P. Ramasamy[a,*], Yutthapong Inkong[b], Prapun Manyum[b]

[a] Centre for Crystal Growth, SSN College of Engineering, Kalavakkam, Chennai 603110, India
[b] School of physics, Institute of Science, Suranaree University of Technology, Thailand

**ARTICLE INFO**

**ABSTRACT**

The effect of the addition of potassium chloride (KCl) in bulk growth unidirectional (0 0 1) potassium dihydrogen phosphate (KDP) grown from aqueous solution by Sankaranarayanan-Ramasamy (SR) method has been studied. The crystal of 15 mm diameter, 95 mm height was grown by SR method. Addition of 5 M% KCl in the bulk growth medium increases the quality as well as the growth rate. The grown crystals were characterized by UV–Vis spectroscopy, microhardness and dielectric studies. It reveals that the SR method grown crystalline quality and perfection is better than the conventional method grown crystal.

© 2008 Elsevier B.V. All rights reserved.

## 1. Introduction

One of the obvious requirements for a non-linear optical crystal is that it should have excellent optical quality. Potassium dihydrogen phosphate, $KH_2PO_4$ (KDP) is a good non-linear crystal material due to its interesting electrical and optical properties, structural phase transitions, and its easy crystallization. The study of KDP is of great interest because of its unique non-linear optical properties and vast applications in the field of high power laser systems. Potassium dihydrogen orthophosphate (KDP) is a model system for non-linear optical device application. Large single crystal of KDP and DKDP are used for frequency conversion and as parts of large aperture optical switches in the laser fusion systems for the inertial confinement fusion program [1]. These crystals are required to have good optical property and high laser-damage threshold. Additives have an important role in improving the qualities of KDP crystal [2,3] and the effect on the adjustment of growth habits. But many ions impurities exist in the KDP solutions. They have various effects both on habit modification and crystal quality. The effects of cationic ions, such as $Fe^{3+}$, $Cr^{3+}$, $Al^{3+}$, etc., have been extensively investigated [4]. It is known that the growth of a crystal in solutions could be suppressed or enhanced by the presence of an impurity. In some cases, [5] crystal growth is suppressed for a wide range of supersaturation. The

KDP crystals were grown with higher quality and different orientation by SR method [6,7]. Already 1–10 M% KCl added KDP crystals have been grown by conventional method and the addition of KCl improves the quality of the KDP crystal [8–10]. From this point of interest an attempt has been made to grow high quality large size KDP single crystals by the addition of 5 M% KCl using SR method. Using the same ingredients KDP crystal was also grown by conventional solution growth method. Identical samples prepared with similar orientation were subjected to all the studies. Several samples were analysed. The results of SR method and conventional method grown KDP with addition of 5 M% KCl are compared.

## 2. Crystal growth

The solution is prepared in Millipore $18\,M\Omega\,cm^{-1}$ resistance, deionized water. The seed obtained from slow cooling was employed for the bulk growth. Best seed crystals were selected for growth. Saturated solution of KDP containing the additive (KCl) to the extent of 5 M% was prepared and used for both conventional and SR method. The saturated solution was filtered and kept inside a constant temperature bath (CTB). A seed crystal was inserted into the solution using nylon thread. The temperature of CTB was reduced at the rate of $0.2\,^{\circ}C\,day^{-1}$. The growth was observed for the entire cooling process and finally the crystal was harvested as soon as the CTB reached the room temperature. The crystal thus grown was used as seed for SR method and also to compare the crystalline quality with SR method grown crystal.

* Corresponding author. Tel.: +91 44 27475166; fax: +91 44 27475166.
  *E-mail address:* ramasamyp@ssn.edu.in (P. Ramasamy).

Fig. 1. (a) The KDP crystal with addition of 5 M% KCl grown by SR method. (b) Cut and polished ingot of KDP + 5 M% KCl crystals grown by SR method.

The SR method experimental setup consists of controllable heating assembly, transparent growth vessel made out of borosilicate glass. A ring heater positioned at the top of the growth ampoule facilitated the solvent evaporation. Depending on the growth rate of the crystal, the bottom ring heater was moved using translation mechanism. It was about 4 mm day$^{-1}$. The seed crystals collected from the conventional slow cooling technique were used for the unidirectional growth. The growth ampoules were carefully mounted with individual seed having the plane (0 0 1) facing the saturated solution of KDP. The seed crystal was mounted in the 15 mm diameter and 300 mm length ampoule. The temperature of the top and bottom portion was set as 38.5 and 34 °C, respectively. The temperature around the growth region is maintained at ±0.05 °C accuracy. The solvent is evaporated with respect to the temperature of the top portion. Highly transparent crystal was obtained which is shown in Fig. 1(a). The size of the harvested crystal is 15 mm diameter and 95 mm height. The cut and polished ingot is shown in Fig. 1(b).

## 3. Result and discussion

### 3.1. Transmittance

Optical transmittance spectra were recorded at room temperature using PerkinElmer Lambda 35 spectrophotometer on 3 mm thick plates of SR method and conventional method grown KDP crystal in the same (0 0 1) plane. The UV–Visible transmittance spectra were recorded in the wavelength region 200–1200 nm. Fig. 2 shows the transparency in the visible spectral range of the samples. The crystal is highly transparent in the entire UV, Visi-
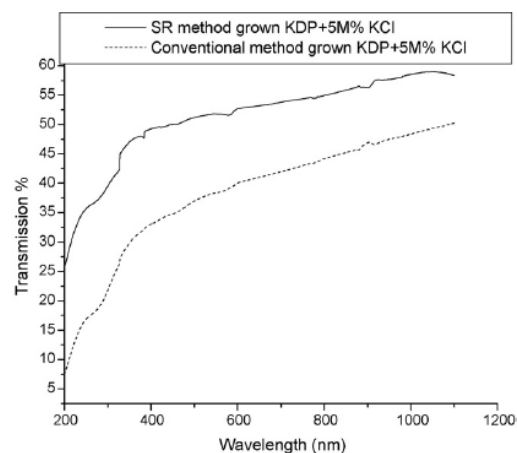


Fig. 2. UV–Vis–NIR spectrum of KDP crystals.

ble and near IR region. From the spectrum it is observed that the transmittance percentage of SR grown crystal is higher than that of the conventional solution grown crystal. The increase in the quality of the KDP crystal in presence of KCl is due to the complexation of trace metal ion impurities in the solution by Cl ion. This complex metal impurity does not get into the crystal lattice [10].

### 3.2. Vickers microhardness measurement

The crystals grown by SR method and conventional method were subjected to Vickers microhardness (using a Shimadzu (Model HMV 2) hardness tester) testing. Load of different magnitudes (10, 25 upto 100 g) were applied. The indentation time was kept at 5 s for all the loads. The plot of Vickers hardness (Hv) versus load (P) for the SR method grown and conventional method grown KDP crystals is shown in Fig. 3. The hardness of ⟨0 0 1⟩ KDP crystals increases with increase of load and then slowly decreases with addition of increased load. The cracks are formed in the crys-
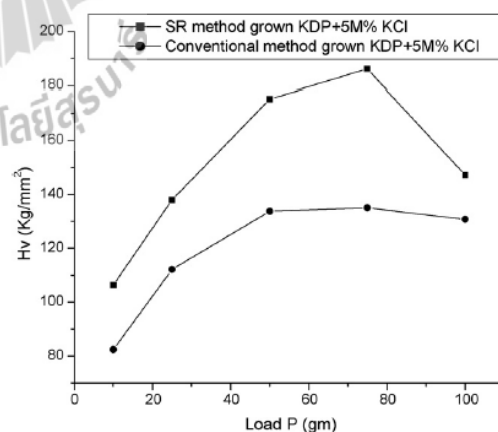


Fig. 3. Microhardness number (Hv) vs load (P) of KDP crystals.

tals around 75 g, which is moderately harder. From the graph, it is seen that the hardness value for SR method grown crystal is higher than the hardness of the conventional method grown crystal. The addition of KCl can make the KDP solution more stable and increase the growth rate of KDP crystal and increase the quality of crystal. The major contribution to hardness is attributed to the high stress required for homogeneous nucleation of dislocation in the small dislocation-free region indented [11]. Hence higher hardness value for SR method grown KDP crystal indicates greater stress required for dislocation which confirms greater crystalline perfection. Though cracks begin to be formed for both the crystals around the same load the influence of crack formation on hardness reduction was found to be higher for SR method grown crystal. A similar behavior is seen in our results on KDP crystals grown without the addition of KCl [7]. It has been reported [12] that harder crystals develop more number of microcracks around the indentation mark. This is possibly, the reason for higher reduction of hardness in SR grown KDP crystal.
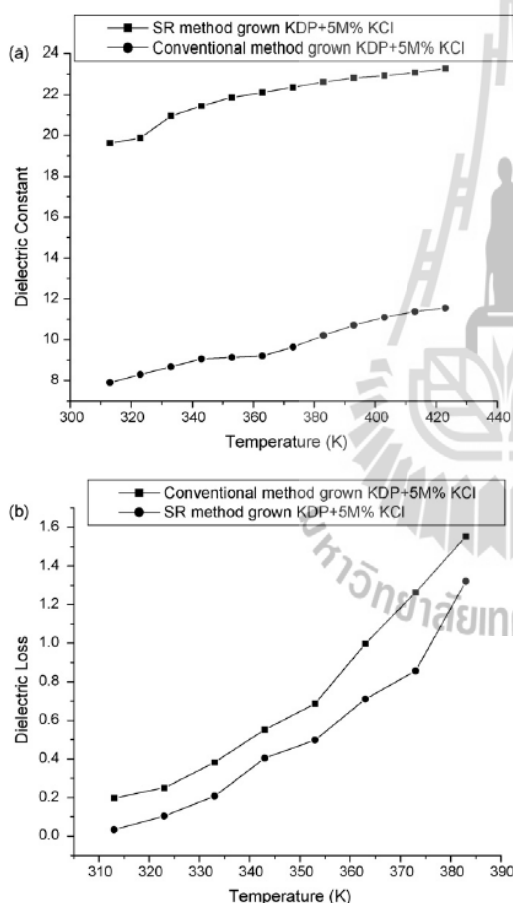
### 3.3. Dielectric studies

The sample dimensions of 3 mm × 3 mm surface area and 2 mm thickness were used for dielectric studies. Dielectric measurement was carried out using a precision (Model4284A) LCR meter in the frequency range 20 Hz–1 MHz. The measurements were taken in the temperature range 40–150 °C. The dielectric constant decreases with increase of frequency. The dielectric constant and dielectric loss increase with the increase of temperature. The dielectric constant of a material is generally composed of four types of contributions, viz. ionic, electronic, orientational and space charge polarization. The above four factors are active at low frequency. The nature of variations of dielectric constant with frequency and temperature indicates the type of contributions that are present in them. The dielectric constant in SR method grown crystal is higher than conventional method grown crystal and is shown in Fig. 4(a). Addition of KCl in the growth medium is found to suppress the metal ion impurities to a large extent and increases the growth rate [9]. The crystal grown from 5 M% KCl added solutions proved that this KCl addition does not affect the crystalline perfection and its quality. Generally the low value of dielectric loss indicates that sample possesses good crystalline quality with fewer defects [13,14]. The dielectric loss was less in SR method grown crystal compared to conventional method grown crystal (Fig. 4(b)) and this agrees with the result of optical transmission studies. The reasons for better quality crystal by SR method: the generation of dislocations is strongly correlated with the formation of inclusions in the crystals, which in turn may arise due to a variety of reasons. Inclusions may also arise due to the shape of the seed crystal. If the seed is not bounded by the important habit faces, the facets of these will be formed in the early stages of growth. The region between these facets develops terraces parallel to the habit faces. In these regions solvent is easily trapped giving rise to the so-called veils. It has also been observed that dislocations can originate from growth sector boundaries [15]. In SR method, the multi faceted growth is avoided so grown crystals have fewer defects.

### 4. Conclusion

The dimension of the bulk KDP crystals grown by SR method using 5 M% KCl is 15 mm diameter, 95 mm height. Addition of 5 M% KCl in the bulk growth medium is found to suppress the metal ion impurities to a large extent and increase the growth rate. The additive KCl blocks the metal ions from entering into the crystal lattice and thus avoiding the chain structure, which enhances the crystalline quality. The SR method grown crystal is found to have excellent crystal quality as determined by transmittance, microhardness and dielectric studies. The SR method grown unidirectional KDP has higher transmittance and higher hardness value as against conventional method grown crystals. The dielectric constant was higher and the dielectric loss was less in SR method grown crystal as against conventional method grown crystal. The improved transparency and size make this crystal suitable for optical device.



Fig. 4. (a) Dielectric constant vs temperature of KDP crystals. (b) Dielectric loss vs temperature of KDP crystals.

### References

[1] Mark A. Rhodes, B. Woods, J.J. DeYoreo, D. Roberts, AthertonF L.J., Appl. Opt. 34 (1995) 5312.
[2] Guohui Li, Genbo Su, Xinxin Zhuang, Zhengdong Li, Youping He, J. Cryst. Growth 269 (2004) 443.
[3] K. Srinivasn, K. Meera, P. Ramasamy, Cryst. Res. Technol. 35 (2000) 291.
[4] Wang Shenglai, Gao Zhangshou, Fu Youjun, Sun Xun, Zhang Jieguo, Zeng Hong, Li Yiping, J. Cryst. Growth 223 (2001) 415.
[5] J. Dugua, B. Simon, J. Cryst. Growth 44 (1978) 280.
[6] S. Balamurugan, G. Bhagavannarayana, P. Ramasamy, Mater. Lett. 62 (2008) 3963.

[7] S. Balamurugan, P. Ramasamy, Mater. Chem. Phys. 112 (2008) 1.
[8] J. Podder, J. Cryst. Growth 237 (2002) 70.
[9] J. Podder, S. Ramalingom, S. Narayana Kalkura, Cryst. Res. Technol. 36 (2001) 549.
[10] Guohui Li, Xue Liping, Genbo Su, Xinxin Zhuang, Zhengdong Li, Youping He, J. Cryst. Growth 274 (2005) 555.
[11] A.G. Kunjomana, K.A. Chandrasekaran, Cryst. Res. Technol. 40 (2005) 782.
[12] K. Kishan Rao, V. Surender, B. Saritha Rani, Bull. Mater. Sci. 25 (2002) 641.
[13] K.B.R. Varma, K.V. Ramanaiah, K.V. Rao, Bull. Mater. Sci. 5 (1983) 39.
[14] P. Suryanarayana, H.N. Acharya, K. Rao, J. Mater. Sci. Lett. 3 (1984) 21.
[15] H.L. Bhat, Prog. Cryst. Growth Charact. 11 (1985) 57.
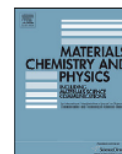
# Investigation of SR method grown ⟨0 0 1⟩ directed KDP single crystal and its characterization by high-resolution X-ray diffractometry (HRXRD), laser damage threshold, dielectric, thermal analysis, optical and hardness studies

S. Balamurugan[a], P. Ramasamy[a,*], S.K. Sharma[b], Yutthapong Inkong[c], Prapun Manyum[c]

[a] Centre for Crystal Growth, SSN College of Engineering, Kalavakkam, Chennai 603 110, India
[b] LMDDD, RRCAT, Indore, India
[c] School of Physics, Institute of Science, Suranaree University of Technology, Thailand

## ARTICLE INFO

## ABSTRACT

⟨0 0 1⟩ directed potassium dihydrogen orthophosphate (KDP) single crystal was grown by Sankaranarayanan–Ramasamy (SR) method. The ⟨0 0 1⟩ oriented seed crystals were mounted at the bottom of the platform and the size of the crystals were 10 mm diameter, 110 mm height. Two different growths were tried, in one the crystal diameter was the ampoule's inner diameter and in the other the crystal thickness was less than the ampoule diameter. In the first case only the top four pyramidal faces were existing whereas in the second case the top four pyramidal faces and four prismatic faces were existing through out the growth. The crystals were grown using same stoichiometric solution. The results of the two growths are discussed in this paper. The grown crystals were characterized by high-resolution X-ray diffractometry (HRXRD), laser damage threshold, dielectric, thermal analysis, UV–vis spectroscopy and microhardness studies. The HRXRD analysis indicates that the crystalline perfection is excellent without having any very low angle internal structural grain boundaries. Laser damage threshold value has been determined using Nd:glass laser operating at 1054 nm. The damage threshold for the KDP crystal is greater than 4.55 GW cm$^{-2}$. The dielectric constant was higher and the dielectric loss was less in SR method grown crystal as against conventional method grown crystal. In thermal analysis, the starting of decomposition nature is similar in SR method grown KDP crystal and conventional method grown crystal. The SR method grown KDP has higher transmittance and higher hardness value compared to conventional method grown crystals.

© 2009 Elsevier B.V. All rights reserved.

## 1. Introduction

Potassium dihydrogen phosphate (KDP) has been extensively studied for many years due to its important applications such as second harmonic generation, Q-switch and quantum electronics [1,2]. KDP and ammonium dihydrogen phosphate (ADP) are nonlinear optical materials and have been used as optical modulation devices and frequency converters. The National Ignition Facility (NIF), being built at Lawrence Livermore National Laboratory (LLNL), requires large single crystal plates of KDP ($KH_2PO_4$) and DKDP ($KD_2PO_4$) for Pockels cells and frequency converters as a part of its design [3]. Particularly, optical crystals with lower impurity and higher damage threshold are required for inertial confinement fusion. The KDP is a transparent dielectric material best known for its nonlinear optical and electro-optical properties. Because of its nonlinear optical properties, it has been incorporated into various laser systems

for harmonic generation and optoelectrical switching [4]. The very high-energy Nd:glass lasers used for inertial confinement fusion research need large plates of nonlinear crystals for electro-optic switches and frequency converters [5]. KDP crystal draws persistent attention of scientists due to its excellent quality and possibility of growing large-size single crystals [6–8]. KDP finds widespread use as frequency doublers in laser applications and has been studied at great detail. KDP, ADP and DKDP are the only nonlinear crystals currently used for these applications due to their exclusive properties. These properties include transparency in a wide region of the optical spectrum, resistance to damage by laser radiation, and relatively high nonlinear efficiency, in combination with reproducible growth to large size and easy finishing.

In all the methods of growth, planar habit faces contain separate regions common to each facet having their own sharply defined growth direction known as growth sectors. The boundary between these growth sectors is more strained than the extended growth sectors due to mismatch of lattices on either side of the boundary as a result of preferential incorporation of impurities into the lateral section [9]. The KDP crystals were grown with higher quality and

different orientation by SR method [10,11]. The grown crystals have better quality compared to conventional method grown crystal.

Already ⟨0 0 1⟩ directional KDP single crystals were grown by SR method and the grown crystals were characterized by laser damage threshold, Raman Spectroscopy, Fourier transform infrared (FTIR) and optical studies [12,13]. In this paper ⟨0 0 1⟩ directional KDP single crystals were grown, two types of different growths were tried, in one the crystal diameter was the ampoule's inner diameter and in the other the crystal size was less than the ampoule diameter. In the first case only the top four pyramidal faces were existing whereas in the second case the top four pyramidal faces and four prismatic faces were existing through out the growth. The crystals were grown using same stoichiometric solution. The results of the two growths are discussed in this paper. The grown crystals were subjected to HRXRD, Laser damage threshold, dielectric, thermal analysis, UV–vis spectroscopy and microhardness studies. With the same ingredients KDP crystal was also grown by conventional solution growth method. The results of SR method grown KDP and conventional method grown KDP are compared.

## 2. Experimental

A saturated solution of KDP is prepared in Millipore 18 MΩ cm resistance, deionized water. The seed obtained from conventional slow cooling method was employed for the bulk growth. Best seed crystals were selected for growth. The saturated solution at 45 °C was prepared, filtered and kept inside a constant temperature bath (CTB). A seed crystal was inserted into the solution using nylon thread. The temperature of CTB was reduced at the rate of 0.2 °C day⁻¹. The growth was observed for the entire cooling process and finally the crystal was harvested as soon as the CTB reached the room temperature. The crystal thus grown was used as seed for SR method and also to compare the crystalline quality with SR method grown crystal.

The SR experimental setup consists of two ring heaters, transparent glass tubes made by borosilicate glass and seed mounting pad. The ring heaters are positioned in the top and bottom of the ampoule. The heaters are connected to a dual channel temperature controller which maintains constant temperature. The entire setup is kept in a water bath. The experimental setup was placed in a dust free hood. The crystal with specific orientation can be grown from solution by

Sankaranarayanan–Ramasamy (SR) method. The SR method is suitable to effectively control the orientation of molecules during the bulk crystal growth from solution at room temperature. Using the above method ⟨0 0 1⟩ directional KDP single crystal was grown.

Highly transparent crystal was obtained which is shown in Fig. 1(a) and (b). With the stoichiometric solution the ratio between length and breadth of KDP crystal in conventional method is ≈2:1 [14,15]. The ratio can be changed by varying the pH [16]. In the present experimentation stoichiometric solution was taken in both the cases. Fig. 1(a) shows a KDP crystal grown by SR method in an ampoule with the bottom cone angle ≈5°. The crystal covers the inner diameter of the ampoule. In this growth only the top four pyramidal faces are existing during the entire growth. Fig. 1(b) shows a KDP crystal grown in an SR method ampoule with bottom cone angle much larger than the previous case. The cone had a flat bottom and the cone angle was ≈15°. In this condition the crystal was not covering the whole ampoule leaving certain space in between the ampoule wall and the crystal during the entire growth. In this case the top four pyramidal faces and the four prismatic faces exist during the growth. Gravity driven concentration is responsible for crystal growth in SR method. Hence the four pyramidal faces at the top receive the most of the nutrient resulting in growth lengthwise. This results in length to breadth ratio different from conventional method. In all the methods of growth, planar habit faces contain separate regions common to each facet having their own sharply defined growth direction known as growth sectors. The boundaries between these growth sectors are more strained than the extended growth sectors due to mismatch of lattices on either side of the boundary as a result of preferential incorporation of impurities into the lateral section. In the crystal shown in Fig. 1(b) the pyramidal face growth was very high but the growth of the prism face was very little. Hence incorporation of defects in this crystal can be expected to be much less than in a conventional method grown crystal. In SR method length to breadth ratio has been changed to as much as 10:1 using the same stoichiometric solution, and without any change of pH. The growth rate 4 mm day⁻¹ was found to be optimum. The size of the harvested ⟨0 0 1⟩ KDP crystal is 10 mm diameter and 110 mm height.

## 3. Result and discussion

### 3.1. High-resolution X-ray diffractometry (HRXRD) studies

The crystalline perfection of the grown single crystals was evaluated by HRXRD using a multicrystal X-ray diffractometer developed at National Physical Laboratory (NPL), New Delhi, India. Fig. 2 shows
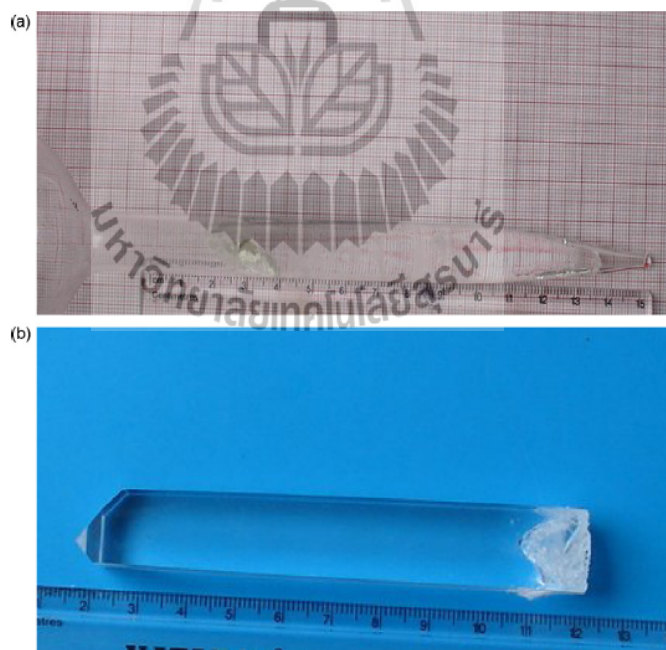


Fig. 1. (a and b) ⟨0 0 1⟩ directional KDP crystal grown by SR method.
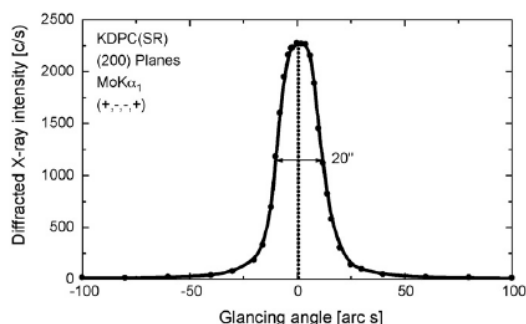
Fig. 2. Diffraction curve recorded for KDP single crystal for (2 0 0) diffracting planes by employing the multicrystal X-ray diffractometer with Mo Kα₁ radiation.
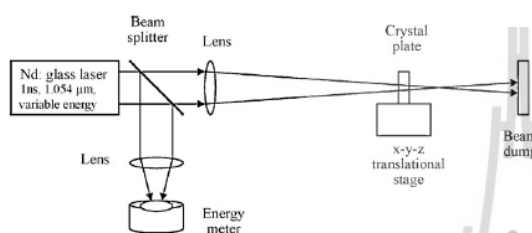


Fig. 3. Schematic of experimental setup for measuring laser-induced damage threshold.

the high-resolution diffraction curve (DC) recorded for a SR-grown ⟨0 0 1⟩ directional KDP single crystal grown by SR technique using (2 0 0) diffracting planes in symmetrical Bragg geometry by employing Mo Kα₁ radiation. As in the figure, the DC contains a single peak and shows that this specimen is free from structural grain boundaries. Full width at half maximum (FWHM) value of this curve is 20 arc s which is expected for a nearly perfect crystal. It is interesting to see the asymmetry of the DC with respect to the peak position (denoted by the dotted line). For a particular angular deviation ($\Delta\theta$) of glancing angle with respect to the peak position, the scattered intensity is much more in the positive direction in comparison to that of the negative direction. This feature clearly indicates that the crystal contains predominantly interstitial type of defects than that of vacancy defects. This can be well understood by the fact that due to interstitial defects which may be due to self-interstitials, impurity atoms including the solvent atoms or molecules in the

crystalline matrix, the lattice around these defects undergo compressive stress [17] and the lattice parameter $d$ (interplanar spacing) decreases and leads to give more scattered (also known as diffuse X-ray scattering) intensity at slightly higher Bragg angles ($\theta_B$) as $d$ and $\sin\theta_B$ are inversely proportional to each other in the Bragg equation ($2d\sin\theta_B = n\lambda$; $n$ and $\lambda$ being the order of reflection and wavelength, respectively, which are fixed). However, these point defects with much lesser density as in the present case hardly give any effect in the performance of the devices based on such crystals.

### 3.2. Laser damage threshold studies

One of the most important considerations in the choice of a material for nonlinear optical applications is its optical damage tolerance. Because of the high optical intensities involved nonlinear materials must be able to withstand high power intensities. The laser damage threshold studies have been carried out for KDP single crystal grown by SR method using a Q-switched Nd:glass laser. Well-polished samples with clean surface were chosen for the present study. Laser-induced surface damage threshold measurements were conducted at RRCAT Indore using a high power Nd:glass laser operating at 1 ns pulse width with beam diameter 62 mm, a convex lens was used to focus it through the crystal. Fig. 3 shows the schematic of the optical layout used for measuring laser-induced damage threshold. Experiments were performed by keeping the positions of the lens and crystal plate as fixed and increasing the laser pulse energy until a whitish visible spot was seen at the surface of the crystal. The crystal was placed at a distance where the beam diameter becomes 2 mm at the exit face of the crystal; the beam diameter was measured using a CCD camera. During laser radiation, the power meter records the energy density of the input laser beam by which the crystal gets damaged. The beam was passed along the ⟨0 0 1⟩ direction for SR method grown KDP single crystal. The experiments were conducted at four different sites (A, B, C and D) in the KDP plate (as shown in Fig. 4) by translating the crystal in the plane perpendicular to the beam direction. The laser has energy stability of the order of ±10%. We measured the maximum non-damaging laser intensity at the four sites of the plate and the results are presented in Fig. 5. The average value of damage threshold for the KDP crystal is greater than $4.55 \pm 0.46\,\mathrm{GW\,cm^{-2}}$, while it is 0.20 GW cm⁻² for conventional method grown KDP single crystal [18]. The laser damage threshold of nonlinear optical components (Pockels cells, frequency doublers, parametric oscillators, etc.) depends on physical and chemical imperfections, particularly on growth imperfection (dislocation, growth ghosts) and impurities concentration and segregation [19]. The most significant features of the dislocation structure were tendency for certain dislocation
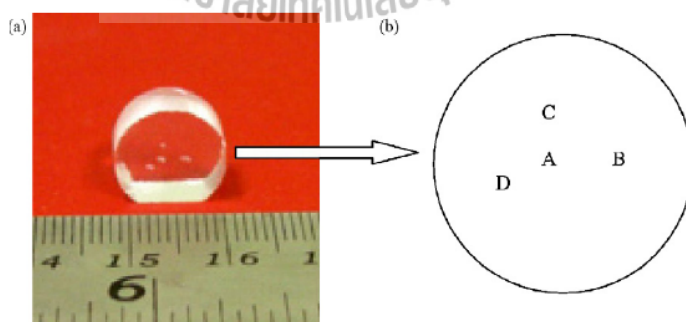


Fig. 4. (a) z-Cut KDP plate prepared for measuring laser-induced damage threshold and (b) schematic for locations of spots (A, B, C and D) in the crystal plate for measuring laser-induced damage threshold.

*S. Balamurugan et al. / Materials Chemistry and Physics 117 (2009) 465–470*
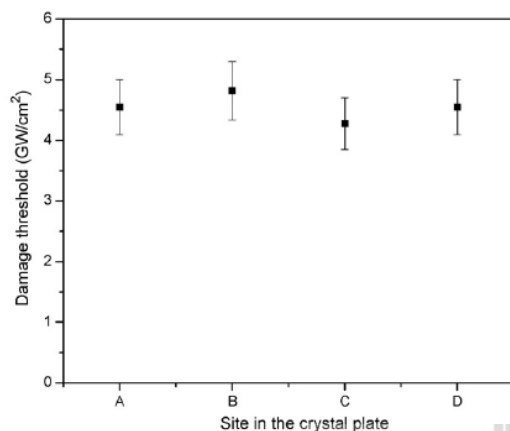


**Fig. 5.** Laser-induced damage threshold of z-cut KDP plate with location in the plate.

types to nucleate in pairs and at growth sector boundaries. Among the numerous processes, which are influenced by crystallographic defects, there can be few situations in which the interconnections are as close as in the case of crystal growth. Crystallization both influences, and is influenced by, the defect structure of the crystal. Some of the dislocation pairs formed at isolated nucleation points originate at growth sector boundaries [20]. In the SR method, the growth sector boundaries are reduced resulting in better quality for the crystal. This is the reason for the high laser damage threshold in the SR method grown crystals.

### 3.3. Dielectric studies

Dielectric measurement was carried out using a precision (Model4284A) LCR meter in the frequency range 100 Hz to 1 MHz. The measurements were made in the temperature range 40–150 °C. The dielectric constant decreases with increase of frequency. The dielectric constant was increased with the increase of temperature. The dielectric constant was measured for SR method grown KDP crystal using two different growths and for conventional method grown KDP crystal (Fig. 6a). In the two different growths of SR method, the higher dielectric constant and low dielectric loss was observed for the crystal which was not covering the whole ampoule during growth compared to the crystal which was covering the inner diameter of the ampoule. But still lower dielectric constant value and higher dielectric loss were observed for conventional method grown crystal. The large value of dielectric constant at low frequency is due to the presence of space charge polarization [21], which depends on the purity and perfection of the sample.

Generally the low value of dielectric loss indicates that sample possesses good crystalline quality with fewer defects [22–24]. The dielectric loss was less in SR method grown crystal as against conventional method grown crystal (Fig. 6b) and this is in agreement with the result of optical transmission studies.

### 3.4. Thermal analysis

TG-DTA of SR method grown KDP crystals grown by two different methods was carried out between 35 and 550 °C at a heating rate 10 °C min$^{-1}$ in nitrogen atmosphere using PerkinElmer Diamond TG/TDA instrument (Fig. 7). In thermal analysis, the starting of decomposition at 185 °C is similar in SR method grown KDP
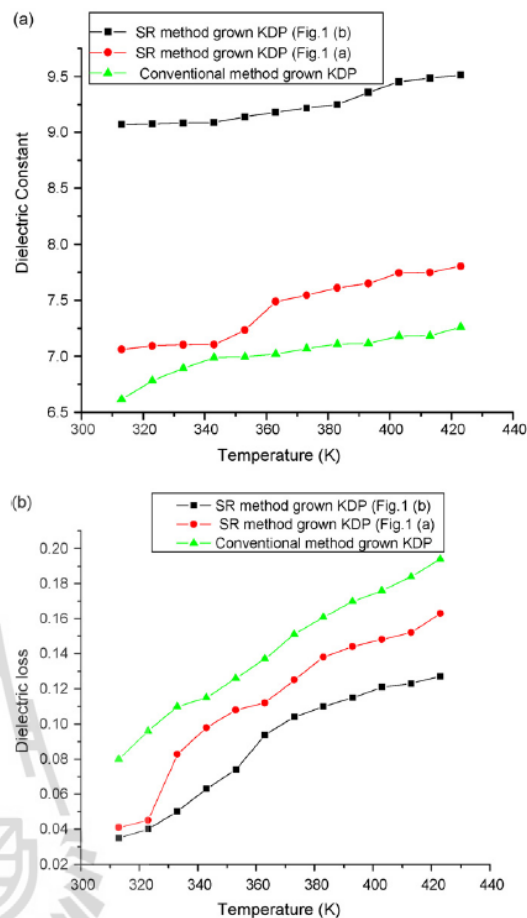




**Fig. 6.** (a) Dielectric constant of KDP single crystal; (b) dielectric loss of KDP single crystal.
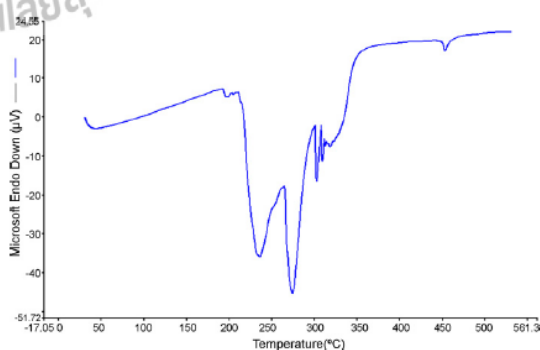


**Fig. 7.** DTA of SR method grown KDP single crystal.
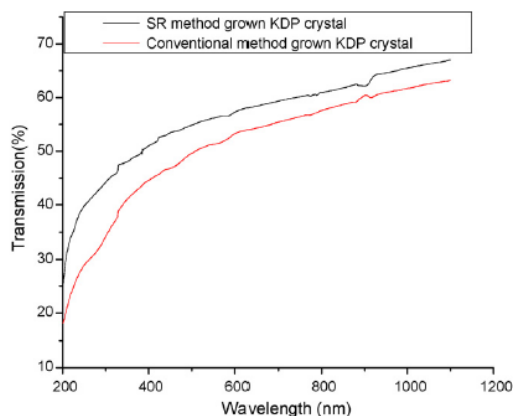
Fig. 8. UV–vis–NIR spectrum of KDP crystals.
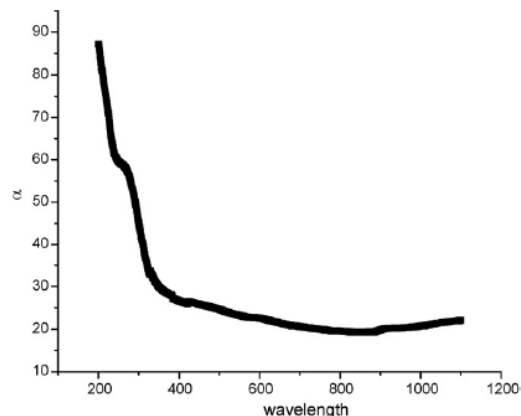


Fig. 9. Absorption coefficient ($\alpha$) vs. wavelength of KDP crystal.

crystal and conventional method grown crystal. The decomposing nature in the temperature range between 185 and 350 °C was similar for both the method grown crystals. The similar behavior was seen with conventional method grown KDP single crystal.

### 3.5. Transmittance

The UV–vis transmittance spectra of SR method grown KDP crystal and conventional method grown KDP crystal in the same (0 0 1) plane (Fig. 3) were recorded in the wavelength region 200–1200 nm. In the visible spectral range the sample shows high transparency (Fig. 8). This is the most desirable property of the materials possessing NLO activity. The crystal is highly transparent in the entire UV, visible and near IR region. From the spectrum it is observed that the transmittance percentage of SR method grown crystal is higher than that of the conventional method grown crystal. The measured transmittance ($T$) was used to calculate the absorption coefficient ($\alpha$) using the formula:

$$\alpha = \frac{2.3036 \log(1/T)}{t}$$

The absorption coefficient was calculated from different location of the grown crystal. Similar absorption coefficient was observed in different sites of the grown crystal (Fig. 9). It reveals that the grown crystalline quality and perfection is good for optical application.

### 3.6. Vickers microhardness measurement

One has to know the mechanical behaviors of the materials that are used for device fabrication. The smooth surface of KDP crystal was subjected to Vickers static indentation test at room temperature (303 K) using a Shimadzu (Model HMV 2) hardness tester. Loads of different magnitude (10, 25 up to 100 g) were applied. The indentation time was kept as 5 s for all the loads. The plot of Vickers hardness (Hv) versus load ($P$) for the SR method grown and conventional method grown KDP crystals is shown in Fig. 10. From the graph it is seen that the hardness value for SR method grown crystal is higher than the hardness of the conventional method grown crystal.

Due to the application of mechanical stress by the indenter, dislocations are generated locally at the region of indentation. Thus the major contribution to hardness is attributed to the high stress required for homogeneous nucleation of dislocation in the small dislocation-free region indented [25]. Hence larger hardness value
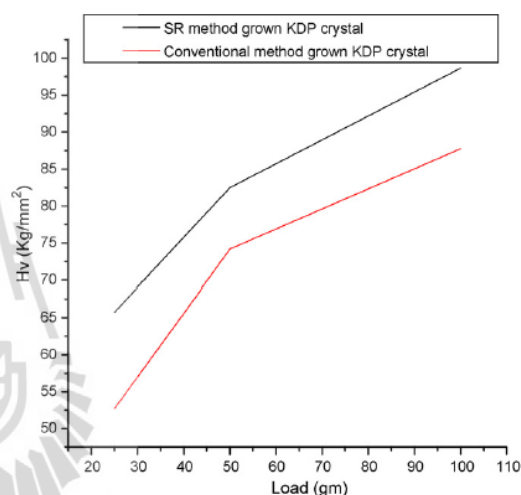


Fig. 10. Microhardness number (Hv) vs. load ($P$) of KDP crystals.

for SR method grown KDP crystal indicates greater stress required to form dislocation thus confirming greater crystalline perfection.

## 4. Conclusion

The bulk single crystals of ⟨0 0 1⟩ KDP with the dimension of 10 mm diameter and 110 mm length have been grown by SR method. Two different growths were tried, in one the crystal diameter was the ampoule's inner diameter and in the other the crystal thickness was less then the ampoule diameter. In the first case only the top four pyramidal faces were existing whereas in the second case the top four pyramidal faces and four prismatic faces were existing through out the growth. In SR method length to breadth ratio has been changed to as much as 10:1 using the same stoichiometric solution, and without any change of pH. The HRXRD analysis indicates that the crystalline perfection is excellent without having any very low angle internal structural grain boundaries. The better laser damage threshold value indicates that direction controlled KDP crystal has high damage resistance and hence the

S. Balamurugan et al. / Materials Chemistry and Physics 117 (2009) 465–470

grown crystals are useful in high power frequency conversion application. The dielectric constant was higher and the dielectric loss was less in SR method grown crystal as against conventional method grown crystal. In thermal analysis, the starting of decomposition at 185 °C is similar in SR method grown KDP crystal and conventional method grown crystal. The SR method grown KDP has higher transmittance and higher hardness value compared to conventional method grown crystals. The improved transparency and size make this crystal suitable for SHG and optoelectronic device fabrications.

## Acknowledgement

## References

[1] A. Yokotani, T. Sasaki, K. Yamanaka, C. Yamanaka, Appl. Phys. Lett. 48 (1986) 1030.
[2] N.P. Zaitseva, J.J. De Yoreo, M.R. Dehaven, R.L. Vital, K.E. Montgomery, M. Richardson, L.J. Atherton, J. Cryst. Growth 180 (1997) 255.
[3] S. Sen Gupta, T. Kar, S.P. Sen Gupta, Mater. Chem. Phys. 58 (1999) 227.
[4] A.J. Nelson, T. van Buuren, E. Miller, T.A. Land, C. Bostedt, N. Franco, P.K. Whitman, P.A. Baisden, L.J. Terminello, T.A. Callcott, J. Electr. Spectr. 114 (2001) 873.
[5] N. Zaitseva, L. Carman, Prog. Cryst. Growth Charact. Mater. 43 (2001) 1.
[6] D. Xu, D. Xue, J. Cryst. Growth 310 (2008) 2157.
[7] X. Ren, D. Xu, D. Xue, J. Cryst. Growth 310 (2008) 2005.
[8] D. Xu, D. Xue, J. Alloys Compd. 449 (2008) 353.
[9] H.G. Gallagher, R.M. Vrcelj, J.N. Sherwood, J. Cryst. Growth 250 (2003) 486.
[10] S. Balamurugan, P. Ramasamy, Mater. Chem. Phys. 112 (2008) 1.
[11] S. Balamurugan, G. Bhagavannarayana, P. Ramasamy, Mater. Lett. 62 (2008) 3963.
[12] Justin Raj, S. Krishanan, D. Dinakaran, R. Uthrakumar, S. Jerome Das, Cryst. Res. Technol. 43 (2007) 245.
[13] N. Balamurugan, P. Ramasamy, Cryst. Growth Des. 6 (2006) 1642.
[14] V. Kannan, R. Birava Ganesh, R. Sathyalakshmi, N.P. Rajesh, P. Ramasamy, Cryst. Res. Technol. 41 (2006) 678.
[15] K.D. Parikh, D.J. Dave, B.B. Parekh, M.J. Joshi, Bull. Mater. Sci. 30 (2007) 105.
[16] S.K. Sharma, S. Verma, B.B. Shrivastava, V.K. Wadhawan, J. Cryst. Growth 244 (2002) 342.
[17] G. Bhagavannarayana, S. Parthiban, S. Meenakshisundaram, Cryst. Growth Des. 8 (2008) 446.
[18] N. Vijayan, G. Bhagavannarayana, R. Ramesh Babu, R. Gopalakrishnan, K.K. Maurya, P. Ramasamy, Cryst. Growth Des. 6 (2006) 1542.
[19] H.V. Alexandru, S. Antohe, J. Cryst. Growth 258 (2003) 149.
[20] G.R. Easter, R. Price, P.J. Halfpenny, J. Phys. D: Appl. Phys. 32 (1999) A128.
[21] P.S. Ramasubramanian, C. Mahadevan, Indian J. Pure Appl. Phys. 29 (1991) 285.
[22] T.H. Freeda, C. Mahadevan, Proc. Intl. Workshop Prep. and Charact. Tech. Imp. Single Crystals, 2001, p. 350.
[23] K.B.R. Varma, K.V. Ramanaiah, K.V. Rao, Bull. Mater. Sci. 5 (1983) 39.
[24] P. Suryanarayana, H.N. Acharya, K. Rao, J. Mater. Sci. Lett. 3 (1984) 21.
[25] A.G. Kunjomana, K.A. Chandrasekaran, Cryst. Res. Technol. 40 (2005) 782.
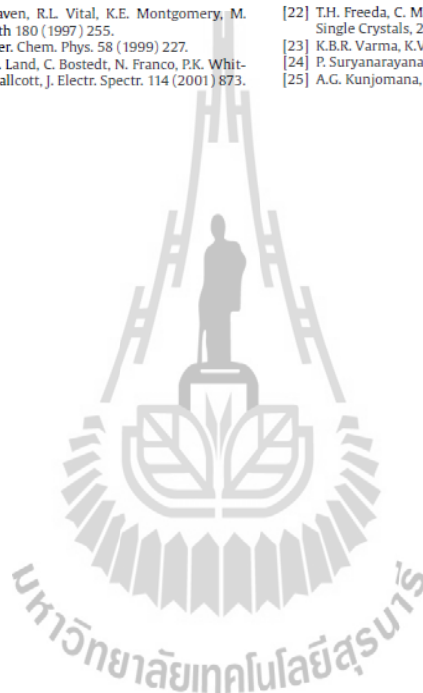
# CHARACTERIZATION OF PURE AND THIOUREA DOPED KDP SINGLE CRYSTALS GROWN BY SLOW EVAPORATION METHOD

Y. Inkong[1*], P.Ramasamy[2] and P.Manyum[1]

[1]School of Physics, Suranaree University of Technology, Nakorn Ratchasima 30000, Thailand
[2]Centre for Crystal Growth, SSN College of Engineering, Kalavakkam, Chennai 603110, India

## Abstract

Single crystal of pure Potassium dihydrogen phosphate (KDP) and KDP doped with thiourea were grown from aqueous solution by slow evaporation method at room temperature. The crystal structure of the grown crystals was determined using powder XRD method. The functional groups of KDP in the grown crystals were analyzed using FT-IR. The physical and optical properties of pure and doped crystals were studied. Dielectric constant measurements of the grown crystals along the [010] direction were carried out. It was found that the KDP crystal with 2%wt thiourea has better physical and electrical properties than the pure KDP crystal.

## 1. INTRODUCTION

Potassium di-hydrogen phosphate $KH_2PO_4$ (KDP) and the KDP type crystals are well known crystals for nonlinear applications. The crystals of the family show nonlinear electromechanical behaviour for acoustic applications such as piezoelectric transducer. They also show electro-optical effect. This nonlinear optical property of KDP type crystals is utilized in optics, especially for laser applications to convert the frequency of a coherent radiation to different one and to mix different frequencies [1-4]. They have very high optical damage thresholds and this can be exploited in intense laser beam applications. The KDP crystal belongs to the class $\overline{4}2m$ of the tetragonal system.

In this present work pure KDP and thiourea doped KDP were grown by slow evaporation method and the grown crystals were characterised.



**FIGURE 1.** As grown KDP single crystals.

## 2. EXPERIMENTAL

### 2.1 Crystal growth

Single crystals of pure and thiourea doped KDP were grown by slow evaporation method at ambient room temperature $30 \pm 1\ ^\circ C$. Analytical grade chemical reagents and distilled water were used in these experiments. Thiourea 2 wt% and 3 wt% were mixed in KDP solution separately and stirred by magnetic stirrer for 30 min then filtered by using filter paper grade no.1. The grown crystals are shown in Fig. 1.

### 2.2 Characterization

The good quality crystals were characterized. Powder XRD was obtained by BRUKER axs D5005 with $CuK_\alpha$ ($\lambda$=1.5418 A°) system. The FT-IR spectra were recorded in the range $400 - 4000\ cm^{-1}$. Microhardness was tested by Anton-Paar, MHT-10 with Vickers method. Optical properties were studied by transmittance of UV-visible spectra and dielectric constant measurements at room temperature were carried out.

## 3. RESULTS AND DISCUSSION

### 3.1 Powder X-ray diffraction

The powder XRD pattern of pure and thiourea doped KDP crystal are shown in Fig. 2. Diffraction patterns of the doped and pure crystal show that the additive has not changed crystal structure.
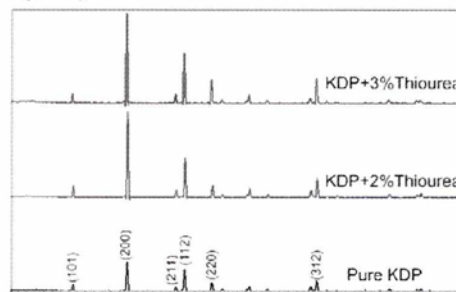


**FIGURE 2.** XRD pattern of pure and thiourea doped KDP.

*Corresponding author. E-mail: Inkong14@hotmail.com

258                                                    Y. Inkong *et al.*

The unit cell parameters of pure and doped crystals were determined by comparisons with standard peaks data. The unit cell parameters are listed in table 1.

**TABLE 1:** Unit cell parameters.

| Sample | a = b (Å) | c (Å) |
|---|---|---|
| Pure KDP | 7.453 | 6.974 |
| KDP+2%Thiourea | 7.447 | 6.974 |
| KDP+3%Thiourea | 7.478 | 6.974 |

### 3.2 FT-IR analysis

The functional group bonding of $(PO_4)^{3-}$ bending, P-O-H Stretching, P- Stretching, P=O Stretching and OP-O-H Stretching present in pure and thiourea doped KDP crystal show small shift in frequency. The FT-IR spectra of 2 wt% thiourea doped KDP is shown in Fig. 3 and sharp vibration peaks of functional group of pure and thiourea doped KDP are compared in table 2.
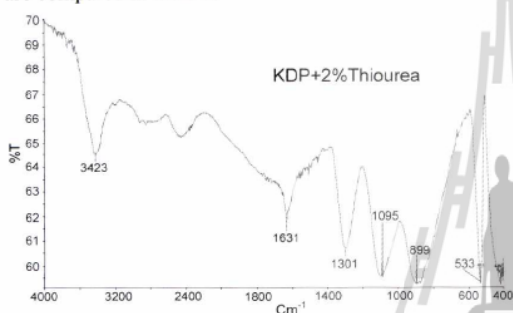


**FIGURE 3.** FT-IR spectra of 2 wt% thiourea doped KDP.

**TABLE 2: FT-IR frequency of functional groups of crystals.**

| Functional group | Pure KDP (cm$^{-1}$) | KDP+2% (cm$^{-1}$) | KDP+3% (cm$^{-1}$) |
|---|---|---|---|
| OP-O-H Stretching | 1633 | 1631 | 1634 |
| P=O Stretching | 1300 | 1301 | 1297 |
| P- Stretching | 1101 | 1095 | 1100 |
| P-O-H Stretching | 898 | 899 | ~900 |
| $(PO_4)^{3-}$ bending | 898 | 899 | ~900 |

### 3.3 Microhardness test

Microhardness test was carried out on (010) direction by Vickers method with load 10 g and holding time 15 s. Each sample was tested in 5 positions at 23 °C. The average hardness of samples is shown in table 3. The hardness of KDP+2%thiourea is more than pure KDP but the KDP+3%Thiourea less than pure KDP.

**TABLE 3:** Microhardness test.

| Sample | Hardness (Hv) |
|---|---|
| Pure KDP | 164.2 |
| KDP+2%Thiourea | 169.4 |
| KDP+3%Thiourea | 161.1 |

### 3.4 UV-visible spectral studies

The (010) faces of crystals were lapped by SiC paper no.800 and no.2000 to 3 mm thickness and then washed with DI water for optical transparency studies. The spectra were recorded in the wavelength range 190 – 900 nm. The UV-vis transmittance spectra of crystals are shown in Fig.

4. Pure and 2 wt% thiourea doped KDP are more transparent than 3 wt% thiourea doped KDP.
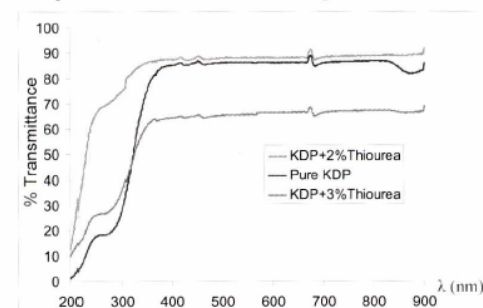


**FIGURE 4.** UV-vis transmittance spectra of pure and thiourea doped KDP.

### 3.5 Dielectric study

For dielectric measurement 1 mm thick sample was used. One side was coated with silver paint and on the opposite side a circle of 5 mm diameter was coated with silver paint. The capacitance of coated crystals was carried out by varying frequency of electric field from $10^2 – 10^7$ Hz at room temperature. The dielectric constant ($\varepsilon_r$) of crystals was calculated by Eq. (1)

$$\varepsilon_r = \frac{C_p d}{\varepsilon_0 A} \qquad (1)$$

Where $C_p$ is the capacitance, d is thickness of samples (in this case d = 1 mm), A is area of circle and $\varepsilon_0 = 8.85 \times 10^{-12}$ F/m. Dielectric constant versus log of frequency of crystals is shown in Fig. 5. The dielectric constant was increased with increasing percentage of addition of thiourea due to high nonlinear properties of organic material.
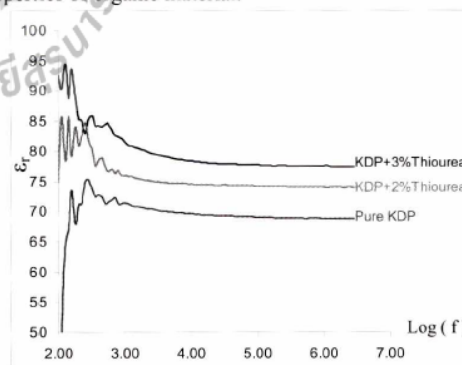


**FIGURE 5.** Dielectric constant along the [010] direction of pure and thiourea doped KDP.

### 4. CONCLUSIONS

- Single crystal of pure and thiourea doped KDP crystals were grown.
- The crystal structure of the grown crystals was confirmed by using powder XRD.

- The FT-IR spectra revealed that the addition of thiourea causes small shift in frequency.
- The 2 wt% thiourea doped KDP is better than pure KDP in physical and optical properties.
- The dielectric constant of 3 wt% and 2 wt% thiourea doped KDP is higher than pure KDP.

## ACKNOWLEDGEMENTS

## REFERENCES

[1] S.S. Hussaini, et. al. Cryst. Res. Technol. 42, No.11(2007) 1110 – 1116.
[2] K.D. Parikh, et. al. Bull. Mater. Sci.30 (2) (2007) 105–112.
[3] N.P. Rajesh, et. al. Mater. Lett. 52 (2002) 326-328.
[4] S. Balamurugan, et. al. Mater. Chem. Phys. 113 (2009) 622-625.
[5] D. Xu and D. Xue, Physica B 370 (2005) 84-89.
[6] M. Priya, et. al. Bull. Mater. Sci.24 (5) (2001) 511–514.
[7] G. Li, et. al. J. Cryst. Growth 274 (2005) 555-562.

# CURRICULUM VITAE

Mr.Yutthapong Inkong was born on the 16th January 1971 in Udornthanee Province, Thailand. After he finished high–school at Udornpithayanukul in 1989, he studied Physics at Department of Physics, Faculty of Science, Ramkhamhaeng University. He received his Bachelor's Degree in 1994. He was a researcher at Thailand Institute of Scientific and Technological Research (TISTR) in 1996. He became a Teaching/Researching Assistant in School of Physics, Institute of Science, Suranaree University of Technology (SUT) in 1997 and he obtained his Master's Degree at this University in 2005. After that, he joined to Rajamangala University of Technology Thanyaburi, as a lecturer. In 2006, he came back to SUT again to enroll for Ph.D. study in the field of Single Crystal Growth under supervision of Assoc. Prof. Dr. Prapun Manyum and Prof. P. Ramasamy from SSN College of Engineer (SSNCE), Chennai, India. During his course of study, he has visited to Centre for Crystal Growth, SSNCE, to practice in crystal growth. His Ph.D. thesis was entitled "Growth and Characterization of Pure and Thiourea Doped Potassium Dihydrogen Phosphate Single Crystals". His Ph.D. study was supported by Rajamangala University of Technology Isan. He successfully obtained his Ph.D. degree in 2012.